Single electron methodology for the synthesis of disubstituted quinolines by chemical and electrochemical catalysis

by

Mark D. Aloisio

A thesis submitted in partial fulfillment of the requirements for the degree of

Master of Science

Department of Chemistry
University of Alberta

Abstract

Radical cation catalyzed methodology was adapted for the synthesis of disubstituted quinolines, to address the requirements for continuous oxygen sparge and high reaction temperatures. Using previously reported aldehydes and 5,6,7,8-tetrahydronaphthylamine, the reaction required optimization of radical cation salt and reaction conditions. A series of radical cation salts were synthesized by the Buchwald-Hartwig amination of para-substituted iodobenzene derivatives screened using similar *para*-substituted anilines. The triarylamines were oxidized to the radical cations using triphenylammonium hexachloroantimonate ($TPASbCl_6$), tris(*p*-methylphenyl)ammonium hexachloroantimonate ($TTASbCl_6$), tris(4-biphenyl)ammonium hexachloroantimonate ($TBPhASbCl_6$), and triphenylammonium hexafluorophosphate ($TPAPF_6$), to compare with commercial tris(4-bromophenyl)ammonium hexachloroantimonate ($TBPASbCl_6$). After optimizing other reaction variables, the best results were obtained using $TPASbCl_6$ as the catalyst.

This method of radical catalysis was compared to our previously optimized acid/iodide methodology with a series of aniline substrates. Radical cation catalysis was comparable to the HI method, with some substrates providing increased yields. Bidirectional MCR reactions were evaluated using 1,5-diaminonaphthalene to target the formation of tetrasubstituted 4,10-diazachrysene compounds under the radical cation conditions. These reactions were successful, but resulted in isolation of the dihydroquinoline as product, which does not undergo aerobic oxidation to the fully aromatic ring system.

Preliminary exploration of an electrochemical method for generating the aniline radical cation was pursued. The electrochemical cell allows for oxidation of a soluble redox mediator, leading to the same radical cation mediated MCR quinoline synthesis. Initial results were poor, but lithium bromide as electrolyte provided improved but still modest yields. The dual role of lithium bromide as the electrolyte and the amine redox mediator requires more investigation to better understand its purpose in the reaction process.

To August, Marion, John, and Jennie

Acknowledgements

I would like to acknowledge several people that made this degree and my time at the University of Alberta possible and enjoyable.

Firstly, I would like to thank Prof. Jeffrey Stryker for allowing me to work in his lab under his mentorship and counseling throughout both my master's and my undergraduate degrees. His patience with the students and allowing them to think and problem solve will always be remembered. The opportunities and lessons he gave to me will be valued too, from fundamental synthetic chemistry to current taste in jazz music, I will take with me on my journey forward.

I would also like to thank my committee members Prof. Rik Tykwinski and Prof. Eric Rivard for their counsel during my MSc. As well as Prof. Rylan Lundgren as my committee chair for my defense.

To current and past Stryker group members. Dr. Robin Hamilton, Dr. Orain Brown, Dr. David Scott, thank you all for the conversations and mentorships, but more importantly the friendship you shared with me. Munashe Chizema, Dr. Sanjay Jadhav, Subrata Patra and Yaowei Guo, thank you all for the conversation and company through years. Dr. Asama Leduc, Dr. Jose Rodriguez, and Fiona Nkala, thank you for the early days in the lab and for the many coffees we shared.

To the staff of the department for their help with my requests, questions, and counselling through my time here, specifically Wayne Moffat, Jennifer Jones, Mark Miskolzie, Laura Pham, Anita Weiler, Ryan Lewis, Michael Barteski, Matthew Kingston, Andrew Yeung, Dr. Karlene Lynch and Jason Dibbs. To my fellow students and friends whom I met in the department; Vitor Cunha, Wesley McNutt, Emily Rodrigues, and more, for their comradery during my MSc. Thank you all.

To the teaching administration and staff in the department. I had the pleasure of working under Dr. Jeffrey Stryker, Dr. Tina Grant and Dr. Sai Yiu as a teaching assistant during my time here. I also would like to thank Dr. Hayley Wan and Connor Part for their time and guidance as I learned patience and skills to educate the students within the lab space.

To my family for their encouragement and support during my degree, Mom, Dad, Veronica, Samantha, Grandma, Grandpa, and Dido, thank you. To my friends outside of the department: Patrick Boyer, Brandon Smith, Ryan Suave, Taylor Knopp, Connor and Shaylee Boucher, Daniel Chu, Brendan Gluth, Eric Hiebert, and Terry Bamlett, thank you for the continued friendship over the years.

Table of Contents

List of Figures

List of Schemes

List of Equations

List of Tables

List of Abbreviations

Å	angstrom
AFM	atomic force microscopy
API	American Petroleum Institute
°C	degrees Celsius
cm^{-1}	wavelength
Cp_2Fe	Ferrocene
CV	cyclic voltammetry
D	days
“DAB”	diazabutadiene
DCM	dichloromethane
DME	dimethoxyethane
DMF	dimethylformamide
equiv	equivalents
g	grams
h	hours
HMDSO	hexamethyldisiloxane
HRMS	high resolution mass spectroscopy
IR	infrared spectroscopy
min	minutes
mA	milliamperes
MCR	multicomponent reaction
Me	methyl

MeCN	acetonitrile
MeOH	methanol
MHz	megahertz
mmol	millimoles
mL	millilitres
mV	millivolts
nm	nanometres
NBS	*N*-bromosuccinimide
NMR	nuclear magnetic resonance
N,N'-DMEDA	*N,N'*-dimethylethylenediamine
OMe	methoxy
Ph	phenyl
PhOMe	anisole
ppm	parts per million
rt	room temperature
RVC	reticulated vitreous carbon
SET	single electron transfer
TBABr	tetrabutylammonium bromide
TBACl	tetrabutylammonium chloride
TBAI	tetrabutylammonium iodide
$TBAPF_6$	tetrabutylammonium hexaflourophosphate
TBPA	tri(4-bromophenyl)amine
TBPA*	tris(4-bromophenyl)ammoniumyl hexachloroantimonate

TBPhA	tri(biphenyl-4-yl)amine
$TBPASbCl_6$	tris(4-bromophenyl)ammoniumyl hexachloroantimonate
THF	tetrahydrofuran
TMEDA	tetramethylethylenediamine
TPA	triphenylamine
$TPAPF_6$	triphenylammoniumyl hexafluorophosphate
$TPASbCl_6$	triphenylammoniumyl hexachloroantimonate
TTA	tri(4-methylphenyl)amine
$TTASbCl_6$	tris(4-methylphenyl)ammoniumyl hexachloroantimonate
UV-Vis	ultraviolet visible spectroscopy
V	volt

Chapter 1: Multicomponent synthesis of quinolines as model compounds for basic nitrogen-driven asphaltene aggregation.

1.1 Introduction

The diverse molecular interactions of asphaltenes found within bitumen are continually under investigation. Synthetic models of the material are needed to simulate the associative interactions produced by the hierarchy of intermolecular interactions present in the complex material. Synthesis of highly substituted quinolines is crucial for "rapid through-put" synthesis of the targeted range of model compounds containing basic nitrogen.

1.1.1 Bitumen asphaltenes. What defines their intermolecular interactions?

The Alberta oil sands constitute one of the largest deposits of crude oil in the world.[1] The vast majority of these deposits consist of a heavy and highly viscous crude oil termed bitumen, which presents unique challenges for transportation to market and processing into fuels and petrochemicals.[2] Crude oils are classified using several parameters including density and viscosity, which are reflected in the American Petroleum Institute gravity API measurement.[3] These measurements invert the density measurements, which reflect the size and composition of the oil. Therefore lower API measurements reveals a lager components found within the bitumen.[3] In addition, heteroatom content and H/C ratios are key metrics for classifying oils. Alberta bitumen

Table 1.1. Comparison of Heavy Oil from Alberta and ExxonMobil Crude Oil

Parameters	Athabasca Heavy Oil	Crude Heavy Oil*
Gravity °API	8.0	19 - 25
Sulfur (wt%)	5.1	0.3 – 3.0

*Data range from ExxonMobil from their crude oil standards

oil is regarded as having a lower quality than global benchmark crudes by all of these metrics.[2] Compared to other geographical regions, Alberta heavy oil has much lower API and H/C ratios, as well as elevated levels of sulfur (Table 1.1).[4,5] Transporting this heavy crude from remote Northern Alberta mines and wells to distant refineries either extensive upgrading to synthetic crude oil or blending with diluents prior to transport.[3] Both methods provide pipeline-grade liquids but add significant costs and lead to increased greenhouse gas emissions.

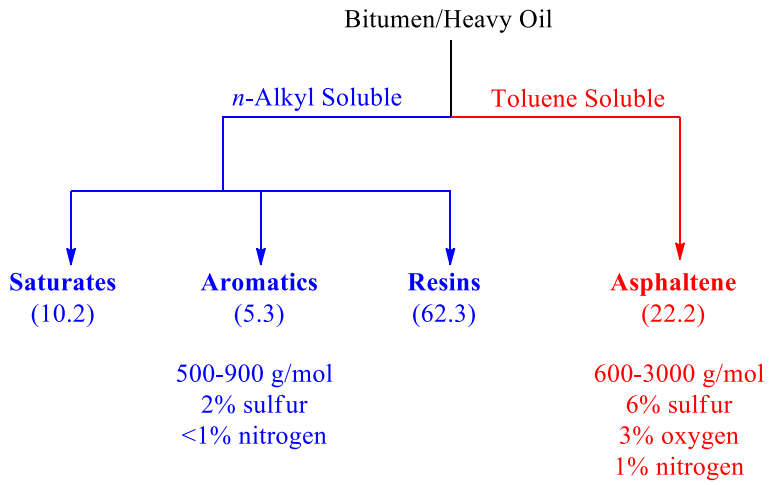

Figure 1.1 Composition of the bitumen by solubility. Values in brackets are weight percent values for Athabasca bitumen found by Gray and co-workers.

Many of the undesirable physical and chemical properties of heavy crude oil result from the high content of asphaltenes.[6] Crude oils are comprised of four major solubility fractions termed saturates, aromatics, resins, and asphaltenes, each having distinct physical and chemical properties (Figure 1.1).[5,7,8] Saturates, aromatics and resins are *n*-alkane soluble and comprise 80-90% by weight of heavy oils and are the principal source of the accessible and useful hydrocarbons in bitumen.[7] In contrast, asphaltenes dissolve in toluene and are by far the least useful fraction because of its extreme molecular complexity, high sulfur and nitrogen content, and presence of

toxic metals (vanadium ppm: 196, nickel ppm: 75).[9] Asphaltenes are prone to spontaneous deposition during processing and transport, leading to fouling of equipment and pipelines.[3]

The standard industrial approach to processing heavy crude oils having a high asphaltene content is to reject this fraction, most often through either high-temperature thermal coking or a solvent based deasphalting.[10] While effective, these processes are less desirable because of the energy consumption, associated greenhouse gas emissions, and the loss of 13-25% of the bitumen as valueless and toxic petcoke.[7] This reality has spurred considerable research towards deciphering the molecular structure of asphaltene constituents, as well as understanding the irreversible aggregation observed for the material.

There are two closely related branches of asphaltene research. In the first, modern analytical techniques are employed to sample naturally occurring asphaltenes, either to isolate intact molecules or identify key substructures present. Modern mass spectroscopy and atomic force microscopy have proven particularly useful, revealing that at least part of the asphaltenes are comprised of polycyclic aromatic hydrocarbons "islands and continents" of varying sizes, decorated by alkyl side chain chains of varying lengths (Figure 1.2).[11,12] The second approach to

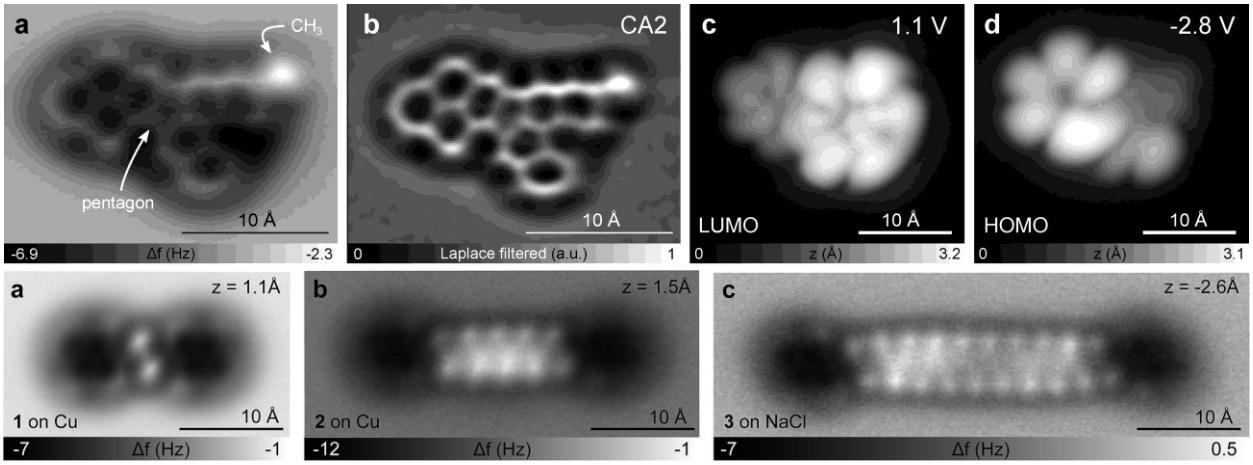

Figure 1.2 AFM imaging of coal derived asphaltenes performed and analyzed by Gross and co-workers. The top line of images is a representation of the continental motif, while the lower images representation for the archipelago motif with the alkyl tether between two polycyclic aromatics

studying asphaltenes involves the synthesis of model compounds guided by the data obtained from studying naturally occurring asphaltenes samples. These synthetic molecules allow for modelling of asphaltene behaviour under controlled experimental and in silico conditions, the results of which may reveal the mechanisms driving asphaltene aggregation and precipitation during

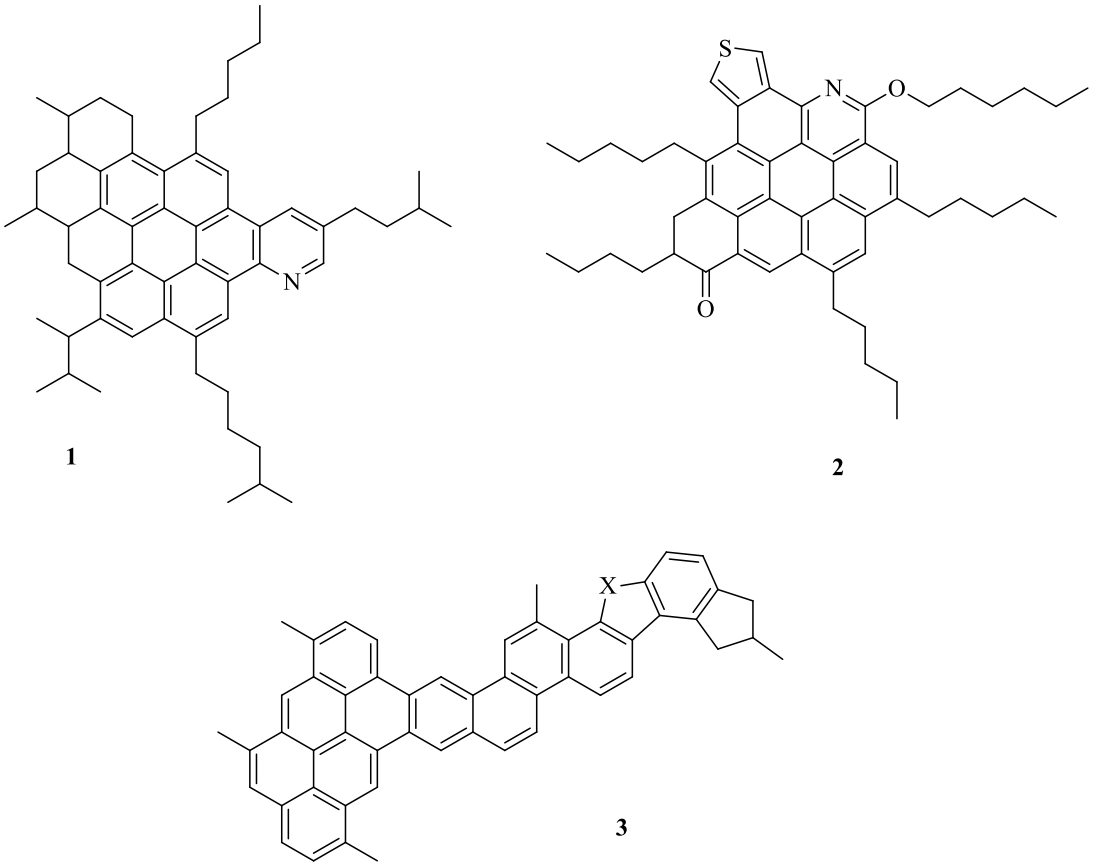

Figure 1.3 Possible structure of different continental motifs 1) The structure suggested by Yen-Mullin. 2) An average structure suggested by the molecular weight and heteroatom percentages 3) A natural structure determined by AFM.

transport and processing in industrial environments. Eventually, data obtained from molecular modelling may guide heavy oil processors in developing new strategies for disaggregating asphaltenes, thus unlocking value from a prominent, costly, yet capricious fraction of heavy crude oils.

There are two distinct, yet partly complementary, hypotheses concerning the structure of naturally occurring asphaltenes and hence the appropriate organic molecules to be used as model compounds. The first hypotheses posits that asphaltenes are primarily comprised of large polycyclic aromatic 'continents' decorated by medium-to-long alkyl side chains (Figure 1.3).[13] In this "continental" motif, the primary force driving aggregation is proposed to be π-π interactions between the faces of the aromatic centers. However, experimental determinations suggest that π-π interactions alone are insufficient to account for the net aggregative forces present in natural asphaltenes. In addition, the continental model all but ignores the contributions of the abundant heteroatoms to driving the intramolecular assembly in asphaltenes. As a result, an "archipelago" model has been proposed to explain asphaltene structure *and* aggregation. In this model, asphaltene is viewed as a series of smaller polycyclic aromatic 'islands' tethered by 1-6 carbon saturated alkyl chains (Fig. 1.4).[14] Intermolecular interactions are not limited to π-π interactions but include acid-base association between carboxylic acid and basic nitrogen residues, porphyrin-metal coordination, aliphatic "pockets", and inclusion complexes.[15] Together, these diverse interactions

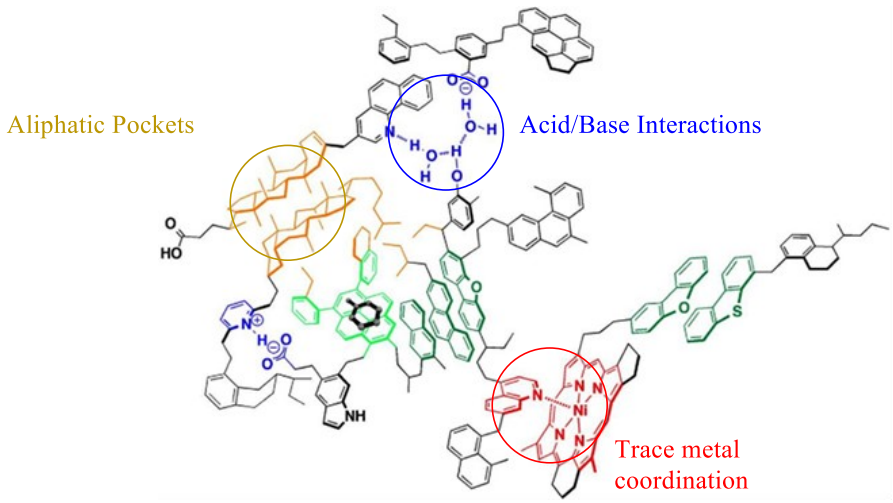

Figure 1.4 Cartoon of Archipelago model, with representation of specific intermolecular interactions

are considered to better reflect the elemental diversity and net aggregation energy observed in asphaltenes. For this reason and because this architecture is virtually unstudied, archipelago asphaltene model compounds will be the principal focus of the remaining discussion.

1.1.2 Model compounds of aggregates of asphaltene compounds .

A range of continental and archipelago asphaltene model compounds have by now been prepared using standard synthetic strategies.[16] For example, hexabenzocoronene, a simple continental model, can be prepared by cobalt-catalyzed cyclotrimerization of substituted diarylacetylenes, followed by oxidative aromatization of the intermediate hexaphenylbenzene (Scheme 1.1).[17] Archipelago type molecules can also be prepared using multi-step syntheses (Scheme 1.2). A simple example of this is Sonogashira coupling of a dibromopyridine with pyrenylethyne, followed by palladium-catalyzed hydrogenation to yield a di-substituted pyridine-centered three island model (Scheme 1.2, top).[18] A more elaborate 5-island archipelago model was prepared by iterative Kumada alkylation of 1,3,6,8-tetrabromopyrene with an appropriate Grignard reagent in the presence of a nickel catalyst (Scheme 1.2, bottom). Varying yield the length of the alkyl 'tethers' and the nature of the aromatic islands yield homologous series.[19]

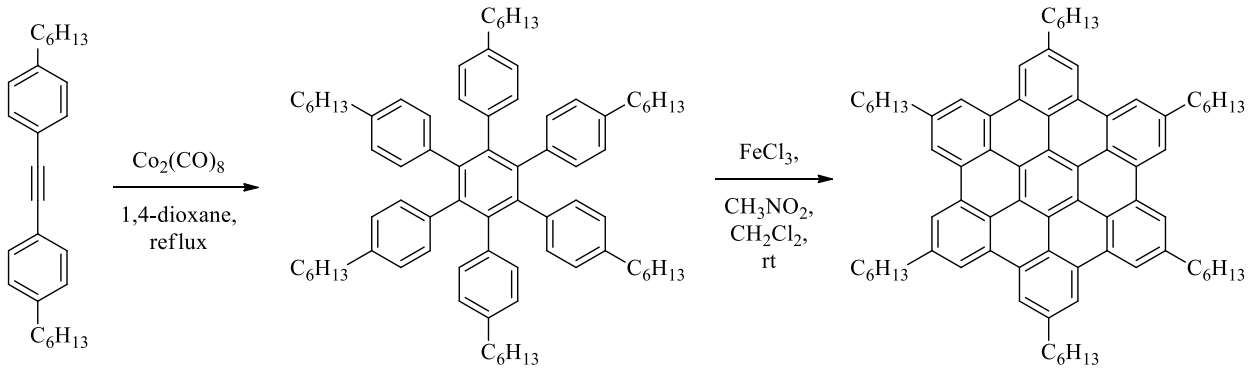

4 **5** (45%) **6** (54%)

Scheme 1.1 Continental model synthesis, building a substituted hexabenzocoronene.

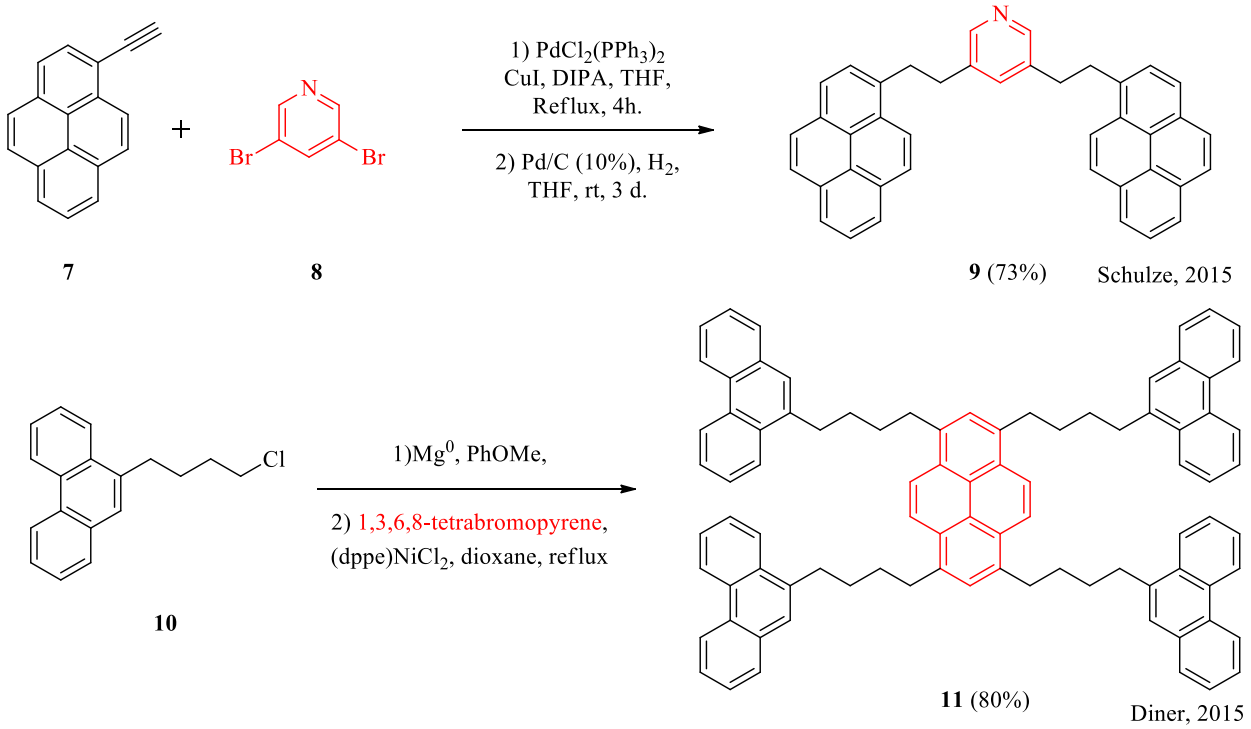

Scheme 1.2 Archipelago model synthesis examples, varying the central "island".

The synthetic routes highlighted above are either multistep or require air-sensitive reagents. Building the large library of diverse molecules needed to model complex asphaltenes at the necessary scale demands rapid, simple, scalable, and inexpensive pathways. In response to these realities, the Stryker group has recently focused on adapting robust air- and moisture-compatible one-pot multicomponent reactions for preparing libraries of archipelago model compounds.

1.1.3 Multicomponent reactions leading to archipelago quinoline synthesis.

An idealized multicomponent reaction (MCR) converts three or more starting materials into a single product, with maximum atom-efficiency.[20] This methodology provides rapid access to molecular diversity and complexity in a single-step. Of the many classes of multicomponent reactions, the one-pot cyclocondensation of anilines and appropriate carbonyl compounds to form

substituted quinolines is of greatest interest for preparing strongly basic asphaltene model compounds. This reaction allows for rapid construction of three-island archipelago molecules, each containing a central N-heterocyclic core attached to variable length tethers and flanking aromatic islands

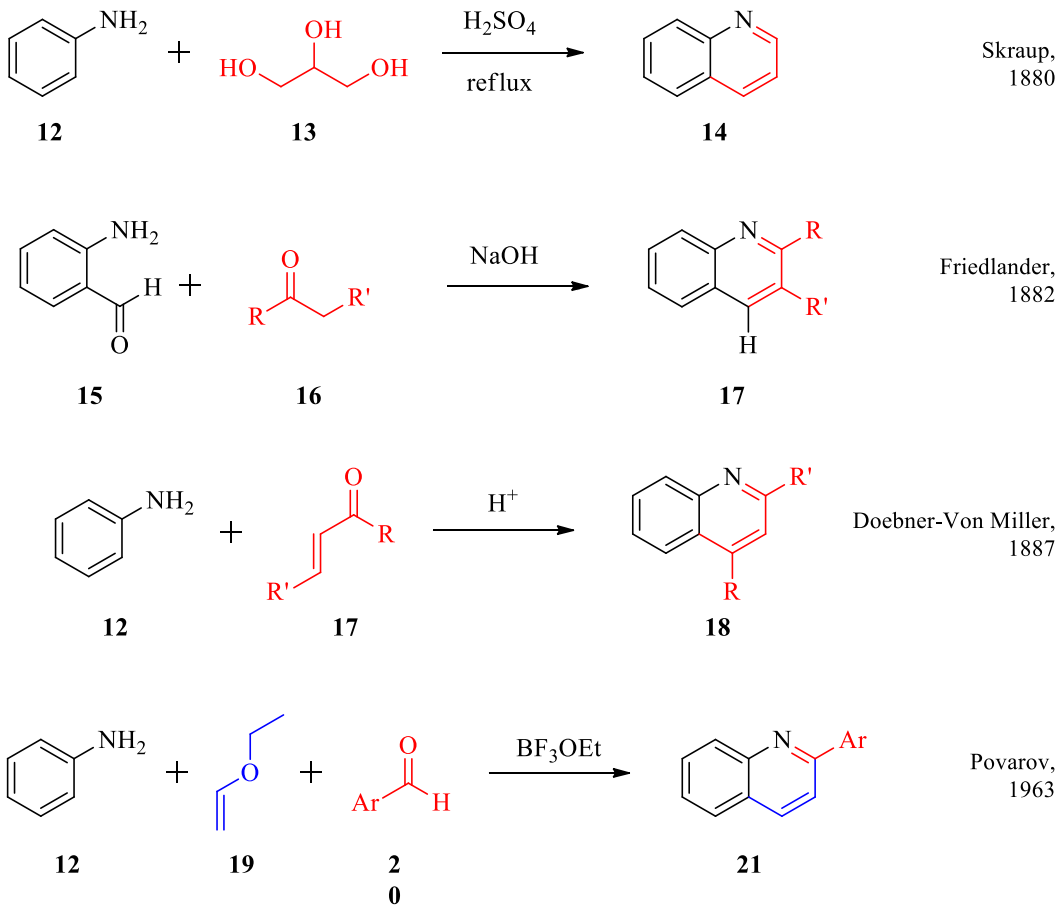

Figure 1.5 Historical examples of quinoline synthesis.

One-pot synthesis of quinolines is neither new nor revolutionary (Figure 1.5). Modern organic chemistry continues to exploit several methodologies for the synthesis of quinolines from anilines initially developed over a century ago.[21] Classical one-pot methods for quinoline synthesis include the Skraup synthesis (1880), which uses glycol and concentrated acid to form the quinoline. Friedlander (1882) used a secondary ketone with 2-aminobenzaldehyde under basic

conditions to form the desired product. The Doebner-Von Miller synthesis (1887) showed that a conjugated ketone could also be used to afford quinolines under acidic conditions.[1x] Pavarov's 1963 report describing Lewis acid-catalyzed cyclcocondensation between aniline, enol ether, and an aldehyde represents the first truly multicomponent quinoline synthesis. Notably, the Povarov multicomponent reaction along with the other methods for quinoline synthesis all have high atom-efficiency, with only water or small molecules such as ethanol eliminated as by-products. This reinforces the relative 'greenness' and cost-effectiveness of this synthetic method.

1.1.4 Acid catalyzed cyclocondensation of quinoline compounds

Povarov MCR protocols have been further developed with a view to improving yields, scope, and accessibility. In 2004, Kozlov and co-workers suggested an acid catalyzed cyclocondensation reaction between an aniline derivative, a substituted benzaldehyde, and a ketone (Scheme 1.3).[22] A diverse scope was realized, giving moderate-to-good yields; however,

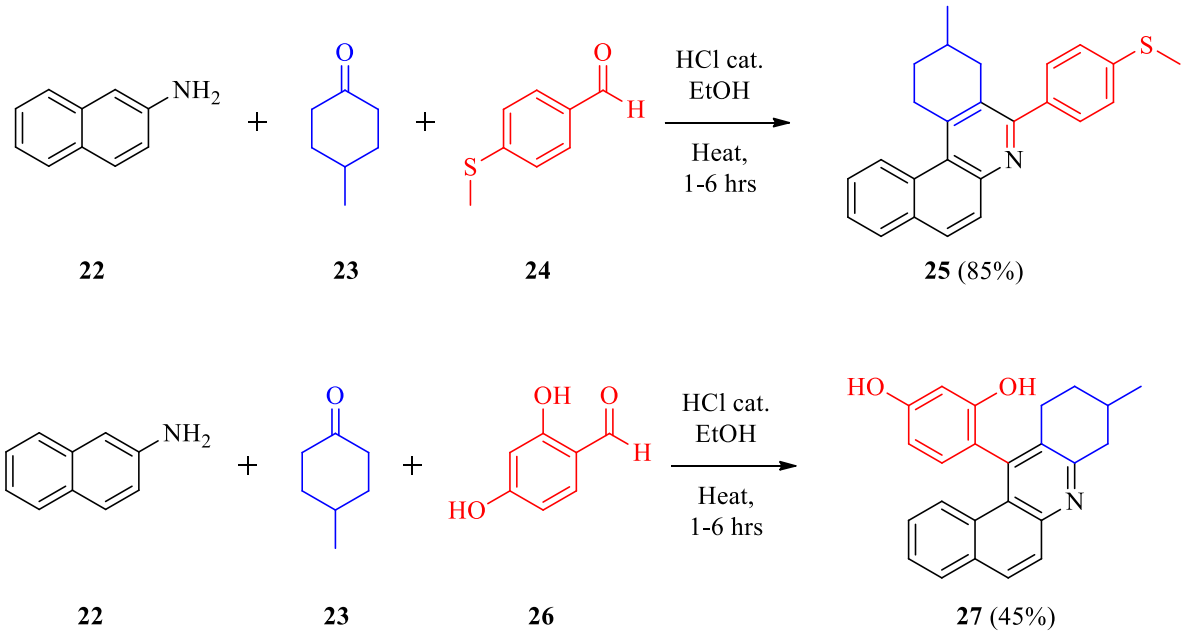

Scheme 1.3 Kozlov and co-workers quinoline MCR.

the challenge of regioselectivity dictated by the substituents on the benzaldehyde led other researchers to explore this method further.

Further development of effective reaction conditions was reported in 2008 when Wang and co-workers published an iodine-catalyzed Povarov-type MCR using similar starting materials (Equation 1.1).[23] The reactions are regioselective and many substitution patterns on the aldehyde and ketone ring sizes are accommodated, with moderate-to-excellent yields. The authors suggest that iodine functions as a mild Lewis acid, coordinating to polar functional groups to promote formation of the imine as well as drive the final cyclization product.

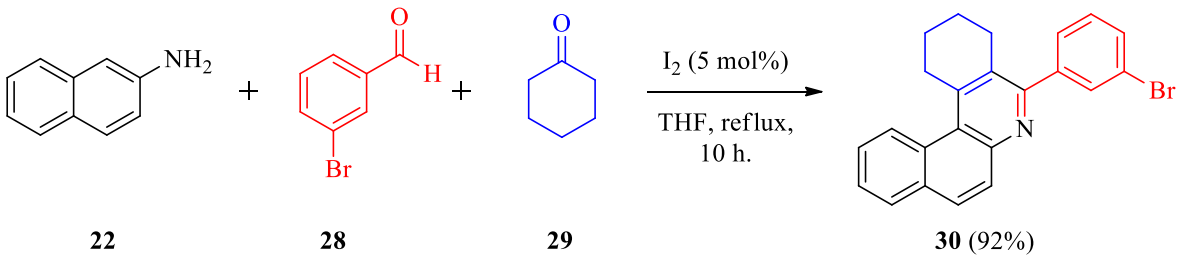

22 **28** **29** **30** (92%)

Equation 1.1 Wang and co-workers quinoline MCR.

The role of iodine turns out to be more nuanced. Schulze, et al., in the Tykwinski and Stryker groups first discovered this by showing that the Wang protocol fails under strictly anhydrous conditions. Only when carefully metered quantities of water were added to the reactor did they obtain selective conversions to the quinolines. The authors established that hydroiodic acid was formed in situ and that buffered HI is the acid catalyst for imine formation and cyclization. Using the modified Wang protocol, Schultz et al. completed the first synthesis of continental asphaltene quinoline model compounds via this MCR.[24] Large steroid substructures and diverse heteroatoms were incorporated into the final product, depending on the choice of ketone and aldehyde coupling partners (Equation 1.2). Limitations of this method include long reaction times and a limited scope of anilines and aromatic aldehydes. While the 2-arylquinoline motif is

accessible through these reaction conditions, these compounds are not archipelago models. The use of alkyl-tethered α,ω-aromatic aldehydes to give satellite polycyclic aromatics of variable length would lead to three-island archipelago compounds that better represent our objectives.

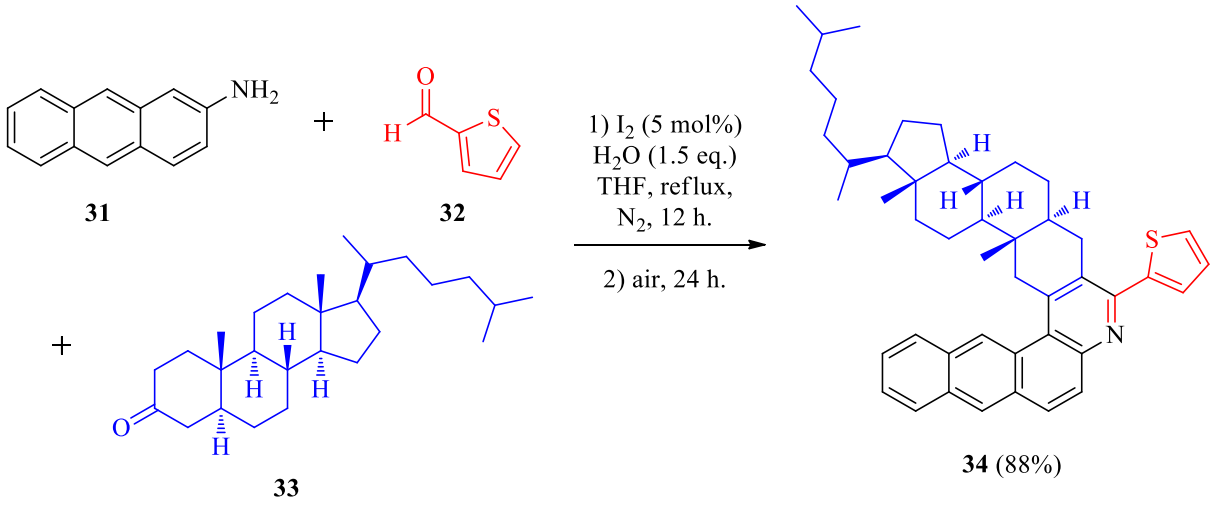

Equation 1.2 Schulze and co-workers quinoline MCR.

Scott, et al., adapted and exploited this multicomponent cyclocondensation to develop a modular synthesis of a quinoline-based archipelago structures, varying the aromatic amine and island-tethered aldehyde.[25] Scott added hydroiodic acid directly instead of molecular iodine/water (Equation 1.3). The use of the aliphatic aldehydes, however, gives rise to issues not previously encountered using aromatic aldehydes. A secondary amine side product resulting from reduction of the imine intermediate is observed, in competition with the final aerobic aromatization to the quinoline. This led Scott to explore the rates and mechanism of the oxidation. A constant sparge of oxygen improves yields but does not suppress the side product, which is difficult to separate during purification. With the addition of stoichiometric soluble iodide (as tetrabutylammonium iodide), the reaction shows significant increases in yield and minimal secondary amine. In this reaction, the iodide is oxidized aerobically, generating I^+ and hydrogen peroxide catalytically in

solution. Optimizing this iodonium/iodide cycle brought this reaction forward substantially, but not sufficiently for our purposes.

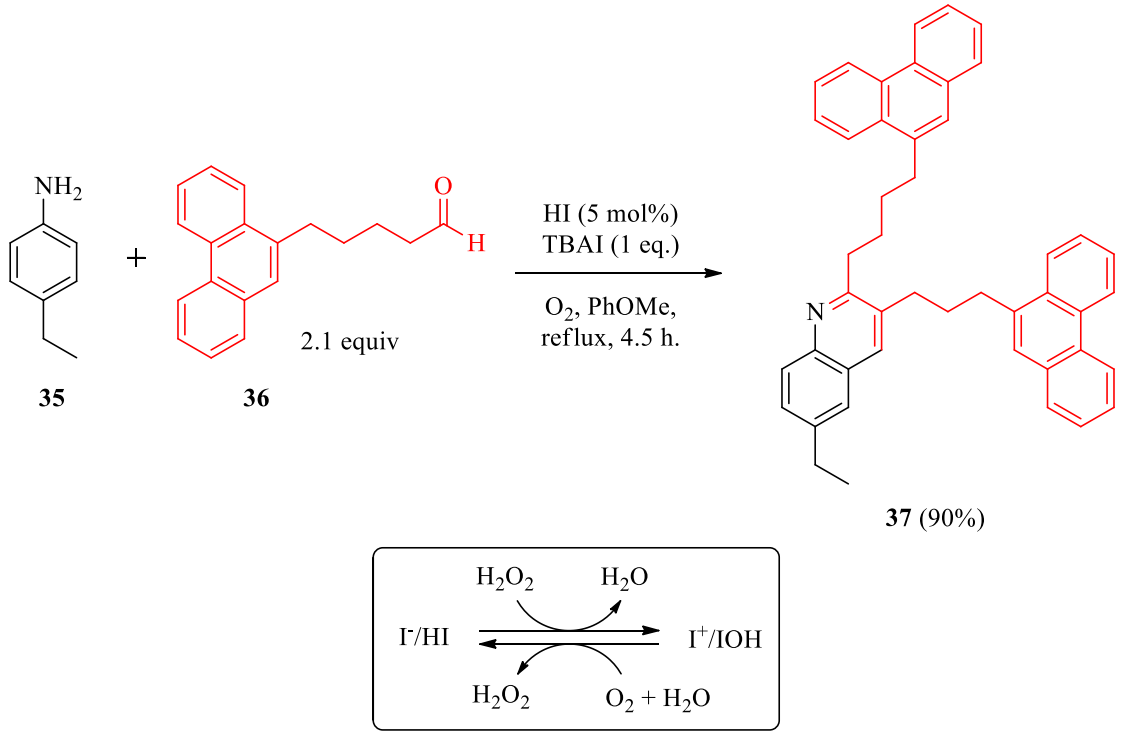

Equation 1.3 Scott and co-workers quinoline MCR and suggested iodine equilibrium.

1.1.5 Limitations to the Acid-Catalyzed Method

With a set of optimal conditions established, the bidirectional synthesis of diazachrysene was explored. This could potentially yield 5-island archipelago molecules in a single-pot synthesis exploiting the iodide/iodonium cycle. Unfortunately, the reaction protocols developed by Scott, et al., are poorly suited to bidirectional synthesis. The reaction halts after one quinoline is formed even at elevated temperatures and under aggressively oxidizing conditions (Scheme 1.4). In any

event, sparging molecular oxygen through organic solvents at elevated temperature is inherently unsafe and certainly not ideal for large scale reactions.

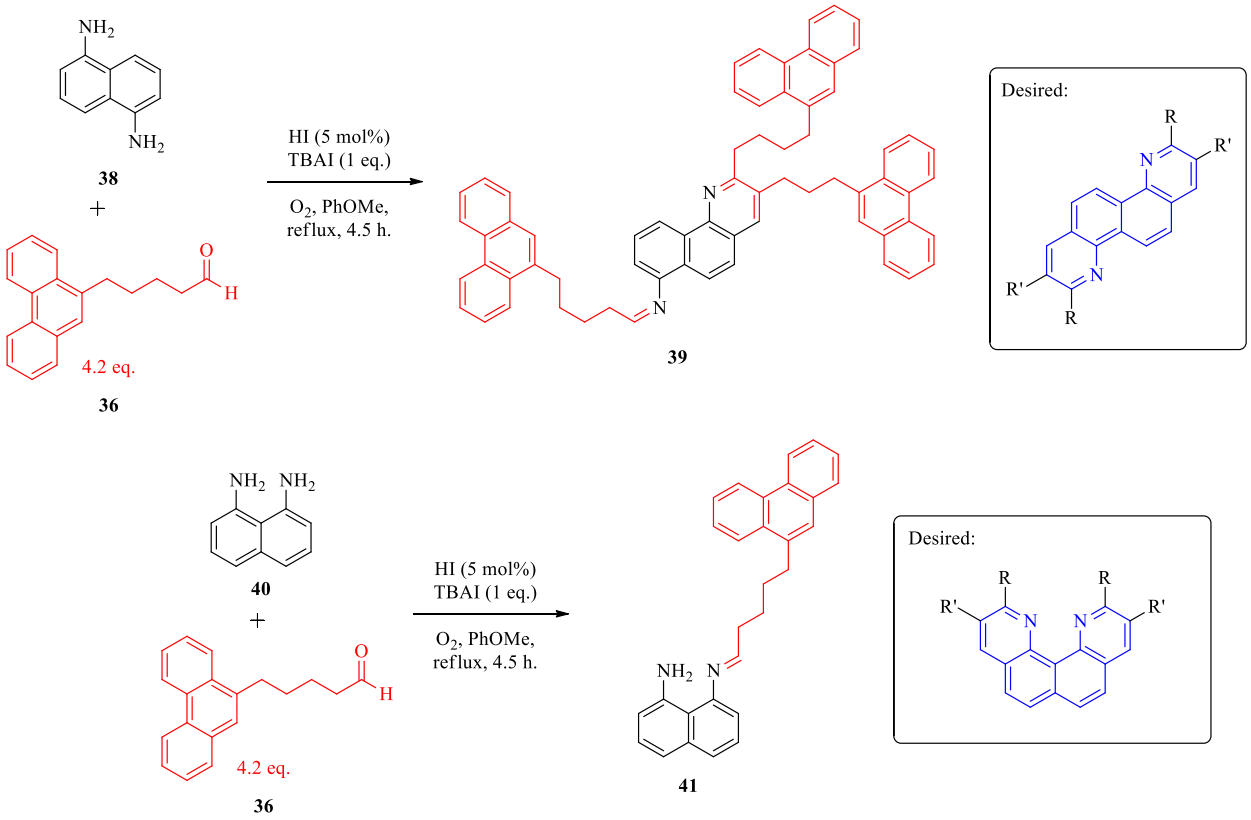

Scheme 1.4 Preliminary bis-quinoline results and limitations.

With these significant limitations identified, my project goals were twofold: (1) develop new protocols to convert simple diaminoaromatic compounds into five-island archipelago model compounds, and (2) explore radical-cation catalysis for MCR cyclocondensation, which proceeds by single electron transfer (SET), generating the catalyst through both chemical and electrochemical methods. In principle, this should avoid the use of high temperature and a pure oxygen atmosphere, and suppress secondary amine formation. Chapter 2 also describes advances in bidirectional MCR methodology catalyzed by chemical oxidants. Importantly, radical cation catalysis induces the MCR to proceed efficiently under air at lower temperatures. Finally, in

Chapter 3, I show that the optimal synthetic approach may well be electrochemical catalysis, which drives the radical cation MCR under ambient conditions (Chapter 3).

Chapter 2: Quinoline synthesis catalyzed by amine radical cation salts.

2.1 Introduction

Radical cation catalysis for the synthesis of substituted quinolines was pursued to address the limitations of the previous methodology. Reaction conditions were optimized, and the scope compared to $HI/O_2/H_2O$ catalysis. Improved yields and oxygen-free turnover were achieved.

2.1.1 Evolution towards radical methodology

Radical cation catalysis is the obvious enabling technology to ensure that the quinoline multicomponent reaction proceeds under milder reaction conditions. For the classic MCR, HI is the nominal catalyst, but its role is not limited to Bronsted/Lewis acid catalysis. Mechanistic analysis reveals that in addition to proton-catalyzed imine condensation, HI also reacts with water and oxygen in situ to generate hypervalent iodine species that promote both cyclocondensation and oxidative aromatization. Both one- and two-electron transfer pathways are involved in these iodine-catalyzed reactions. As described in Chapter 1, with a deficiency of oxidants, some of the imine also acts as the terminal oxidant in the reaction, abstracting hydride from the tetrahydroquinoline intermediate and forming the secondary amine. While this is an undesired side reaction, it is nevertheless instructive. Radical cation catalysis can uniquely drive the quinoline MCR by mimicking both hydride abstraction and facilitation electron transfer reactions typical of hypervalent iodine.[26] Furthermore, we anticipate that the radical cation catalyst will eliminate the need for oxygen (or air), and create a lower energy pathway for the MCR, potentially allowing ambient temperature synthesis of the desired quinolines in high selectivity.

Radical cation catalysis for the synthesis of substituted heterocycles is not new. Since the 1980s, commercially available radical cation salts such as tris(4-bromophenyl)ammoninyl hexachloroantimonate, commonly referred to as "Magic Blue", have been used for promoting cyclocondensation reactions to make substituted quinolines (Figure 2.1).[27,28] The quinoline is typically prepared from a styrene derivative and a secondary aminoester; because of this, the substituents on the *N*-heterocycle of final products are limited to aryl and ester groups.

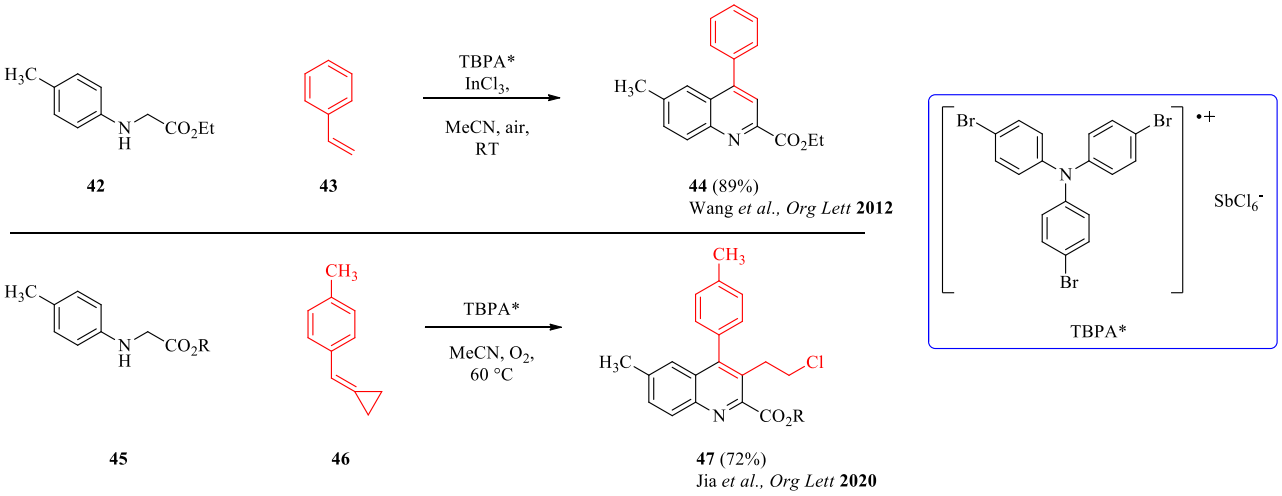

Figure 2.1 Examples of TBPA* mediated quinoline syntheses

More recently, Wang et al. adapted this method to accommodate aliphatic aldehydes and anilines, giving 2,3-alkylquinolines in moderate to good yields (70-80%) (Equation 2.1).[29] Importantly, high temperature and oxygen are not needed to drive the oxidation. The anilines and linear alkyl aldehydes used in this study are nearly identical to those needed to access alkyl-

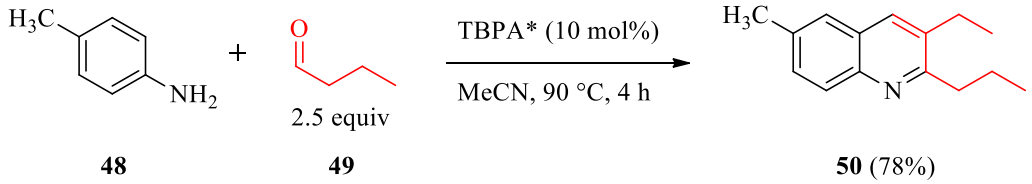

Equation 2.1 Wang and co-workers use of the triaryl amine radical cation salt in the synthesis of quinolines.

tethered ‘multi-island’ molecules. We therefore explored similar radical cation catalysts for promoting the synthesis of the quinoline archipelago compounds.

2.2 Results and Discussion

2.2.1 Synthesis of α,ω-arylalkyl aldehydes

Archipelago model compounds feature polycyclic aromatic groups (i.e., pyrene, phenanthrene, dibenzothiophene) tethered to a central aromatic core, in this case quinoline or benzoquinoline. The arene-terminated alkyl aldehydes are the source of these ‘satellite islands’ and are not commercially available. Fortunately, these aldehydes can be prepared using a simple yet versatile two-step procedure. First, a commercially available bromoarene is converted into the iodide by copper-catalyzed halogen exchange. (Figure 2.2).[25,30] For dibenzothiophene, an adapted synthesis was used, using direct ortho-lithiation using *N,N,N’,N’*-tetramethylethylenediamine (TMEDA) to activate butyllithium.[31] Followed an iodine quench, 4-iododibenzothiophene is

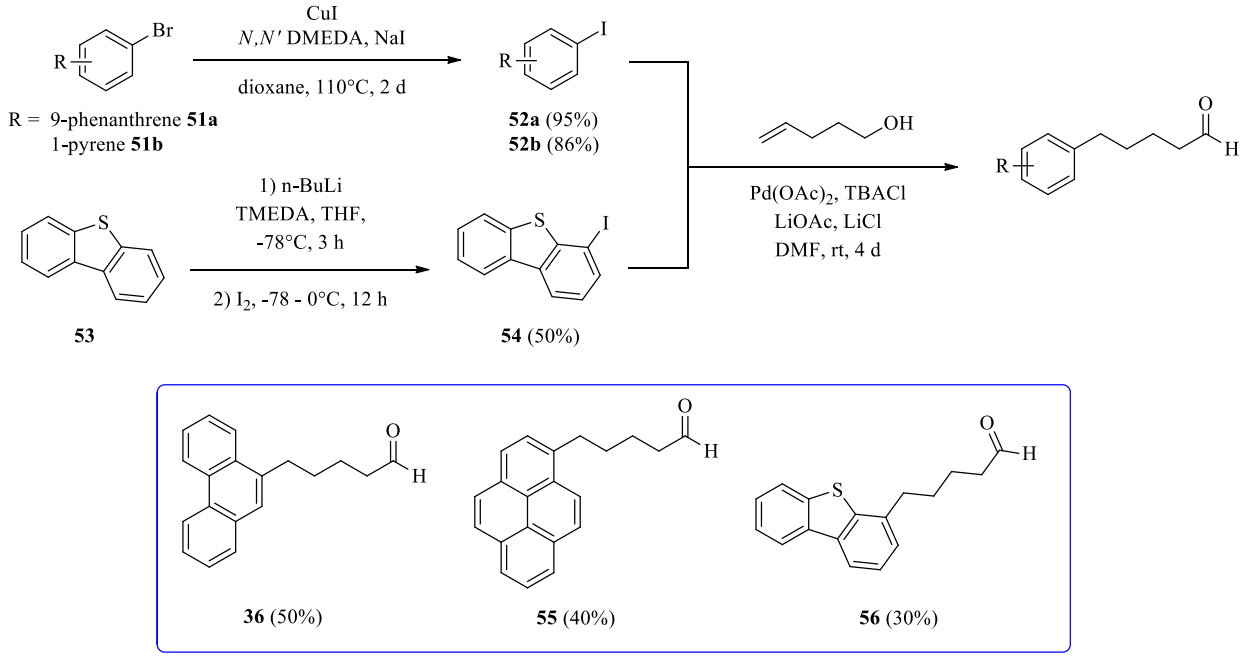

Figure 2.2 Aldehyde synthesis, from a brominated polycyclic aromatic and dibenzothiophene.

formed in reasonable yield.[32] The iodoarene is subsequently subjected to a palladium-catalyzed migratory Heck reaction with a commercial ω-alkenylalcohol (Figure 2.2).[25,33] After initial metalation and insertion, palladium catalyzes a migratory 'chain-walk' mechanism via successive β-elimination and reinsertion reactions to give the aldehyde. In this way a variety of tethered 'designer' aldehydes were prepared for use in quinoline synthesis.

2.2.2 Initial MCR screening

Throughout the screening processes, single reactions were run without reproduction. Subsequent reactions need to be performed for publication. With the appropriate aldehydes in hand, we turned our attention to probing the MCR using triarylamine radical cation catalysts. Using Wang's conditions, the initial yield of quinoline at ambient temperature was disappointing (40%), much lower than Wang reported (79%) using simple *n*-alkyl aldehydes. The yield increases

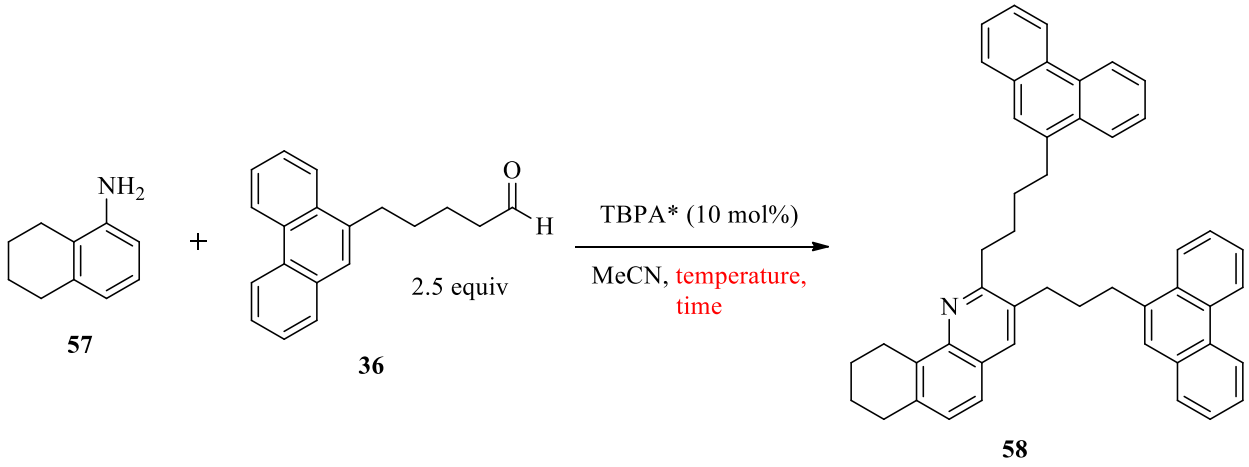

57 **36** **58**

Table 2.1 Temperature and time trials for the quinoline synthesis.

Entry	Temperature	Time (hrs)	Yield[a] (%)
1	rt	4	40
2	90 °C	4	40
3	rt	18	40
4	90 °C	18	60

[a] ^{1}H NMR conversion using HMDSO as an internal standard

to 60% upon heating to 90 °C for 18 h. Although amine radical cations are known to be photoactive, this MCR appear to be unaffected by visible light (Table 2.1).

Gratifyingly, the concentration of the aldehyde can be decreased from 2.5 to 2.0 equivalents without a noticeable decrease in yield (Equation 2.2). Under previously reported conditions (aq. HI/O_2), excess aldehyde is required to compensate 90 °C for oxidative decomposition, which occurs during slowly during the reaction via autoxidation of the aldehyde

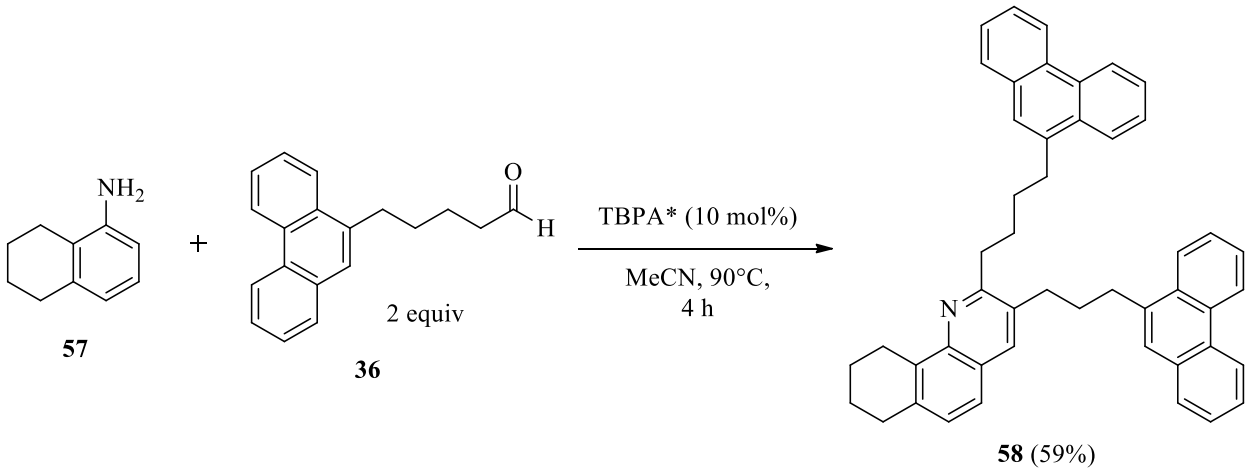

Equation 2.2 Loading of the aldehyde reduced to 2 equivalents.

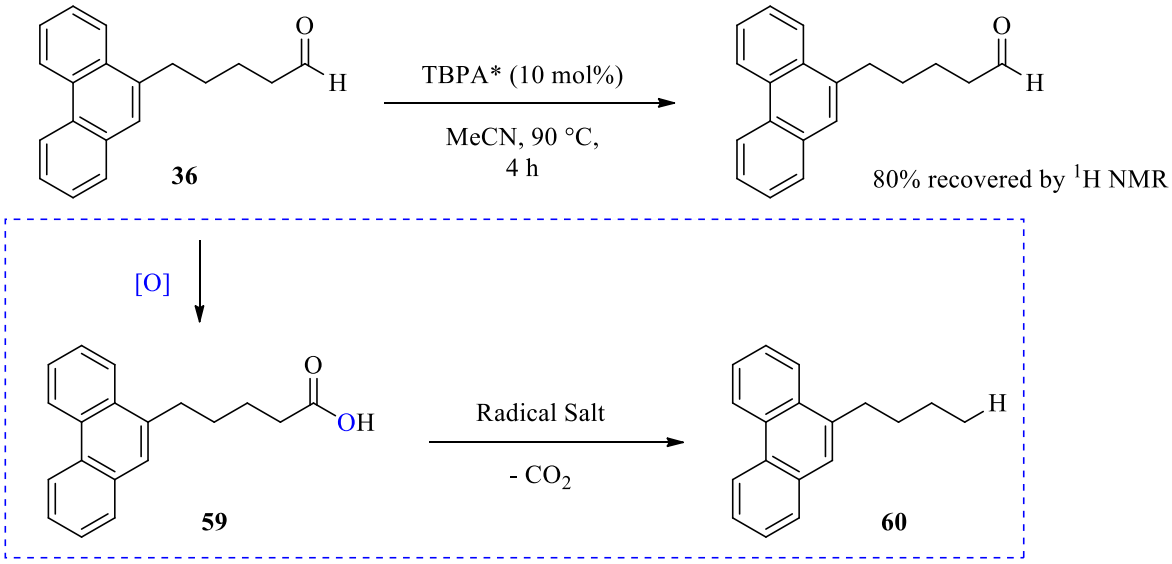

Figure 2.3 Aldehyde recovery and potential loss of material through an oxidative route. Non of the by-product was observed in the reaction mixture.

to the carboxylic acid, followed by a Barton-like radical decarboxylation.[34] This improvement in efficiency suggests that TBPA* is a more selective catalyst, enabling cyclocondensation and aromatization to the quinoline without significant decomposition of the aldehyde. Notably, a control reaction run in the absence aniline reveals that up to 20% of the starting aldehyde is consumed (Figure 2.3). Because of this, we persisted in using a slight excess of aldehyde for most of the subsequent reactions.

The effect of oxygen on the TBPA*-driven synthesis was assessed by using a medium-walled resealable glass reactor containing all reagents, charging the atmosphere with nitrogen, air, or oxygen prior to heating. The quinoline was formed in moderate yields in all cases, but the reaction run under static air proved most efficient. It should be noted that a larger reaction vessel was used for the reaction under air; the greater efficiency may have resulted from more effective mass transfer of oxygen from the headspace into solution (Table 2.2, entry 3). It is particularly illuminating that the reaction proceeds under anaerobic conditions, indicating that oxygen is

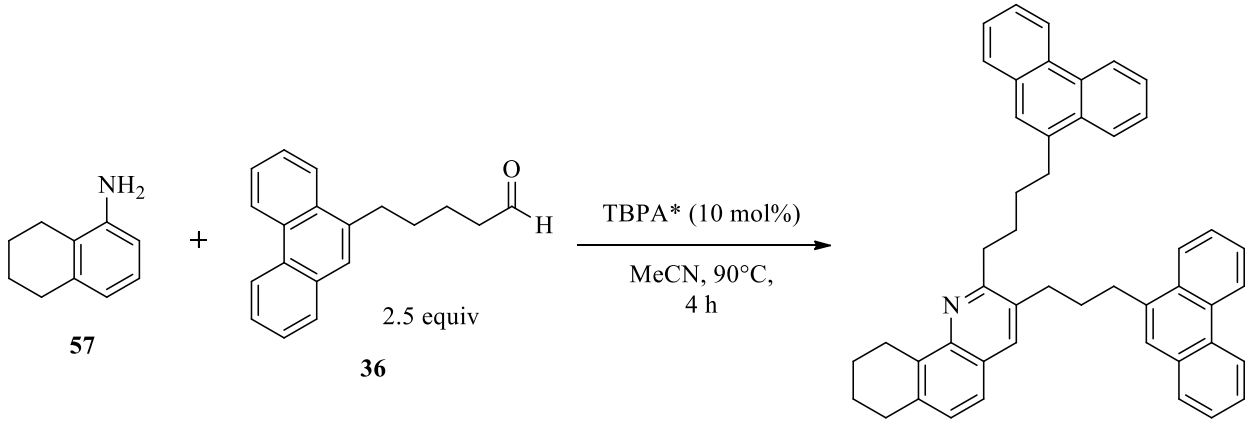

57 **36** **58**

Table 2.2 Effect of the oxygen in the overall reaction.

Entry	Atmosphere	Yield[a] (%)
1	O_2	75
2	N_2	70
3[b]	Air	80

[a] ^{1}H NMR conversion using HMDSO as an internal standard. [b] Reaction ran in a larger reaction flask

unnecessary to carry the radical chain processes involved here. This discovery is pivotal; heating a flammable organic solvent under oxygen sparge is the most glaring safety concern of our previous work and what prompted this new avenue of research.

The aldehydes required for the MCR are only partially soluble in acetonitrile; therefore, a range of solvents was evaluated to boost the conversion and yields (Table 2.3). Benzene and anisole, both of which have been used successfully in HI-catalyzed quinoline synthesis, are inferior to THF and DME in the TBPA-catalyzed reaction. Dimethoxyethane, however, proved to be a particularly effective solvent (81% ^{1}H NMR yield to quinoline at 90 °C). Even reactions conducted at ambient temperature under air still produce at least 60% yield of the quinoline.

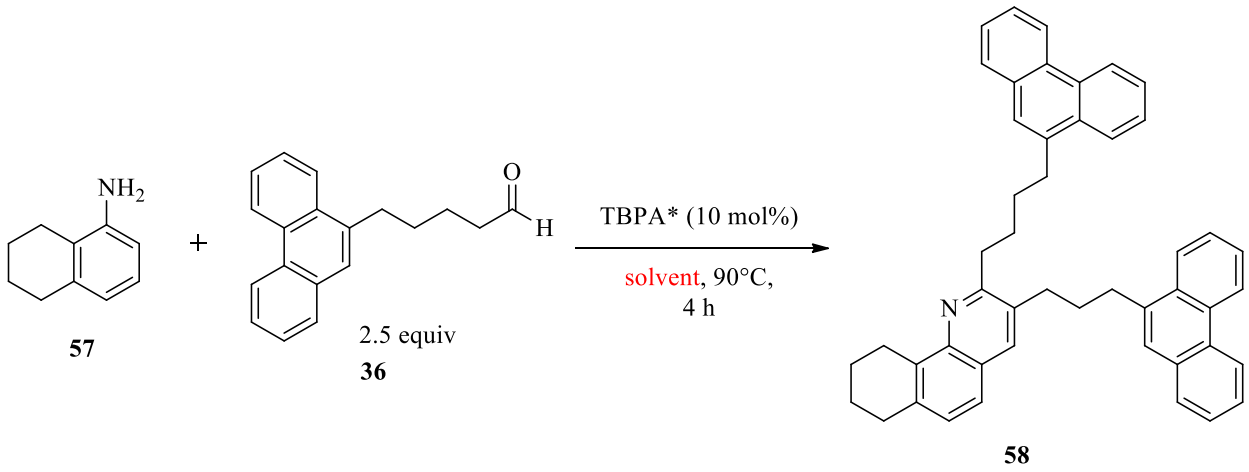

Table 2.3 Solvent screening for the quinoline synthesis

Entry	Solvent	Yield[a] (%)
1	Benzene	67
2	Anisole	55
3	THF	70
4	DME	81
5[b]	DME	60

[a] ^{1}H NMR conversion using HMDSO as an internal standard. [b]Reaction performed at room temperature.

The concentration and molecular structure of the radical cation catalyst were also obvious parameters to optimize. First, the effect of the concentration was evaluated using commercially

available TBPA*. As shown in Table 2.4 a low loading of TBPA* is ideal for achieving high yields. At just 2 mol% TBPA*, the ^{1}H NMR yield of quinoline is 80%, while a ten-fold increase in catalyst concentration causes a 25% drop in yield. It is likely that the high concentration of radicals in solution leads to unproductive couplings among catalysts and/or propagating intermediates. Indeed, dimerization of triaryl amines radical cations under oxidizing conditions is well-known, and high concentrations of TBPA* in our system is expected to promote unproductive chain termination. To assess this, a typical reaction mixture was charged with fresh TBPA* after two hours (Table 2.4, entry 4). The yield of quinoline in this case was quantitative, clearly implicating catalyst deactivation as the key limitation to achieving high yields. Curiously, slow-

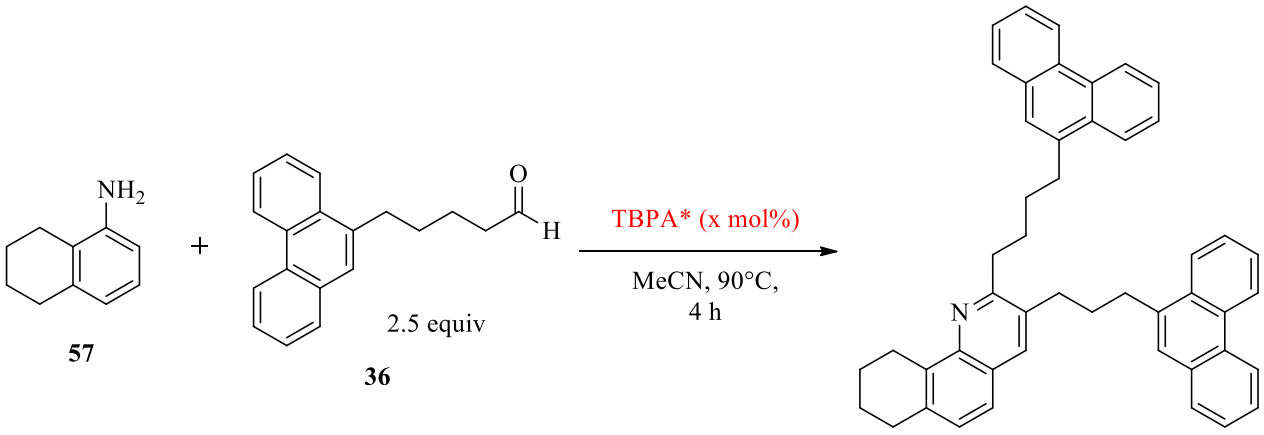

57 **36** **58**

Table 2.4 TBPA loading variations for the quinoline synthesis.

Entry	TBPA* (mol%)	Yield[a] (%)
1	10	80
2	20	61
3	2	80
4	10/2 hr[b]	Quant
5	1/10 min[c]	64

[a] ^{1}H NMR conversion using HMDSO as an internal standard.
[b] 10 mol% of TBPA* added at the onset of the reaction. After 2 hours, another 10 mol% of TBPA* was added
[c] 1 mol% of TBPA* was added at 10 minute intervals over the course of the reaction.

metering of TBPA* into the reaction by syringe pump does not improve the yield (Table 2.4, entry 5). Notably, the loading of catalyst in this trial was lower than used before and may have negatively affected conversion. It is also possible that a constant supply of the amine radical cation might lead to uncontrolled dimerization of the catalyst (Figure 2.4).[35,36]

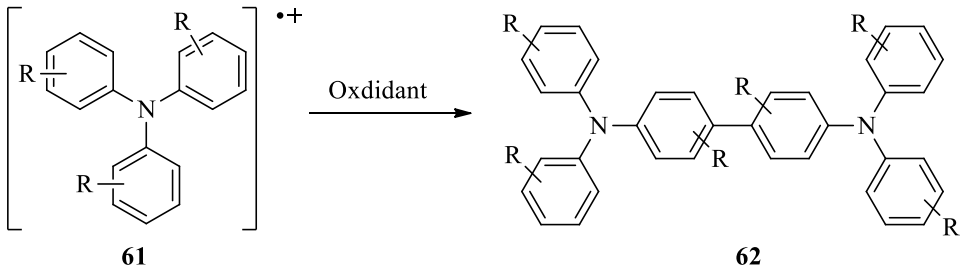

Figure 2.4 Known dimerization of triaryl amine radical cation within the presence of an oxidant to generate the radical cation.

The influence of the structure of the triarylamine radical cation was then investigated. The substituents on the aryl groups of triarylamines have a significant influence on catalyst longevity, redox potential, and rate of electron transfer. For these reasons, four triarylamines with electronically distinct para-substituents were selected for comparison to TBPA*. So do so, the amine radical cations needed to be synthesized.

2.2.3 Synthesis of radical cation triarylamine salts.

The Buchwald-Hartwig amination is one of the most common and efficient methods for the preparation of tertiary amines. Typically, a bromoarene derivative is aminated using a secondary amine and metal catalyst under basic conditions. Homo-triarylamines can also be prepared by a one-pot iterative arylation of ammonia. The reactions are typically catalyzed by palladium complexes bearing an exotic phosphine ligand, which is used to control regioselectivity and stereoselectivity. More recently, less-expensive first-row transitional metals such as nickel

and copper in an appropriate ligand environment have emerged as highly competent N-arylation catalysts.[37]

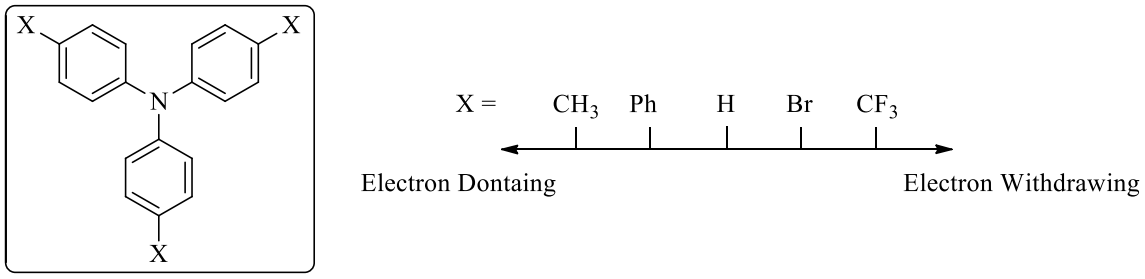

Figure 2.5 Target substitutions for triaryl amine synthesis. With the commercially available bromo derivative for comparison.

The first attempt to prepare the target triarylamines was a ligand-free copper-catalyzed triarylation of lithium amide using *para*-iodotoluene. This one-pot procedure was adapted from a

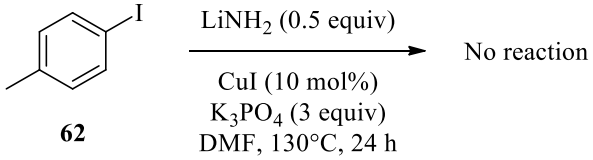

Equation 2.3 Preliminary reaction conditions for triaryl amine synthesis

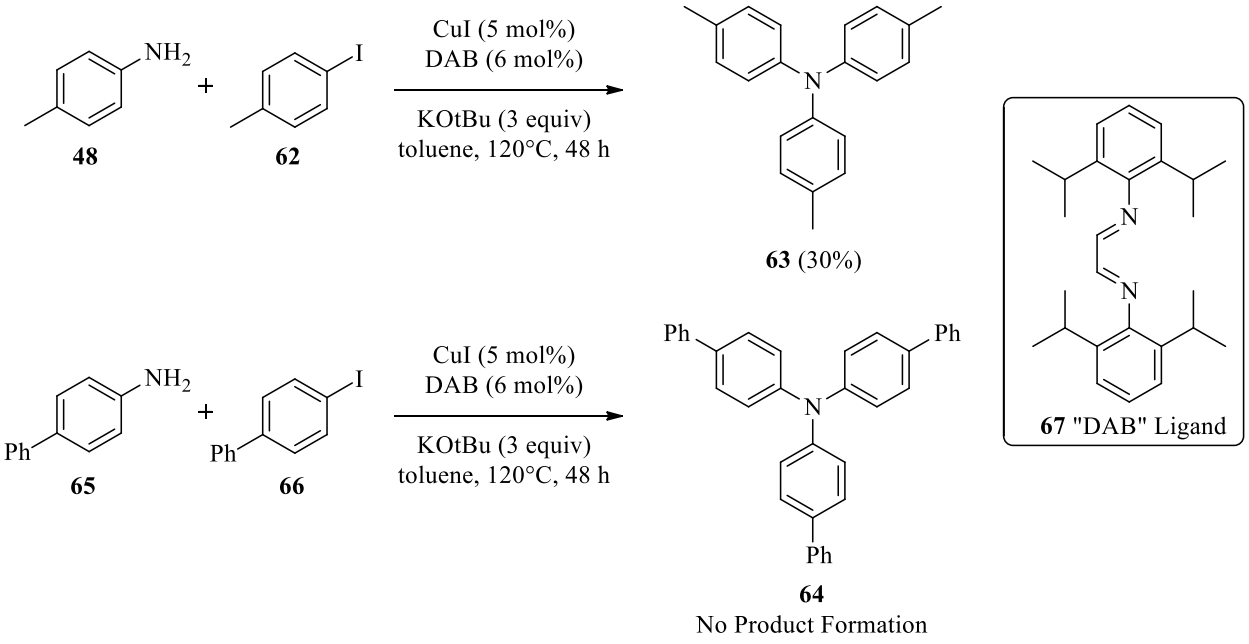

Figure 2.6 Copper/Ligand catalyzed synthesis of triaryl amines.

report by Tlili and co-workers.[38] Unfortunately, in our hands, no conversion to the triarylamine was observed, even when using freshly prepared copper iodide (Equation 2.3). Switching to a copper(I) diazabutadiene complex as the catalyst, the reaction of *p*-toluidine and *p*-iodotoluene as reagents was modestly successful, giving a 30% yield of tri-*p*-tolylamine. The inexpensive diazabutadiene ligand used in this reaction was prepared by condensation of glycol and 2,6-disiopropyl aniline.[39] Unfortunately, this method is not general: no triarylamine was detected from the combination of *p*-phenylaniline and *p*-phenyl(iodo)benzene (Figure 2.6). More efficient palladium catalysts were then considered.

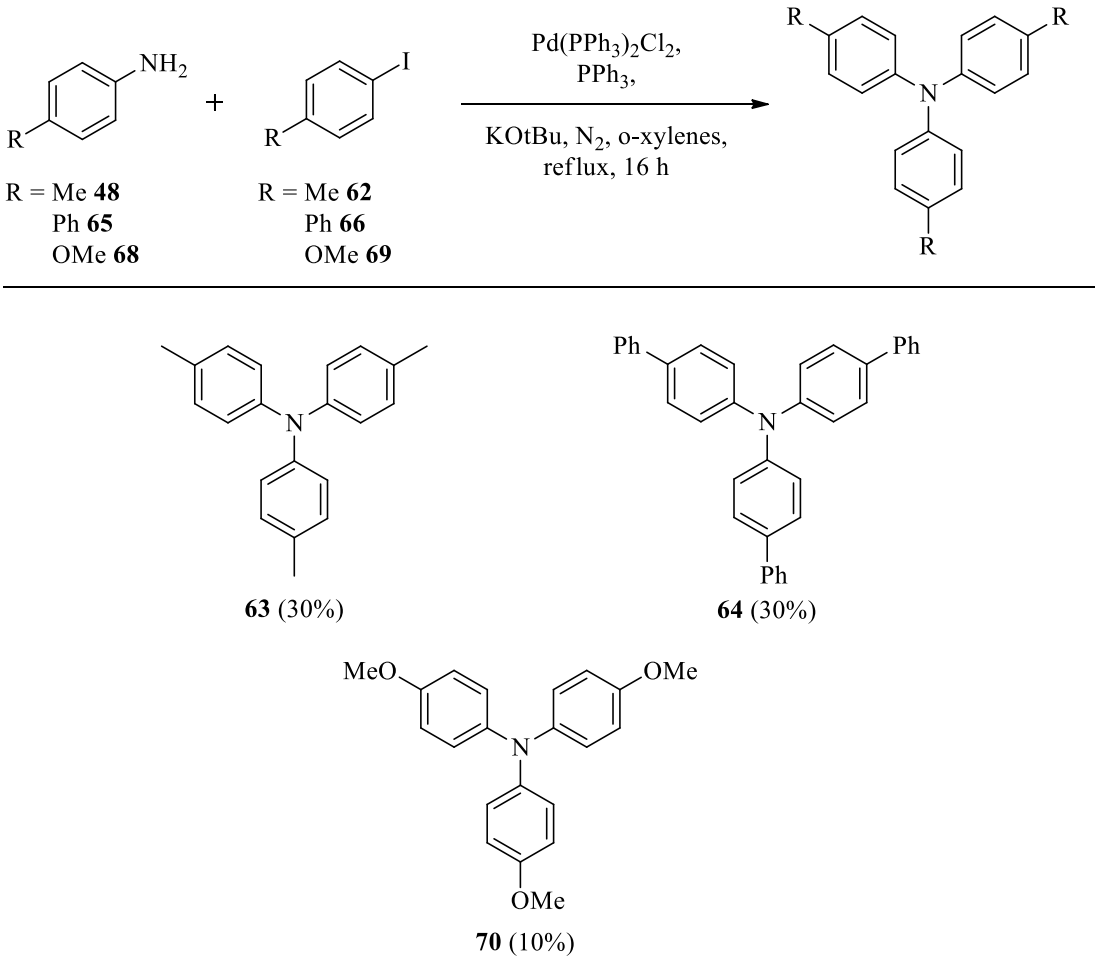

Figure 2.7 Palladium catalyzed synthesis of targeted triaryl amines.

For this particular reaction, commercially available bis(triphenylphosphine)palladium dichloride was used as catalyst.[40] Importantly, this method allows one-pot diarylation of a primary amine, allowing ready access to these amines (Figure 2.7).[40] Tri(4-methylphenyl)amine and

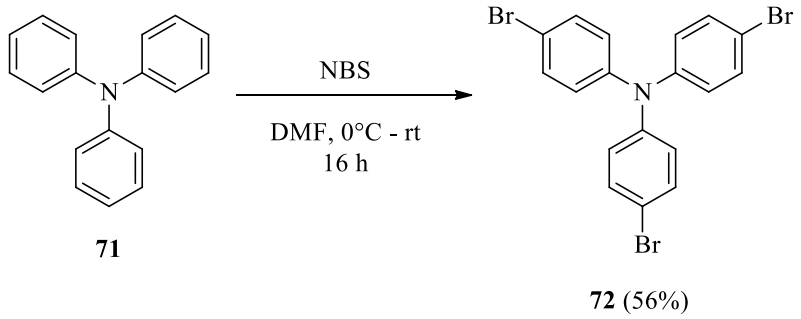

Equation 2.4 Bromination of triphenyl amine.

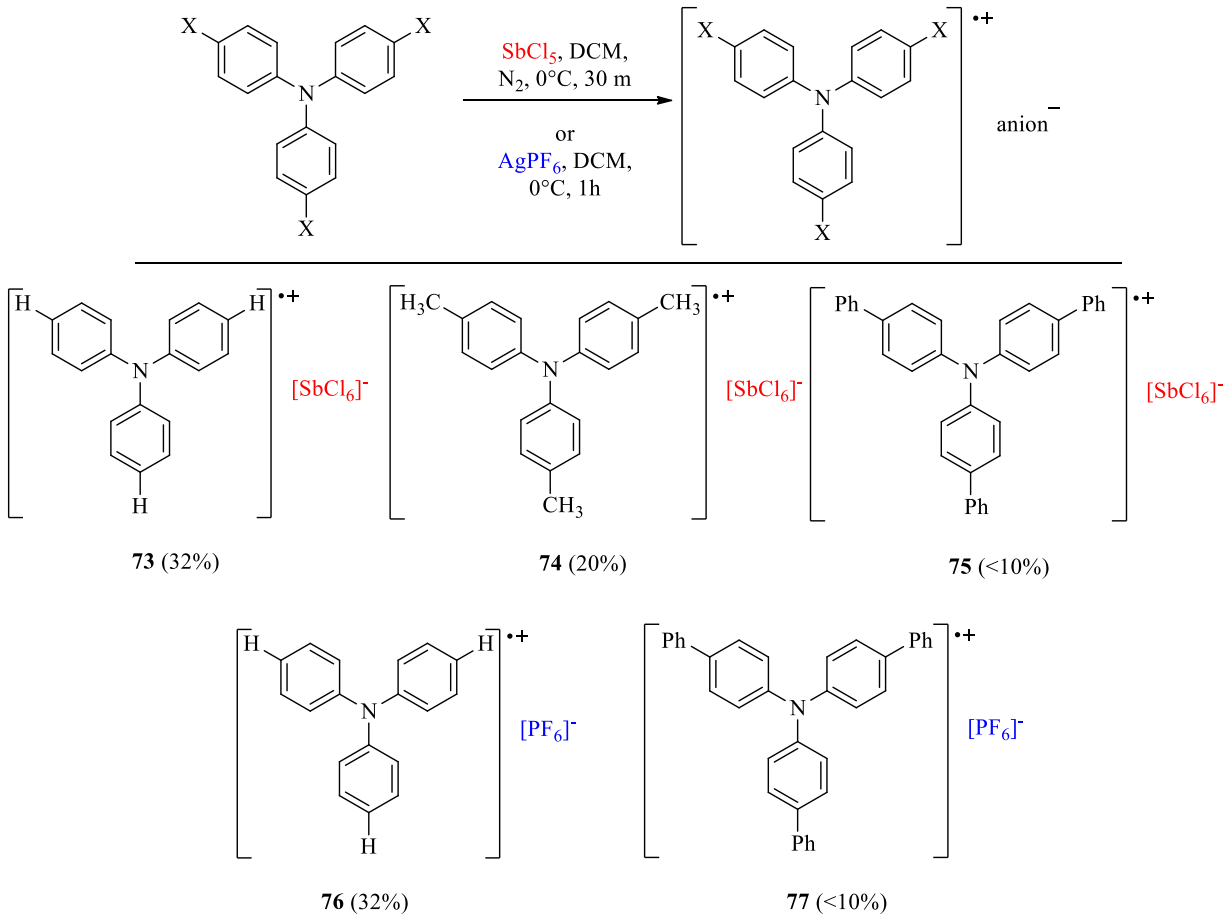

Figure 2.8 Single electron oxidation of triarylamines using antimony pentachloride or silver hexafluorophosphate.

tri(biphenyl)amine were each isolated in 30% yield, but only 10% of tri-p-methoxyphenyl amine was obtained. The inductive effect of the strong electron donor presumably improves the oxidative addition step in this reaction but could inhibit the reductive elimination.

Para-halogenated triarylamines can be obtained by nucleophilic aromatic substitution. Commercial triphenylamine is brominated three times using *N*-bromosuccinimide (Equation 2.4).[41] Radical cation derivatives were then prepared by oxidation using either antimony pentachloride or silver hexafluorophosphate (Figure 2.8).[42–44] The hexachloroantimonate counterion is present in the commercially available TBPA*, but hexafluorophosphate analogues were prepared to determine the effects of counterion on the performance of the radical cation catalysts.

2.2.4 Comparative scope: radical cation versus acid-catalyzed methodology

The triarylamine radical cations were tested as catalysts for the multicomponent cyclocondensation of 5,6,7,8-Tetrahydro-1-naphthylamine and 5-(phenanthren-9-yl)pentanal. Gratifyingly, in this case, all of the oxidants are excellent promoters for quinoline formation. The best results were obtained using the simplest possible radical cation, $Ph_3N^+SbCl_6^-$ (Figure 2.9). Varying counter ions does not seem to have a great effect on product formation.

A comparison of oxidation potentials give better insight into the radical initiation (Figure 2.10).[40,45] The highest oxidation potential catalyst provided the best yield. The rate of the oxidation determines whether dimerization is competitive; ultimately dictating the turnover number. The triarylamine with the highest oxidation potential oxidizes the reactant before the concentration is high enough to dimerize competitively. Alternatively, at lower oxidation potential, nucleophilic attack of the neutral amine on the starting radical catian can intervene, restricting catalyst lifetime.

Dimerization occurs via the most accessible site on the triphenyl amine, if the para-position is unsubstituted. Radical dimerization terminates radical chain propagation. Neutral dimers are derived from two subsequent 1e-oxidations, with a net loss of hydrogen (Fig. 2.11).[35]

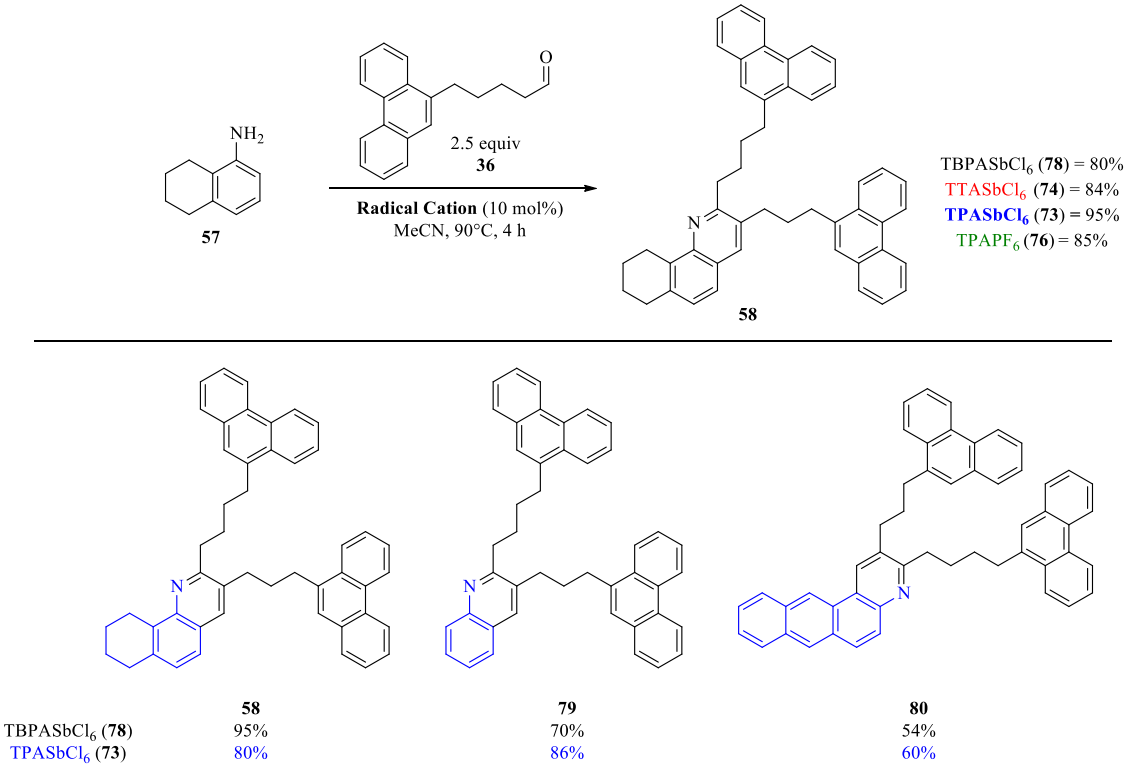

Figure 2.9 Top: Comparison of the radical cation salts on the conversion of product. Bottom: Comparison of the conversion of product based on the specific radical cation salt

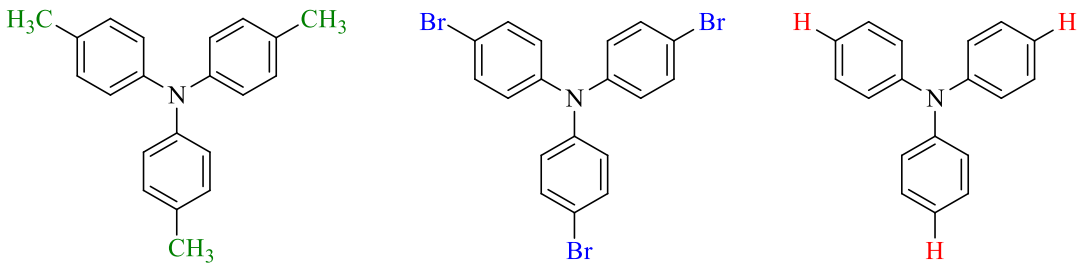

Figure 2.10 Comparison of the range of oxidation potentials based on the triaryl amine substitution.

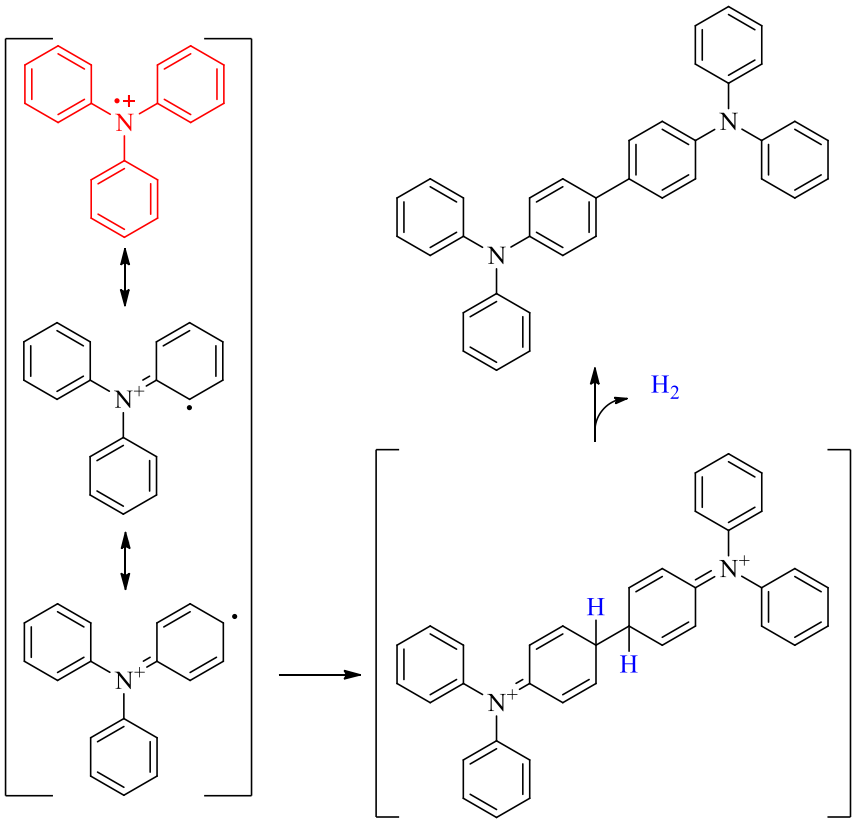

Figure 2.11 A possible dimerization pathway of triphenyl amine. The species in red would be the radical cation salt added at the onset of the reaction.

With optimal conditions in hand, the scope of the radical cation catalyzed MCR was explored. For each substrate, the best results were compared to the best yields obtained using the HI/O_2 method. Moderate to excellent yields of the desired quinolines are obtained using radical cation catalysis. For all substrates, the odd-electron reaction is superior – sometimes vastly so (Figure 2.12). Substitution on the starting amine affects the yield: electron-donating groups, e.g., 4-ethylaniline (Figure 2.16; **81**, 92%) and dimethylamine (**85**, 85%), return substantially higher yields than do electron-withdrawing groups, such as halogen (**84**, 62%) and trifluoromethyl (**83**, 41%). Electron-donating groups may stabilize radical character on the imine nitrogen in a downstream intermediate (Figure 2.16). However, an electron withdrawing group would destabilize the radical, which is preferentially reduced to the neutral imine. Interestingly, the

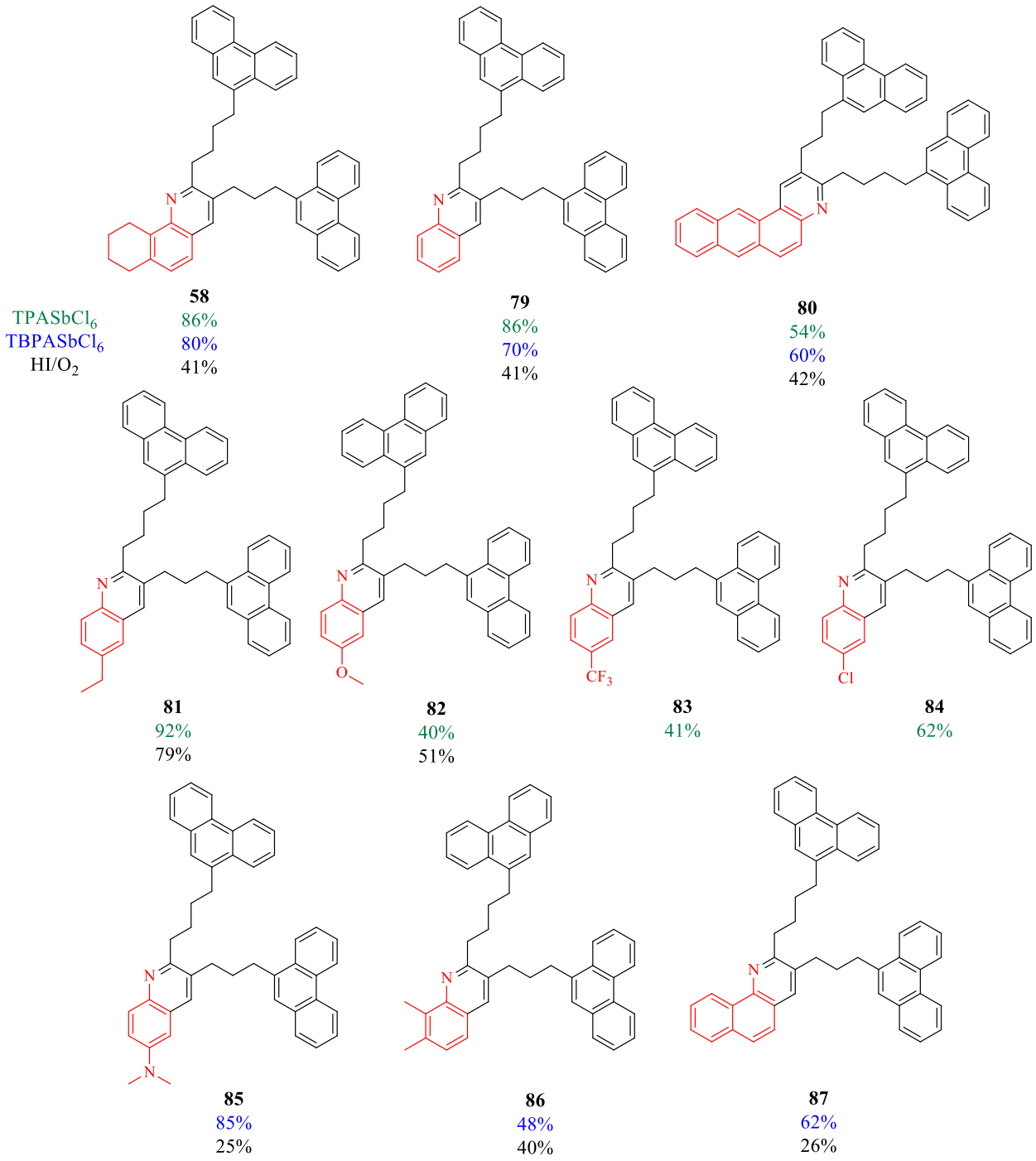

Figure 2.12 Comparative scope of using radical cation salts. Yields were determined by ^{1}H NMR spectroscopy against an internal standard. Yields in green (TPA) and blue (TBPA) were obtained from radical cation catalysis; values in black are by aerobic HI catalysis.

methoxy derivative (**82**, 40%) yielded much lower than other electron donating groups possibly due to greater stabilization of the radical cation. Further variation in electronic effects of the

substituent continues by other hands. The use of the radical cation salt for the tetrahydronaphthylamine (**58**, 80%) and 2,3-dimethylaniline (**86**, 48%) quinolines had notable difference in yields. Even though the substitution on the aniline ring in both cases was similar, the dimethyl has a pronounced effect on the reactivity. Considering the reaction mechanism (Scheme **2.1**) the driving force to de-aromatize the ring for the cyclization would be high, however the ring-strain of the fused cyclohexene could be a contributing factor for the higher yield compared to the dimethyl. Beyond a methyl substitution, further exploration of scope will include other 2-substituted and 2,3-disubstituted anilines.

Notably, the aromatic ring system of the aniline influences the overall selectivity. 2-Aminoanthracene (**80**, 60%), 1-aminonaphthalene (**87**, 62%), and aniline (**79**, 70%) all give comparable yields. Taken together, these results provided an incentive to pursue bidirectional multicomponent reactions using 1,8-diaminonaphthalene, which failed under acid catalysis. To

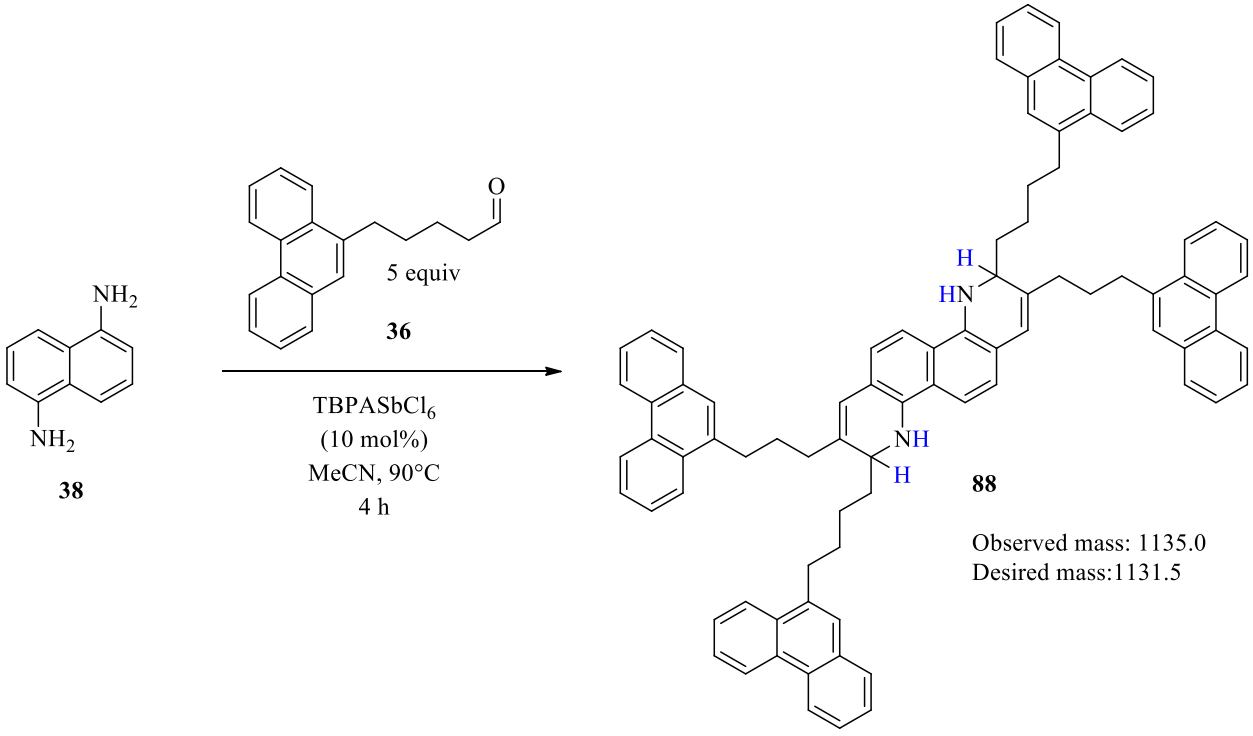

Equation 2.5 Bidirectional MCR yielding a tetrahydrobisquinoline

our delight, radical cation catalysis provides the five-island archipelago compound **88**, but with a tetrahydrodiazachrysene core that does not undergo spontaneous aromatization under these conditions (Equation 2.5). This possible isomer of the target compound was isolated in an indeterminate yield and is only partially characterized through high-resolution mass spectrometry. ^{1}H NMR data was inconclusive for determining the exact isomer isolated. Oxidation to the aromatic diazachrysene clearly requires a stronger oxidant. Optimization of this reaction, complete characterization, and the oxidation to diazachrysene remain under investigation.

2.2.5 Proposed mechanistic pathway

A rational mechanism for the radical-catalyzed quinoline synthesis is proposed, with due consideration of the synthetic results. The mechanism, shown in Scheme 2.1, builds upon the one proposed by Wang.[29] Initial formation of imine **I** and equilibration to enamine **II** is followed by oxidation to iminium radical-cation **III**, stabilized by the conjugated π-system. Enamine **II** then undergoes electrophilic radical cyclization to intermediate **IV**. Either the initiator or the cyclized radical cation can then act as chain propagator. The imine radical cation **III** is regenerated during this propagation. The now-neutral tetrahydroquinoline **V**, as the aromatic tautomer of the enamine, loses the extra aniline, either through acid-catalyzed EI elimination or *syn*-elimination, resulting in dihydroquinoline **VI**. The mechanism of the oxidation to quinoline **VII** remains unclear; it may be a consequence of the aqueous work-up under air.

The proposed elimination of the second aniline (Scheme 2.1, **V→VI**) also requires a deeper understanding. The crude product after workup contains some starting aniline by ^{1}H NMR analysis, as expected. The elimination could proceed via the attack of tetrahydroquinoline **V** on the aldehyde, yielding cation **VIII** in equilibrium with the neutral tertiary amine **VIII'**. However,

ionic intermediate **VIII** could proceed to cyclize through a six-membered ring transition state comparable to a Cope elimination, yielding dihydroquinoline **VI** and secondary amine **IX**. Condensation of this amine with additional aldehyde produces imine **I**, restarting the radical chain (Scheme 2.2) .

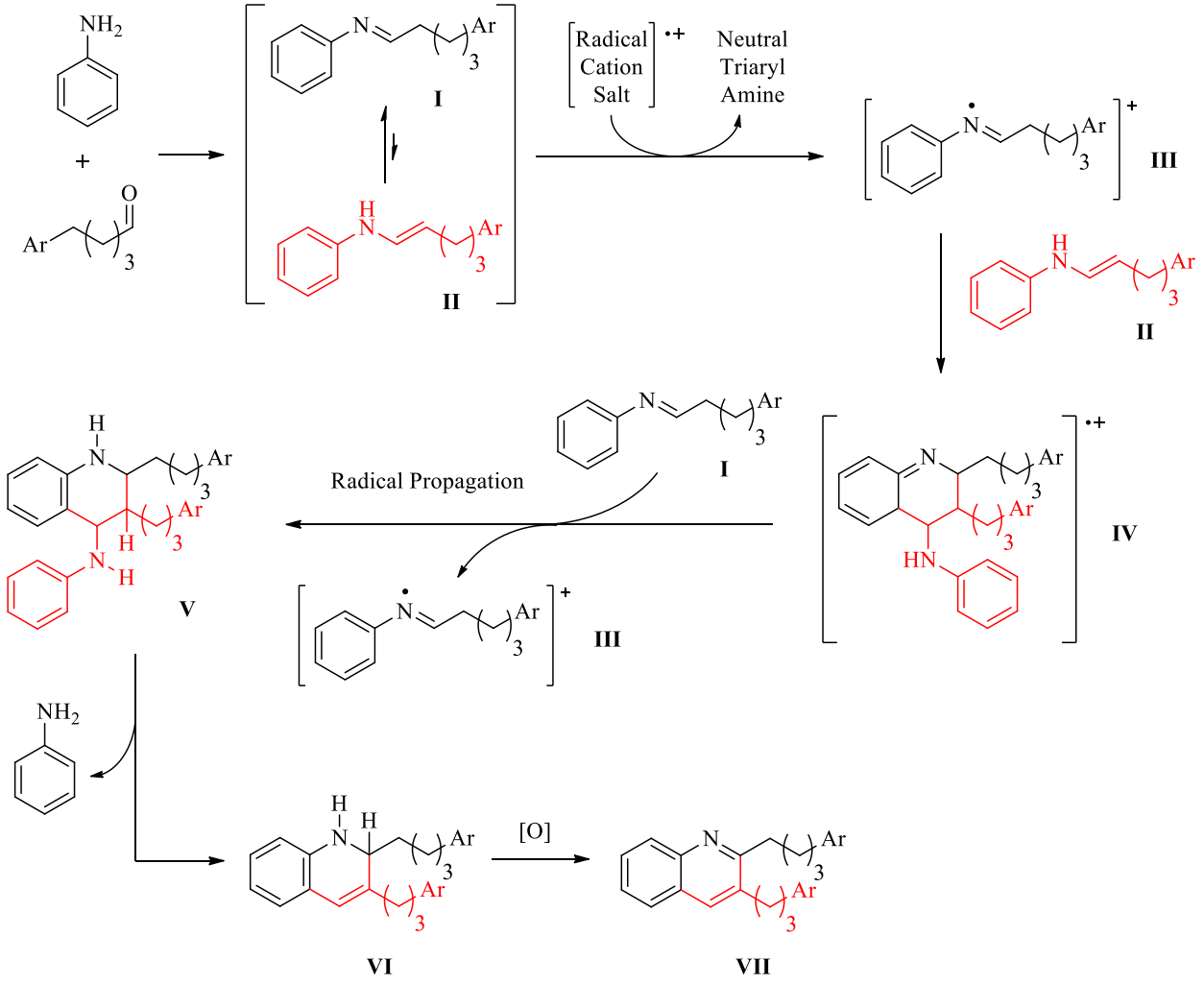

Scheme 2.1 Proposed mechanism for the radical cation quinoline synthesis.

Radical cation methodology thus affords ready access to three-island archipelago compounds defined by a central quinoline core tethered to two satellite islands. The quinolines are formed more efficiently and under milder conditions than obtained by the optimized HI/O_2 procedure. Importantly, no sparging of pure oxygen is required; aerobic oxygen is sufficient to

drive the MCR to completion. A series of substituted triarylamine radical cations proved to be effective catalysts for quinoline synthesis. Further mechanistic analysis is ongoing.

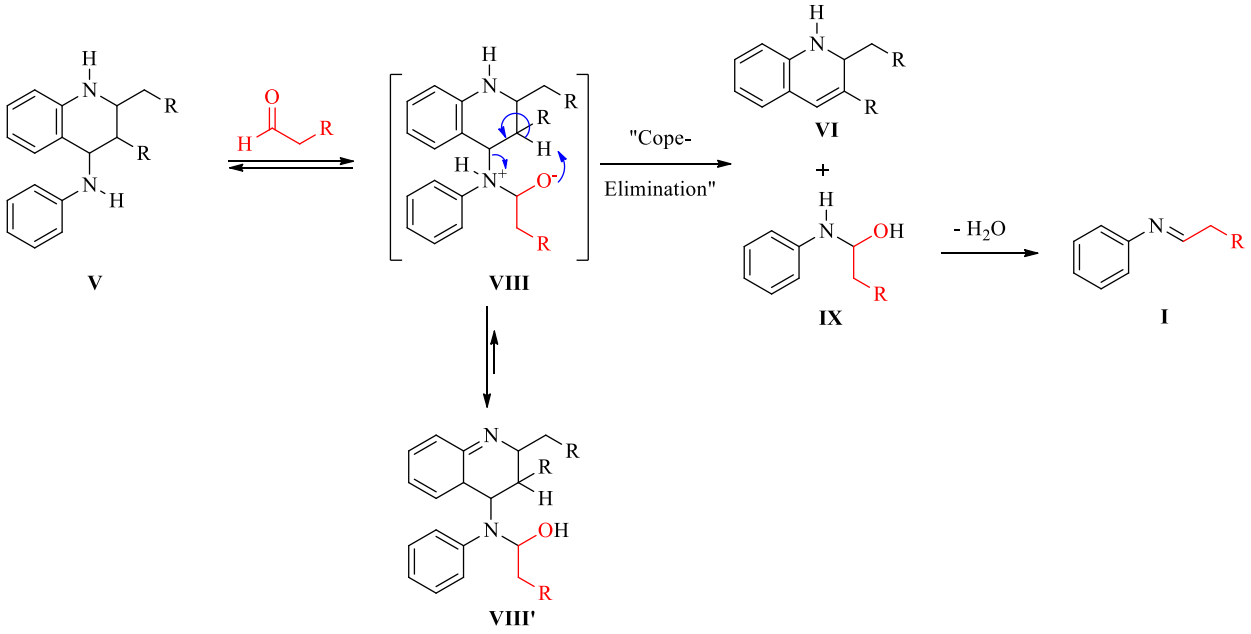

Scheme 2.2 Potential Cope-like elimination of the aniline to yield the imine.

Significant limitations remain in radical cation catalysis for multicomponent cyclocondensation. Inefficient oxidation remains an issue in bidirectional synthesis and these reactions do not proceed efficiently at ambient temperature. This led us to investigate generating radical cation catalysts electrochemically in situ, in the hope that electrocatalysis might overcome the last of the challenges to obtaining high yields on larger scale. Results from this preliminary study are presented in Chapter 3.

Chapter 3: Preliminary Exploration of the Electrocatalytic Synthesis of Quinolines

3.1 Introduction

With temperature limitations and the requirement for a more potent oxidant, the methodology for quinoline synthesis needed to evolve to address these issues. Electrochemical synthesis allows for generation of radical ion species in situ at room temperature. With the ability to control cell potential and reactor variables, electrocatalysis potentially allows for the reaction control necessary to address these limitations.

3. 1.1 Rationale for pursuing electrochemical synthesis.

Electrochemical organic synthesis is undergoing a modern revival, driven by renewed interest in green chemistry, readily available equipment, and greater understanding, the latter leading to greater control over reaction pathways and products. (Figure 3.1).[46] Organic synthesis

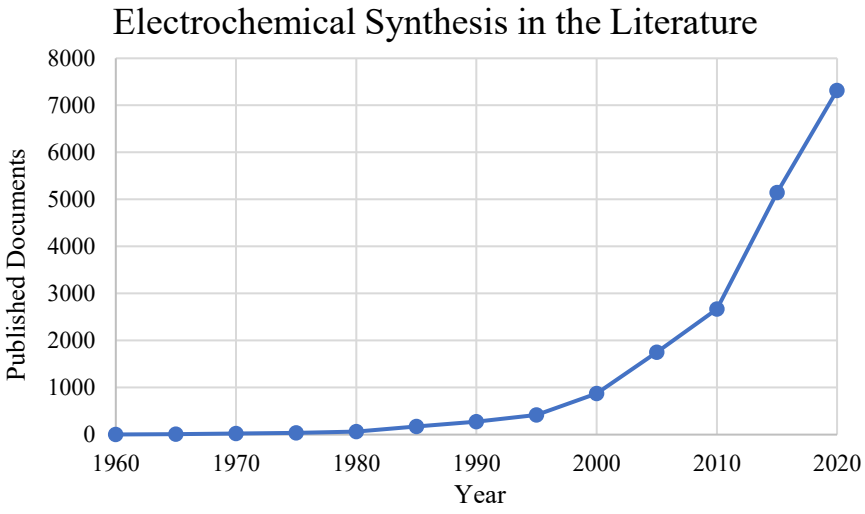

Figure 3.1 Scopus data for the trend of electrosynthesis in the scientific literature over the last 60 years. Documents included are from research articles, reviews, book chapters, etc. Obtained from Scopus April 2021.

within an electrochemical cell is attractive because reactions typically proceed under ambient conditions with reasonable control of electron transfer processes. Moreover, challenging chemical transformations that fail under traditional reaction conditions can sometimes be easily accomplished via electrochemical synthesis.[47] The ability to forgo strong chemical oxidants or reductants in the desired reaction often allows for safer, greener, and more efficient reactions, particularly on large scale.[48]

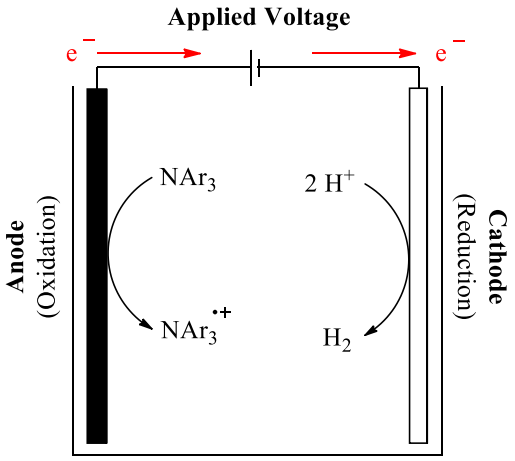

Figure 3.2 Generic electrochemical cell. With the anode, or the working electrode, performing the oxidation of the substrate, and the cathode reducing a protic source to complete the circuit of the cell.

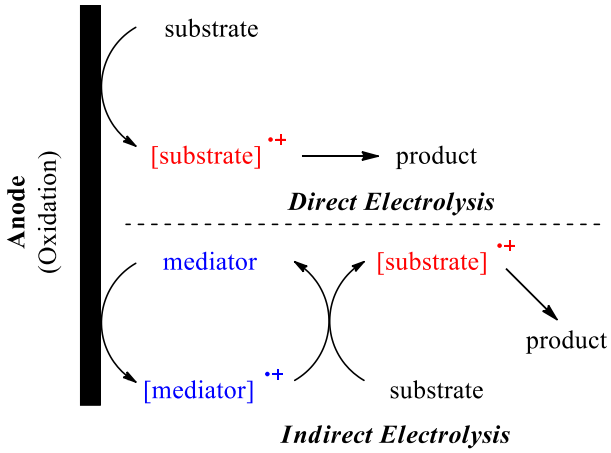

Figure 3.3 Direct versus mediated electrolysis.

A typical electrochemical cell is comprised of several components that connect two half-cells together. When a voltage is applied across the electrodes, oxidation of the reactant occurs at the anode to yield a radical cation, donating an electron to the current. This electron is transported through an external circuit to the cathode, where a one-electron reduction occurs. Both electrodes are immersed in an electrolyte sufficient to support efficient charge transfer. The simplest electrochemical cells place both electrodes suspended in the same electrolyte, with the substrate or electrocatalyst migrating to the electrode of interest based mostly upon electrostatic attractions (Figure 3.2).[49] For greater control, typically of reactions sensitive to both oxidative and reductive processes, a divided cell can be used. In this case, each electrode is contained within a separate compartment, separated by a membrane that prevents substrate from migrating to the opposite electrode. This ensures that only the desired oxidative or reductive event occurs; a complementary redox reaction takes place in the other half cell.[49]

Electrochemical organic synthesis can proceed by direct or indirect electrolysis. For direct electrolysis, the substrate itself contacts the electrode, where it is oxidised or reduced. Conversely, indirect electrolysis relies on soluble redox mediators – often catalysts – that contact the electrodes, transforming into potent solution oxidants or reductants. The "activated" mediator reacts with the target substrate to furnish the desired oxidized or reduced species (Figure 3.3).[50] Common redox mediators include main group and transition metal ions: alkali metal halides, ferrocene derivatives and triarylamines.[49] Meditators are particularly useful when direct electrolysis requires a very high cell (over)potential and where careful control of single-electron redox events is crucial.

Electrochemical synthesis can be tuned for reductive or oxidative transformations. Oxidation is the key step for 'multi-island' quinoline synthesis using an MCR. As seen in Chapter 2, oxidation of the imine to the iminium radical cation is the initiating step in the

cyclocondensation/aromatization process that eventually furnishes the quinoline. As an example, radical cation intermediates are involved in Shono-type oxidation of *N*-acyl amines (Scheme 3.1, top).[51,52] In this case, single electron oxidation of the amine to an iminium radical cation leads to α-functionalization of the starting amine. Similarly, electrochemical oxidation of a substituted urea (Scheme 3.1, bottom) furnishes a nitrogen-centred radical cation, which reacts with a tethered

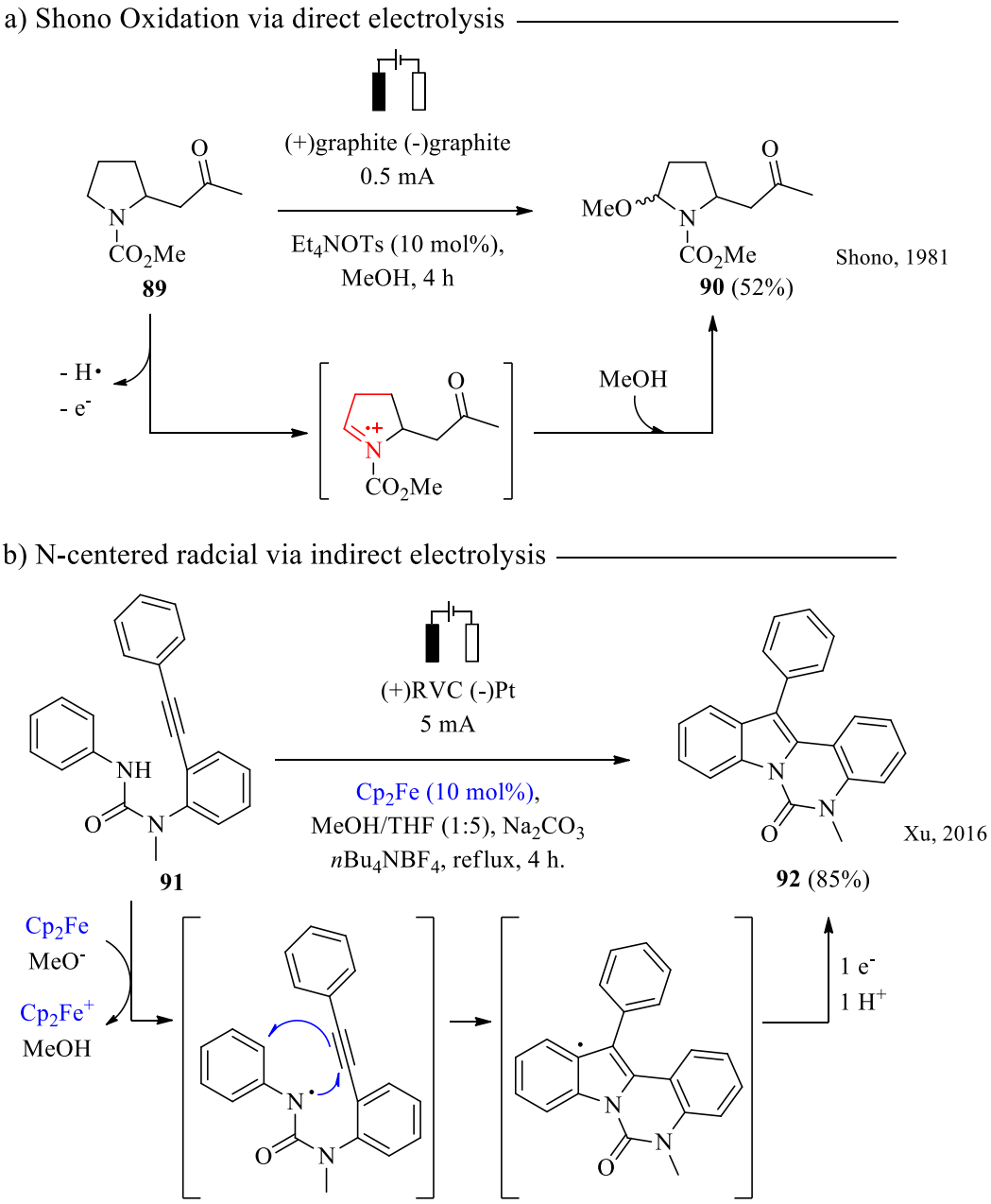

Scheme 3.1 Select *N*-centered radical generation by direct (a) and indirect (b) electrolysis.

alkyne by radical cyclization, giving the aza-indole.[53] In this oxidation, ferrocene is used as a redox mediator for indirect oxidation. These examples support the notion of N-centered radical generation in an electrochemical cell, either through direct or indirect electrolysis.

In Chapter 2, triarylamine radical catalysts were shown to promote the formation of iminium radical cations, which eventually became incorporated into quinolines. Triarylamine radical cations are easily generated under electrochemical conditions and have been used as redox mediators for indirect electrolysis.[47,54,55] In these reactions, the amine radical cation is formed at the anode and diffuses into solution, oxidizing the target substrate on contact. Triarylamine redox transfer reagents have also been used to promote oxidative carbon-sulfur bond cleavage of thioesters and carbon-carbon bond formation between arenes and enamides (Equation 3.1), among other important reactions.[56,57]

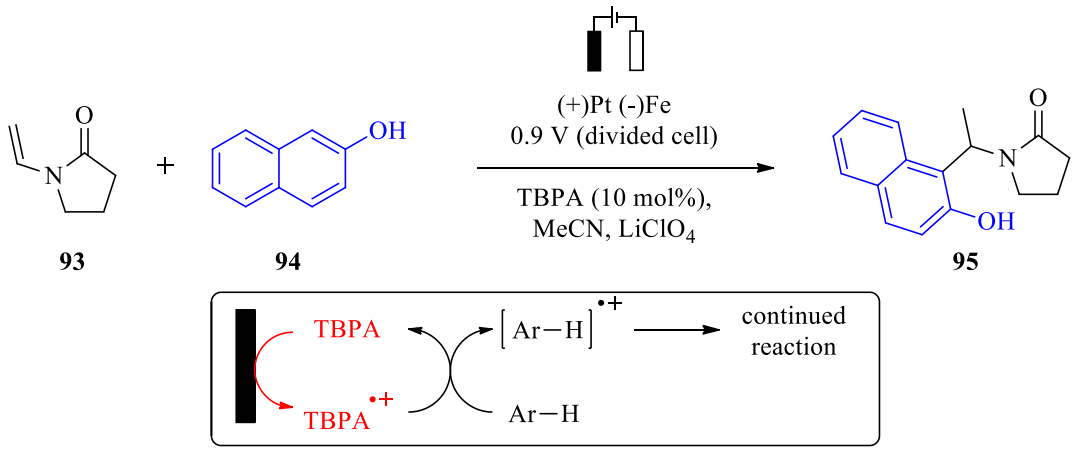

93 94 95

Equation 3.1 Synthesis using a triaryl amine mediator for the oxidation of the aryl starting material.

In the remainder of this chapter, I will discuss the configuration of our electrochemical cell and the reaction variables that affect the synthesis of quinolines. I will also discuss the role of the triarylamine and preliminary optimization of its oxidation potential.

3.2 Results and Discussion

3.2.1 Surveying electrochemical and reaction parameters

Throughout the following screening processes, single reactions were run without reproduction. Subsequent reactions need to be performed for publication.

Triarylamine radical cation catalysts were first prepared by chemical oxidation as described in Chapter 2, typically using antimony pentachloride or nitrosonium hexafluorophosphate as the oxidant. This requires a synthetic step involving expensive, difficult-to-handle reagents, and remediation of toxic wastes. Furthermore, once the anime radical cation is consumed, the neutral amine must be isolated before it can be converted back to the radical cation for reuse. Electrochemical synthesis offers many advantages, generating the radical cation in situ, and functioning as an electrocatalyst, re-oxidizing to the radical cation at the anode.

We tested the electrochemical MCR using simple commercially available reactants, aniline, and valeraldehyde, along with various triarylamine redox mediators. Starting with

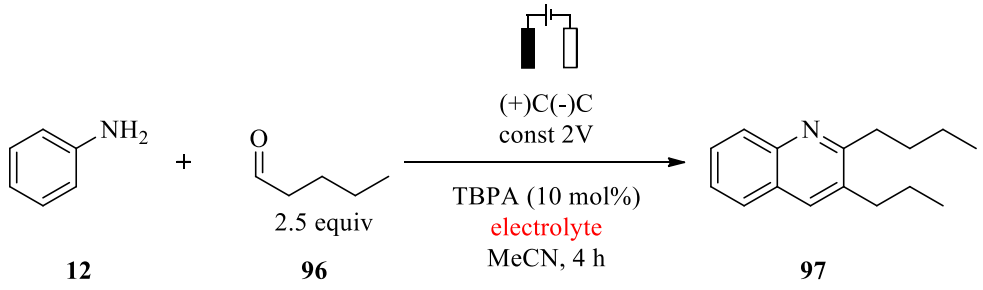

12 **96** **97**

Table 3.1 Electrolyte screening

Entry	Electrolyte	Yield[a]
1	$TBAPF_6$	8
2	LiBr	30
3	LiCl	8
4	LiI	9
5	TBACl	2
6	TBABr	3
7	TBAI	2

[a] ^1H NMR conversion using HMDSO as an internal standard.

purchased reactants allows for straightforward optimizations, without consuming copious amounts of the more valuable ω–arylaldehydes.

Supporting electrolytes were screened first, using a potential of 2V across two carbon electrodes in an undivided cell. Tetra-*n*-butyl ammonium salts are ineffective, regardless of the counterion. Similarly low conversions are observed using lithium chloride and lithium iodide as supporting electrolyte (Table 3.1). Lithium bromide, on the other hand, is much better, affording moderate yields of the quinoline. Previous reports establish that lithium bromide functions as a non-innocent electrolyte, key to efficient electrochemical synthesis of the quinoline. This effect will be addressed later in this chapter.

The yield of quinoline is also dependent on the electrodes. Chemically inert carbon electrodes for both cathode and anode provided the highest yields. A sacrificial anode comprised of strongly reducing magnesium metal performed poorly, while slightly higher yieds were obtained using less-reducing zinc and nickel anodes paired with stainless steel cathodes. Unexpectedly, a reticulated vitreous carbon (RVC) foam anode with much higher surface area was entirely

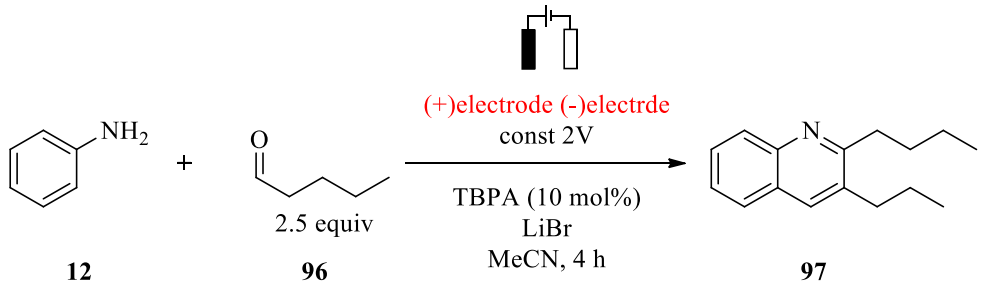

12 **96** **97**

Table 3.2 Electrode screening

Entry	Anode (+)	Cathode (-)	Yield (%)[a]
1	C (graphite)	C (graphite)	30
2	Mg	Stainless Steel	13
3	Zn	Stainless Steel	20
4	Ni	Stainless Steel	19
5	RVC	Platinum	5

[a] ^{1}H NMR conversion using HMDSO as an internal standard.

ineffective. High surface area RVC electrodes suffer from reduced current density, which has a greater impact on charge transfer than the increased surface area, resulting in lower conversion.[58,59]

The choice of voltage and current density is critical for controlling the rate and outcome of most electrochemical reactions. The voltage applied in an electrochemical cell is equivalent to the energy supplied in a thermally-driven chemical reaction. The rate of the reaction is defined by the current supplied. Running the reaction under constant current conditions ensures that the rate of reaction does not slow as the reaction progresses, except such as is caused by decreasing concentration of the reactants. Unfortunately, chemoselectivity typically suffers at high current density, often due to unwanted side reactions involving substrates, intermediates, or products. In contrast, constant voltage electrolysis allows better control over chemoselectivity, because the energy supplied never rises above the threshold voltage needed to accomplish the desired transformation. Unfortunately, as the reaction progresses and the current falls alongside the concentration of reactants, the rate of reaction slows considerably.

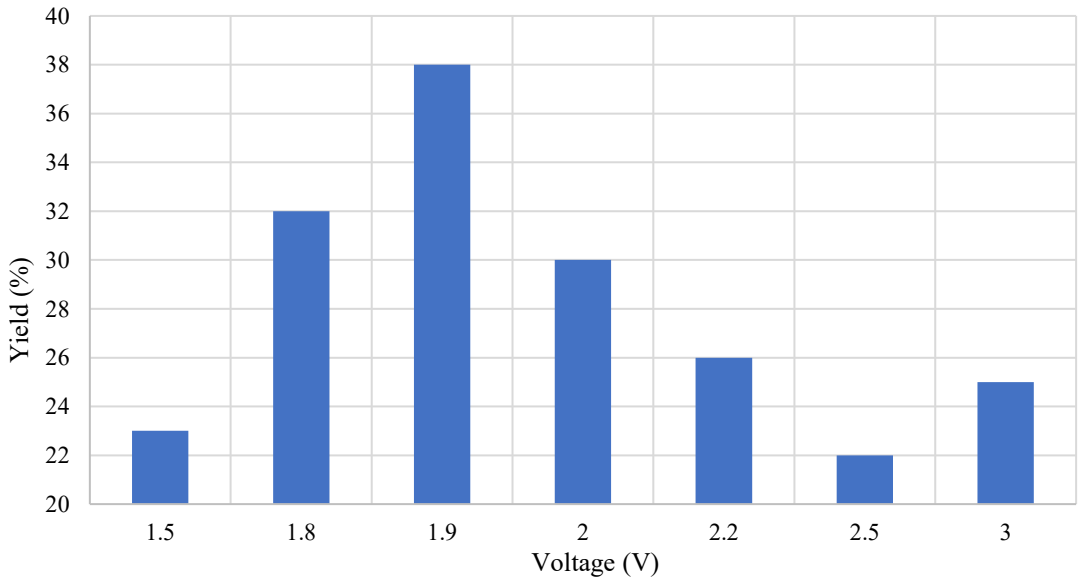

Figure 3.4 Applied cell voltage effect on 2-butyl-3-propylquinoline yield. ^{1}H NMR yield calculated with internal standard of HMDSO

The best yield of the 2-butyl-3-propylquinoline was obtained by running the electrochemical MCR at a constant potential of 1.9 volts (Figure 3.4). The quinoline is formed using potentials as low as 1.3 V, but the current and product yield were low. Conversely, increasing in voltage beyond the optimal value leads to deleterious side reactions, resulting in lower yields of the quinoline.

3.2.2 Optimizing the redox potential of the triarylamine

We also assessed effect of triarylamine substituents on the efficiency of the electrochemical MCR. Electron donating and withdrawing substituents on the aromatic rings alter the redox potential, determining relative suitability for mediating a specific electrochemical reaction. Table 3.3 shows the redox potential for each triarylamine mediator, along with the yields obtained under benchmark reaction conditions. Interestingly, no significant change in yields was observed among triarylamines, even though the measured redox potentials varied between 0.42 V and 0.74 V.

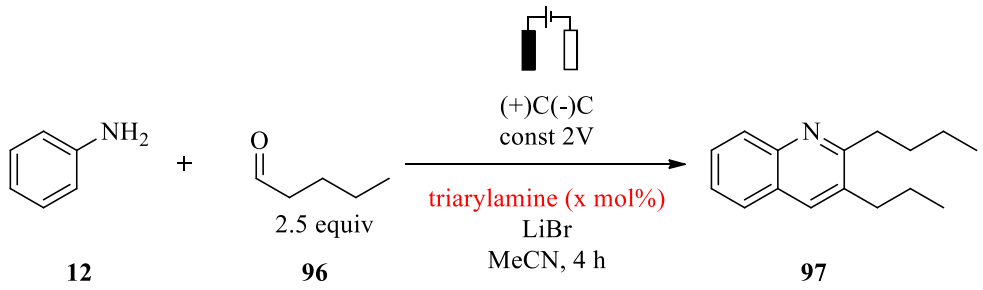

12 **96** **97**

Table 3.3 Triarylamine screening

Entry	Additive (mol%)	Yield[a]
1	TBPA (10%)	30
2	TBPA (20%)	37
3	**TBPA (1 equiv)**	**40**
4	TPA (10%)	32
5	TPA (20%)	32
6	TPA (1 eq)	30
7	TBPhA (10%)	29
8	TTA (10%)	30

[a] ^{1}H NMR conversion using HMDSO as an internal standard.

Similarly, the concentration of triarylamine has little effect on the reaction outcome. The absence of impact raises the question of whether the triarylamines are even required for mediating the electrochemical MCR. (Figure 3. and Table 3.3).[40,60]

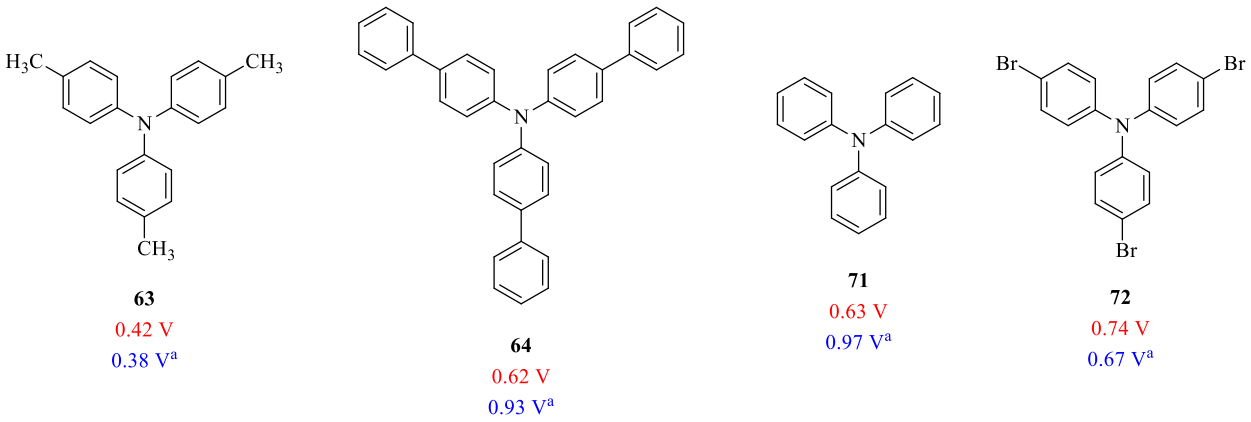

Figure 3.5 Oxidation of triarylamines. [a] Literature value measured against Fc/Fc*.

3.2.3 Assessing other electrochemical parameters, the redox mediator, and side-products.

A control reaction using stoichiometric TBPA (Table 3.3, Entry 3) was analyzed to evaluate the role and fate of the triarylamine (Equation 3.2). Here, 40% yield of product was observed by ^{1}H NMR spectroscopy, along with the triarylamine mediator present at its original loading. Trace aldehyde remained, but no aniline as per ^{1}H NMR spectroscopy. This led to led to attempts to isolate and identify the remaining material from the intractable mixture. Unfortunately, the mixture was inseparable by column chromatography and inconclusive data were obtained from mass spectroscopy. This mixture is assumed to be a series of side-products, possibly formed by bromination or reduction from cathodic interactions.

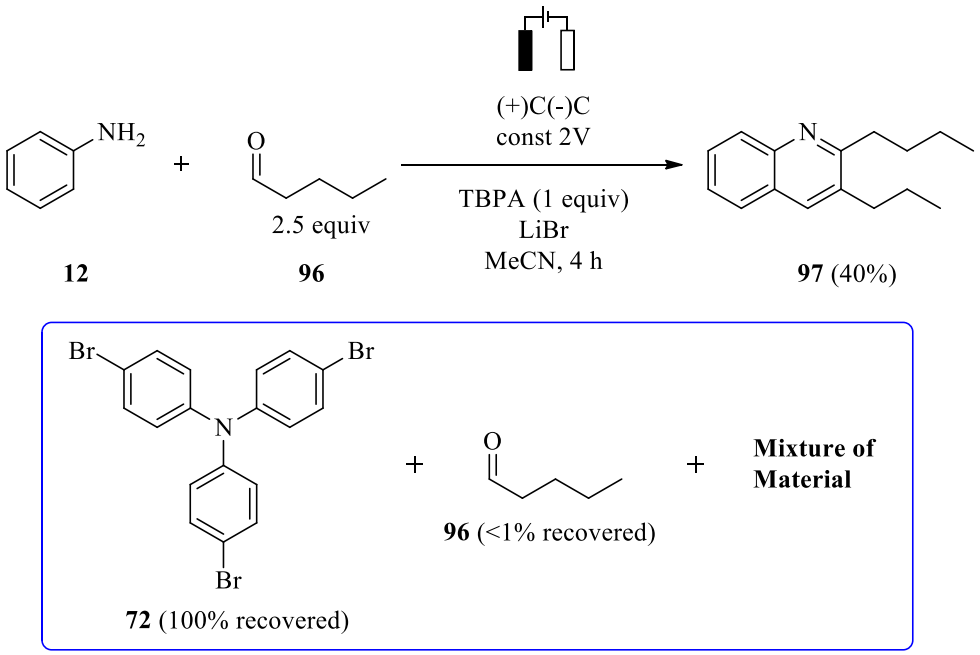

Equation 3.2 Assessment of material from crude mixture of electrochemical reaction

A white coating, likely Li_2O, forms on the cathode over the course of the reaction. This basic species can passivate the electrode surface and inhibit product formation. Alternating the polarity of the electrodes, effectively switching the roles of the anode and cathode, can reduce this passivation.[61] Surprisingly, alternating the polarity of the electrodes every 30 minutes (Equation 3.3) caused the yield of quinoline to fall dramatically. Visual inspection of the electrodes confirmed that both were coated with the same white precipitate. We attribute the low yields of quinoline to progressive fouling of the anode, the electrode that drives this oxidative transformation.

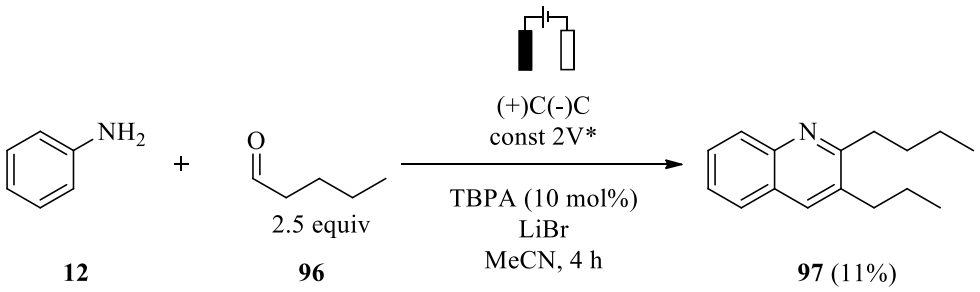

Equation 3.3 Control using alternating current.

We also considered the potential advantages of the cation pool method.[62] This method generates the radical cation mediator prior to adding the substrate. In this way, the triarylamine can potentially be used as an electrocatalyst. Two cation pool reactions were performed. In both

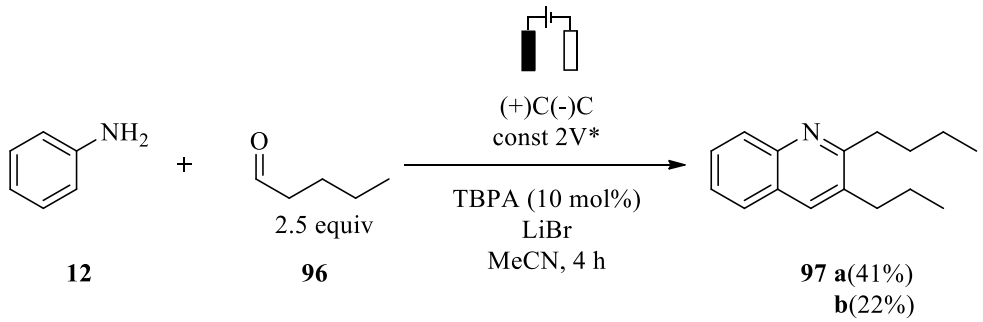

Equation 3.4 Cation pool method. Result **b** is the reaction performed at room temp with no continuous voltage applied.

cases the triarylamine was oxidized electrochemically before the amine and aldehyde were added. In one case, the applied voltage was then turned off, while in the other, a continuous voltage was applied (Equation 3.4). The best yield (41%) was obtained under constant voltage conditions; without a continuous applied voltage, the yield dropped by half.

The lithium bromide electrolyte is indispensable for electrochemical quinoline synthesis. Lithium cations are strongly Lewis acidic, binding to any of the basic nitrogen atoms in each reactive intermediates, potentially accelerating any step in the reaction mechanism (Figure 3.6). Notably, Lewis acids have been shown to be effective promoters for the aza-Diels-Alder reaction

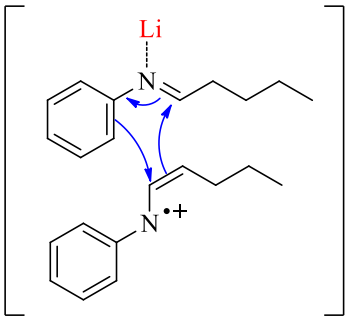

Figure 3.6 A Lewis acidic lithium could coordinate to the basic imine and accelerate the possible cyclization step of the mechanism (Scheme **3.2**)

between aromatic imines and enamines.[63,64] To test the hypothesis, N,N,N',N'-tetramethylethylenediamine (TMEDA) was added, anticipating that this chelating agent would inhibit metal cation binding. As anticipated, chelation of Li+ by TMEDA leads to as significant drop in yield (Equation 3.5). TMEDA chelation can also interfere with the formation of reactive intermediates. Unfortunately, lithium cations also promote competitive reduction of the imine by electron or hydrogen radical transfer, possibly affording secondary amine (Figure 3.7).

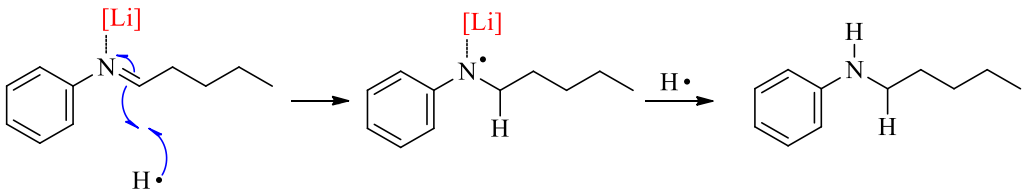

Figure 3.7 Proposed reduction of the imine by hydrogen radicals in an electrochemical cell

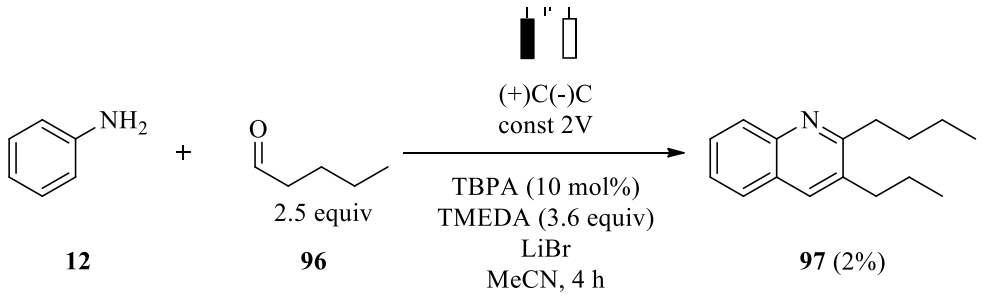

Equation 3.5 TMEDA effect on yield of the electrochemical MCR

The bromide counterion can undergo oxidation at the anode at high overpotentials (≥1.96 V) to give bromine radicals.[65] Bromine radicals are potent oxidants and may be a stoichiometric mediator for MCR. Our group has already demonstrated that iodonium cations are ideal oxidants for the chemically driven reaction. While the iodonium-catalysed reaction is efficient only at elevated temperatures, the electrochemical oxidation of bromide ions and the MCR both proceed rapidly under ambient conditions. Surprisingly, however, lithium iodide is ineffective as an

electrolyte or promoter. Chloride ions are also ineffective, but the high oxidation potential of chloride (2.43 V) likely accounts for this limitation.[65]

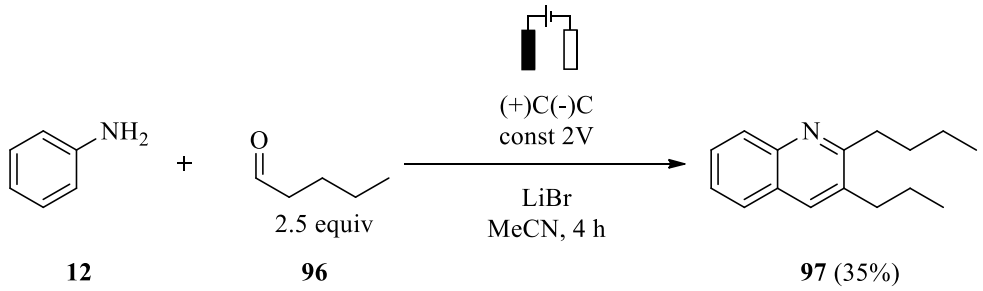

Equation 3.6 Control performed without the triarylamine additive

To resolve the ambiguity regarding the role of the triarylamine in the electrochemical MCR, a control reaction was run in its absence (Equation 3.6). The yield of quinoline in this case is 35%, just 5% lower than under the best conditions in the presence of the triarylamine (40% yield). This suggests a few options. Notably, that the electrochemical MCR does not depend on the triarylamine mediator, which suggests that the oxidation occurs via oxidation of the bromide electrolyte, acting as the mediator for indirect electrolysis.

3.2.4 Role of the redox mediator and a proposed reaction mechanism

Electrochemical mediators are especially important for reactions having large activation barriers to electron transfer. The high overpotential necessary for electron transfer between the electrode and substrate can greatly increase the occurrence of undesired side reactions. Mediators prevent this by making electron transfer and transport more facile, allowing the reaction to proceed at lower potential with fewer deleterious reactions.

Several key electron transfer events presumably occur during the course of the MCR, any of which may be accelerated by a redox mediator. The oxidation potentials of some of the dissolved species were taken from the literature or determined in our labs by cyclic voltammetry and compared to those of the triarylamine mediators (Figure 3.8).[66,67] The oxidation potential of monoarylamines (0.4 V for aniline), imines (0.7 V), and tetrahydroquionline (0.6 V)[68] are all around the range of the triarylamine oxidation (0.4 V – 0.7 V). Indeed, the differences are small enough that the triarylaramine mediator is not required to provide a more facile pathway for oxidation; bromide alone does the job. Moreover, these N-arylamines and imines may themselves functions as redox mediators and/or propagators for a radical chain mechanism.

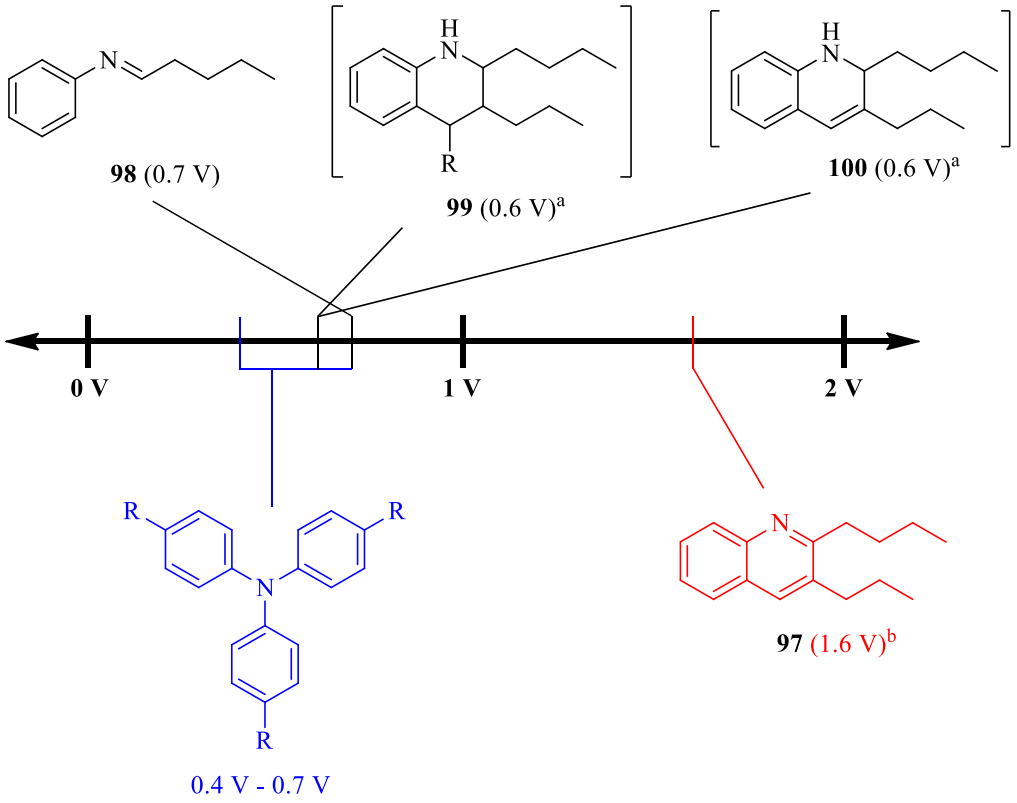

Figure 3.8 Oxidation potentials of suggested quinoline intermediates. [a] Oxidation potential of 1,2,3,4-tetrahydroquinoline for comparison. [b] Oxidation potential of benzoquinoline.

Understanding these potentials as well as the requirement for a mediator, a reasonable mechanistic cycle can be proposed (Scheme 3.2). Similar to the mechanism proposed in Chapter 2, the imine is initially formed thermally from pentanal and the aniline. This imine would exist in

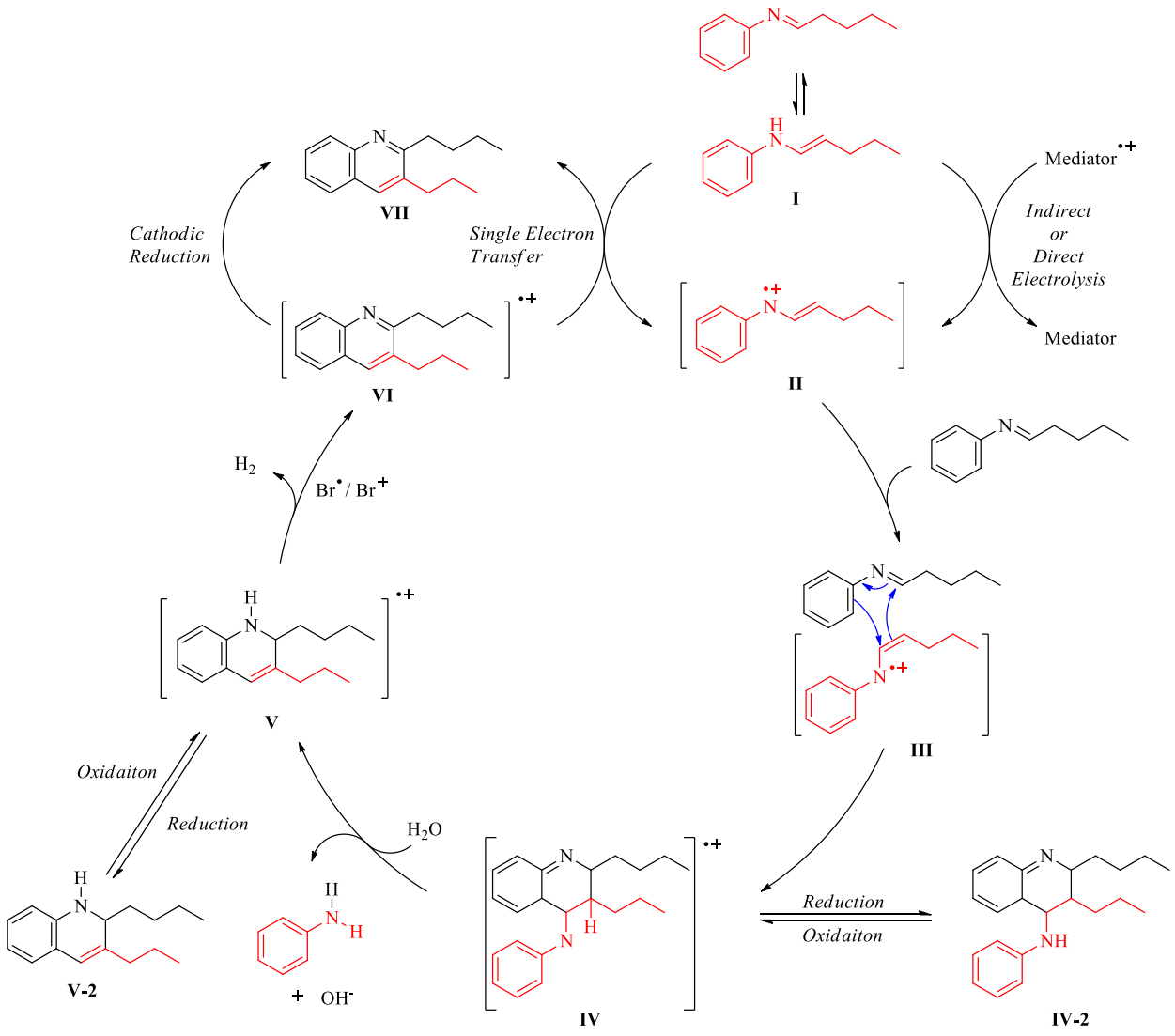

Scheme 3.2 Proposed mechanistic cycle.

equilibrium with its tautomer enamine (**I**). The enamine is much more readily oxidized to the radical cation though (similar to the tetrahydroquinolines) direct electrolysis by interaction with the cathode or through indirect electrolysis by the mediator (**II**). This equivalent of enaminium radical cation can then cyclize with another equivalent of the neutral enamine, similar to an aza-

Diels-Alder cycloaddition (**III**). Alternative to this pathway, the imine could be oxidized instead of or in competition with the enamine, which reacts with another equivalent of the enamine by an inverse-demand aza-Diels-Alder reaction (Scheme 3.3, **III-2**).

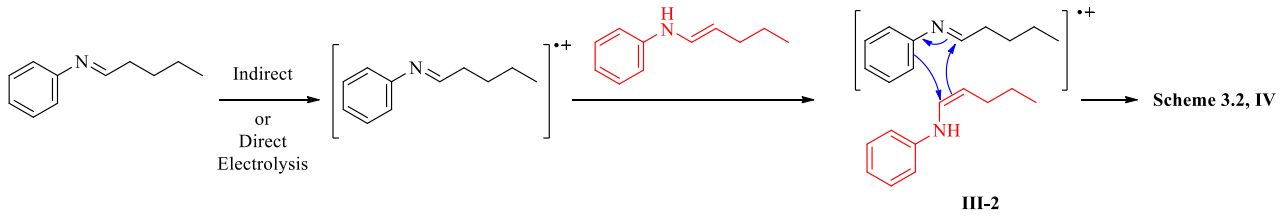

Scheme 3.3 Alternative Diels-Alder pathway to **IV**

From this bicyclic radical (Scheme 3.2, **IV**), elimination of aniline yields the dihydroquinoline radical cation (Scheme 3.2, **V**). The quinoline radical cation then forms via dehydrogenation, mediated by the bromonium cation or bromine radical present in solution (Scheme 3.2, **VI**). This reaction presumably proceeds similarly to the thermal aromatization process using iodonium as the oxidant. The quinoline radical cation can propagate the radical chain by oxidizing either imine or enamine or be reduced directly at the cathode to give the neutral product (**VII**).

This cycle varies from the mechanism proposed in Chapter 2 by the multiple redox equilibria involved in the electrochemical mechanism. As shown in Scheme 3.2, the radical cation may be reduced to the neutral species in solution. These side-equilibria may inhibit the reaction or divert it into a two-electron pathway similar to the thermal iodonium reactions.

3.2.5 Future directions: investigating the reaction mechanism and synthetic scope

Significant limitations to the electrochemical MCR still need to be addressed. The limited selectivity is the major issue. Why we have been unable to improve the yields from 40% and what

befalls the rest of the starting material remain to be determined. At a minimum, identification of the major side-products is required to better understand the mechanism(s) and control these undesired reactions.

The role of the lithium bromide clearly must be reconsidered. From the preliminary controls, lithium bromide is not only the ideal electrolyte, but also has plays the dominant role in the redox process. If bromide is the true mediator for the reaction, the reaction must be re-optimized to compensate for the absence of the triarylamine mediator (Equation 3.7). An electrolyte that does not impact the reaction can be used to optimize bromide concentration.

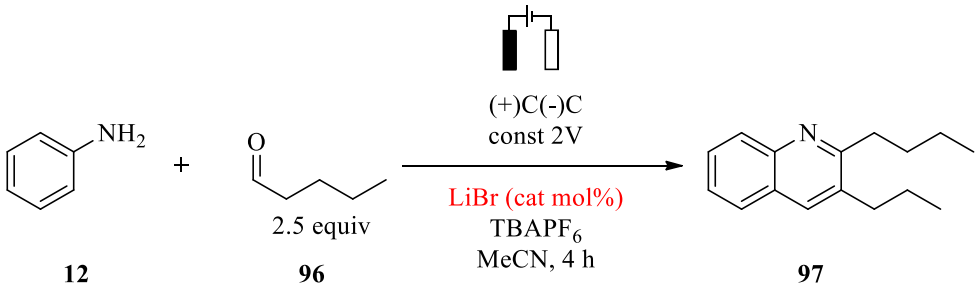

Equation 3.7 Proposed control with LiBr mediator

Once optimal conditions have been found, the scope and scale of the reaction can be investigated. Without a requirement for heating or oxygen, multigram scale reactions should be readily achieved. Further understanding of the oxidation process and optimization of potential may allow for complete aromatization of bidirectional MCR adducts, integral to the next generation of model compounds, featuring higher molecular weights and heteroatom content, consistent with molecular formulas known to be present in native asphaltenes (Figure 3.7).[5,7,8]

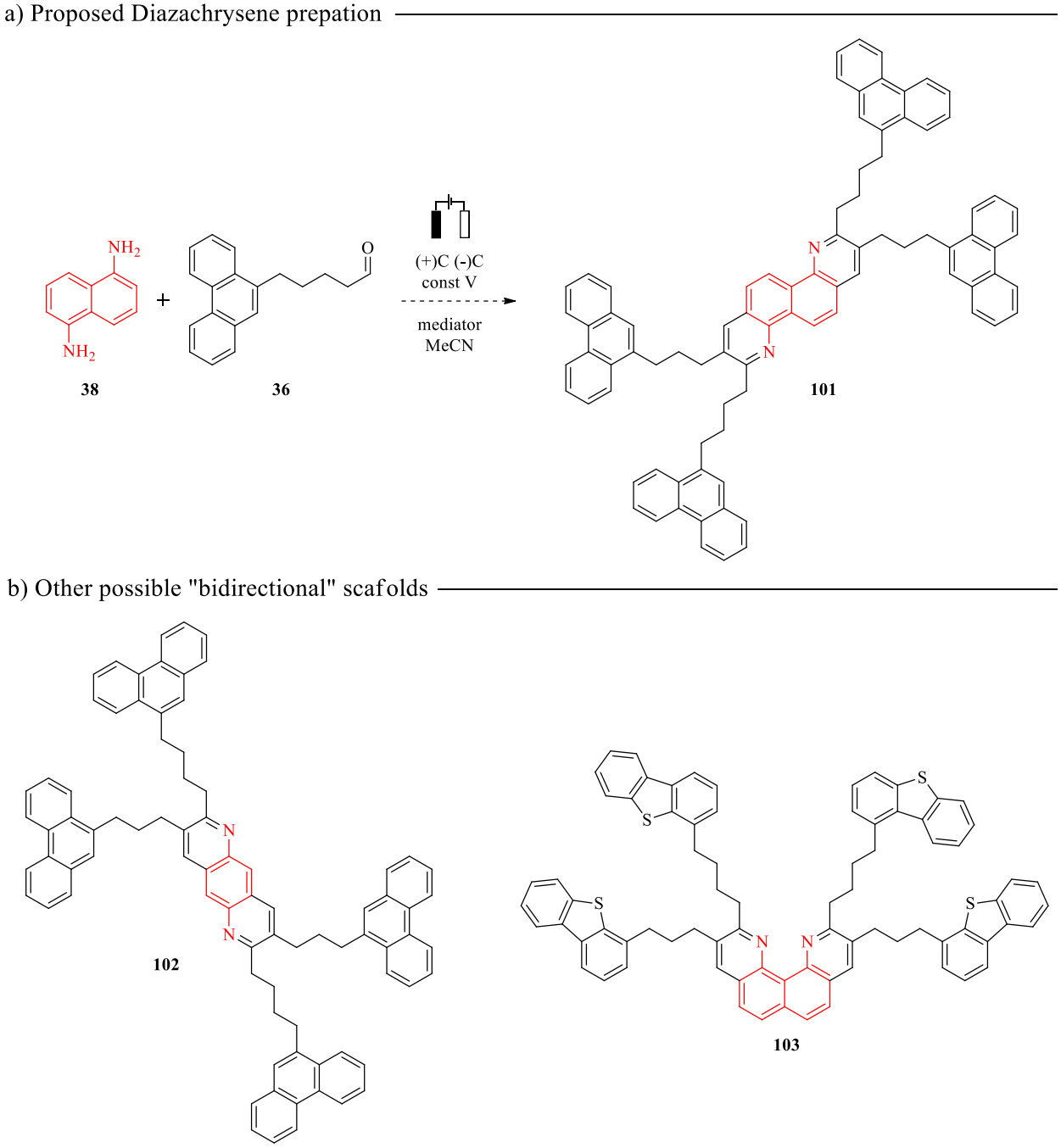

Figure 3.9 Possible outcomes of electrochemical bidirectional synthesis

3.3 Conclusions

Radical cation methodology has begun to address the limitations to the HI-catalyzed multicomponent quinoline synthesis. Removal of the requirement of the oxygen sparge is a crucial step forward in the development of the reaction and applications to asphaltene science. At worst, this method affords comparable yields to the thermal process. However, limitations of the radical cation salt method remain, including substrate/substitution sensitivity and the requirement for high temperature. The electrochemical variant, while preliminary, may provide a simpler and more flexible synthesis of quinolines, but for the moment, radical cation catalysis is best done under chemical rather than electrochemical methodology.

Chapter 4: Experimental Procedures

4.1 Instrumentation

All air sensitive reactions were performed under a nitrogen atmosphere using either Schlenk techniques or in a well-maintained glovebox with pre-purified nitrogen. Solvents (THF and dioxane) were distilled from sodium/benzophenone ketyl under nitrogen atmosphere. DMF was dried by passing over activated alumina and storing over 3 Å molecular sieves under nitrogen atmosphere. CuI was purified by known procedures[69] and stored in an amber glass bottle in the glovebox. N, N'-DMEDA was degassed through freezing and thawing under vacuum and stored under nitrogen atmosphere. All other reagents were used without further purification.

NMR spectra were obtained on an Agilent/Varian instrument (500 MHz for ^{1}H, 125 MHz for ^{13}C, or 400 MHz for ^{1}H, 100 MHz for ^{13}C). Chemical shifts are referenced to residual solvent peaks ([δ in parts per million (ppm) $CHCl_3$ ^{1}H: 7.26 ppm]. ^{1}H NMR coupling constants are reported to 0.1 Hz. UV-vis spectra and IR spectra were obtained by the instrumentation laboratory under the supervision of Wayne Moffat, using HP (Agilent) 8453 UV-Vis and Thermo Nicolet 8700 FTIR spectrometers. High resolution mass spectra (HRMS) were recorded by the mass spectroscopy laboratory staff under the supervision of Dr. Randy Whittal, on several instruments (Bruker 9.4T Apex-Qe FTICR, Bruker MALDI TOF/TOF, or Agilent Technologies 6220 oaTOF).

4.2: Experimental Procedures for Chapter 2

4.2.1: General procedure 1: Copper-catalyzed aromatic halogen exchange

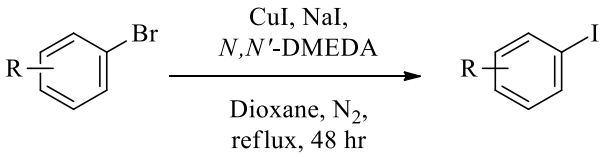

In the glovebox, the polycyclic bromoaromatic derivative (1 equiv), copper (I) iodide (5 mol%), sodium iodide (2 equiv), and dioxane (~20 mL) were charged into an oven-dried 3-neck round bottom flask containing a Teflon magnetic stir bar. The flask was fitted with a condenser and sealed with rubber septa, removed from the glovebox, and brought to a Schlenk line, where a static atmosphere of N_2 was established. *N,N'*-dimethylethylenediamine (*N,N'*-DMEDA) (10 mol%) was added via syringe and the reaction mixture heated to reflux over 48 h. The reaction mixture was allowed to cool to room temperature, after which NH_4OH (~15 mL) was added. After completion (TLC), the reaction mixture was transferred to a separatory funnel, and extracted with DCM. The organic layer was washed 3X with water, then brine. The organic layer was dried over $NaSO_4$, filtered, concentrated under vacuum, and carried forward without further purification.

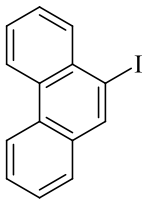

52a

9-Iodophenanthrene (52a) General procedure **1** was followed. 9-Bromophenanthrene (5.0 g, 19 mmol), CuI (0.18 g, 0.97 mmol), NaI (5.8 g, 38 mmol), N,N'-DMEDA (0.17 g, 1.9 mmol), and

dioxane (20 mL) were used, giving the product (5.6 g, 95%). Spectroscopic data (^{1}H NMR, ^{13}C NMR and mass spectroscopy) of the purified product was identical with that previously reported.[70]

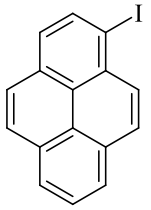

52b

1-Iodopyrene (52b) General procedure **1** was followed. 9-Bromopyrene (4.0 g, 14 mmol), CuI (0.13 g, 0.71 mmol), NaI (4.2 g, 28 mmol), N,N'-DMEDA (0.12 g, 1.4 mmol), and dioxane (18 mL) were used, giving the product (5.0 g, 86%). Spectroscopic data (^{1}H NMR, ^{13}C NMR and mass spectroscopy) of the purified product was identical with that previously reported [70]

4.2.2: General Procedure 2: Palladium catalyzed transmigratory Heck reaction

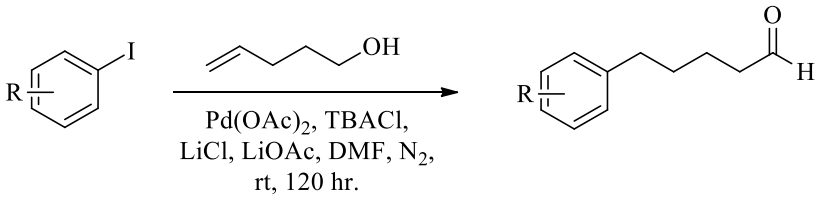

Polycyclic iodoaromatic (1 equiv), palladium (II) acetate (3 mol%), tetrabutyl ammonium chloride (2 equiv), and lithium chloride (1 equiv) were all charged to a 3-neck round bottom flask containing lithium acetate (2.5 equiv) and a Teflon magnetic stir bar. Sealed with rubber septum, an atmosphere of N_2 was established on a Schlenk line. Dry and degassed dimethyl formamide (~30 mL) was added, followed by 5-penten-1-ol (1 equiv) via syringe. The reaction mixture is

allowed to stir for 5 days at room temperature. Upon completion, dichloromethane (~30 mL) is added, and reaction mixture poured into a separation funnel. Organic layer was washed 5X with water, then brine. The organic layer was dried with sodium sulfate, filtered, concentrated, and passed through a silica plug (2:1, hexanes: ethyl acetate). The resulting organic fractions were concentrated and recrystalized from hexanes and ethyl acetate to afford desired material.

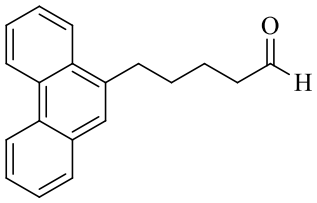

36

5-(phenanthren-9-yl)pentanal (36) General procedure **2** was followed. 9-Iodophenanthrene (5.0 g, 16 mmol), $Pd(OAc)_2$ (0.11 g, 4.9 mmol), TBACl (8.9 g, 32 mmol), LiCl (0.69 g, 16 mmol), LiOAc (2.7 g, 41 mmol), DMF (38 mL), and 5-penten-1-ol (1.4 g, 16 mmol) were used, giving the product (2.8 g, 65%). Spectroscopic data (^{1}H NMR, ^{13}C NMR and mass spectroscopy) of the purified product was identical with that previously reported.[25]

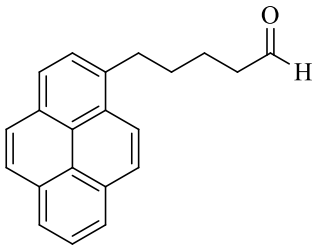

55

5-(pyren-1-yl)pentanal (55) General procedure **2** was followed. 1-Iodopyrene (3.0 g, 9.1 mmol), $Pd(OAc)_2$ (0.061 g, 0.27 mmol), TBACl (4.9 g, 18 mmol), LiCl (0.38 g, 9.1 mmol), LiOAc (1.5 g,

22 mmol), DMF (21 mL), and 5-penten-1-ol (0.78 g, 9.1 mmol) were used, giving the product (1.7 g, 40%). Spectroscopic data (^{1}H NMR, ^{13}C NMR and mass spectroscopy) of the purified product was identical with that previously reported.[25]

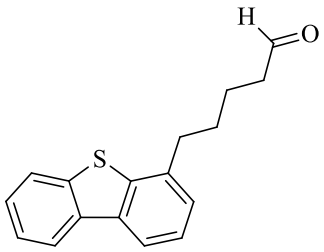

56

5-(dibenzo[b,d]thiophen-4-yl)pentanal (56) General Procedure **2** was followed using 4-iododibenzo[b,d]thiophene (1.0 g, 3.2 mmol), $Pd(OAc)_2$ (0.021 mg, 0.096 mmol), TBACl (1.7 g, 6.4 mmol), LiCl (0.13 g, 3.2 mmol), LiOAc (0.53 g, 8.1 mmol), DMF (7.5 mL), and 5-penten-1-ol (0.27 g, 3.2 mmol) were used. Product purified by column chromatography (0.26 g, 30%). Residual lithium remained coordinated to product.

^{1}H (400 MHz, $CDCl_3$) δ 9.77 (t, *J* = 1.6 Hz, 1H), 8.14 (dd, *J* = 6.0, 3.2 Hz, 1H), 8.02 (d, *J* = 8.0 Hz, 1H), 7.87 (dd, *J* = 6.0, 3.2 Hz, 1H), 7.46 (dd, *J* = 6.0, 3.2 Hz, 2H), 7.42 (t, *J* = 7.6 Hz, 1H), 7.28 (d, *J* = 7.6 Hz, 1H), 2.93 (t, *J* = 7.2 Hz, 2H), 2.50 (td, *J* = 7.6, 1.6 Hz, 2H), 1.87 (quintet, *J* = 6.8 Hz, 2H), 1.80 - 1.75 (m, 2H)

^{13}C (100 MHz, $CDCl_3$) δ 201.9, 138.7, 138.6, 135.7, 135.3, 126.2, 125.7, 124.4, 123.9, 122.4, 121.3, 119.0, 114.5, 43.3, 34.4, 28.2, 21.4

IR (cm^{-1}): 3063, 2940, 2861, 1443, 1402, 1308, 750

HRMS−EI (m/z): [M + Li]+ calcd for $C_{17}H_{16}LiOS$, 275.134; found, 274.058.

4.2.3: Ortho-substitution of Dibenzothiophene

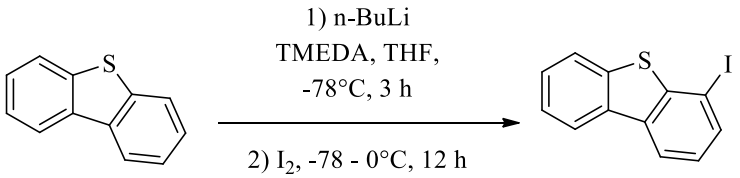

53 **54**

4-iododibenzo[b,d]thiophene (54) In the glovebox, dibenzothiophene (2.0 g, 10 mmol, 1 equiv) and distilled THF (8.0 mL) were charged into a Teflon sealed medium walled glass reactor with a Teflon magnetic stir bar. The vessel was sealed, removed from the glovebox, and brought to a Schlenk line where atmosphere of N_2 was established. The reaction mixture was cooled to -78°C in a dry ice/acetone bath, where N, N, N', N'-tetramethylethylenediamine (1.2 g, 10 mmol, 1 equiv) and 2.5 M solution of n-butyl lithium (0.76 g, 11 mmol, 1.1 equiv) were both added sequentially via syringe. The reaction mixture was allowed to warm up to 0°C in an ice water bath and stirred for 3 hrs. A solution of THF (8.0 mL) and iodine (2.7 g, 10 mmol, 1 equiv) was added at -78°C, via syringe. The reaction mixture was allowed to warm up to room temperature over night. Dichloromethane (~10 mL) is added to reaction mixture and the organic layer is washed with water, dried over sodium sulfate, filtered and concentrated. The crude material was recrystallized in acetonitrile giving the product as light yellow solid (1.6 g, 50%) Spectroscopic data (^{1}H NMR, ^{13}C NMR and mass spectroscopy) of the purified product was identical with that previously reported.[71]

4.2.4: General Procedure 3: Palladium catalyzed Hartwig coupling[40]

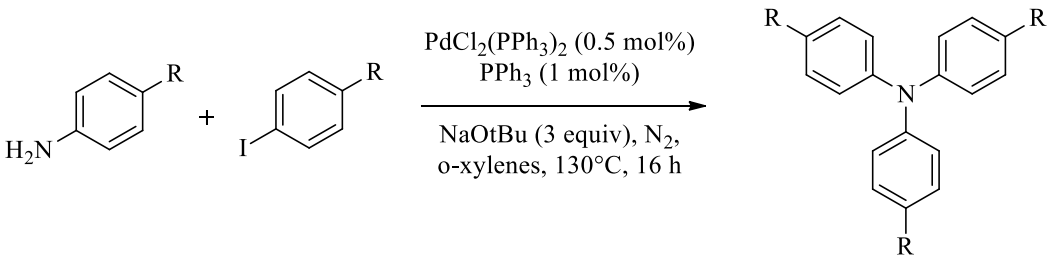

In the glovebox, aniline derivative (1 equiv), 4-iodobenzene derivative (2.5 equiv), $PdCl_2(PPh_3)_2$ (0.5 mol%), PPh_3 (1 mol%), and NaOtBu (3 equiv) charged into a Teflon sealed, medium walled glass reactor with a Teflon magnetic stir bar. Sealed and removed from the glove box and brought to a Schlenk line where atmosphere of N_2 was established. Dried and de-gassed o-xylenes (~8 mL) added to the reactor via syringe. The reactor sealed and heated to 130°C for 16 hours. The reaction mixture is allowed to cool and additional PPh_3 (1 mol%) is added. The reaction mixture is again heated to 130°C for another 4 hours. Reaction mixture is allowed to cool to room temperature, concentrated under vacuum, and the crude material was purified by column chromatography (hexanes: ethyl acetate). Products were carried forward without further purification.

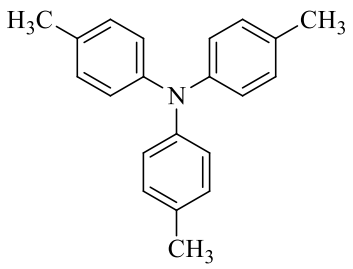

63

Tri-p-tolylamine (63) General Procedure **3** was followed using p-toluidine (0.10 g, 0.93 mmol) and 1-iodo-4-methylbenzene (0.50 g, 0.23 mmol), $PdCl_2(PPh_3)_2$ (0.0032 g, 0.0046 mmol), PPh_3 (0.0024 g, 0.0093 mmol), NaOtBu (0.26 g, 2.8 mmol), and o-xylenes (7.0 mL) The product was purified by column chromatography (9:1, hexanes: ethyl Acetate) (80 mg, 30%). Spectroscopic data (^{1}H NMR, ^{13}C NMR and mass spectroscopy) of the purified product was identical with that previously reported.[40]

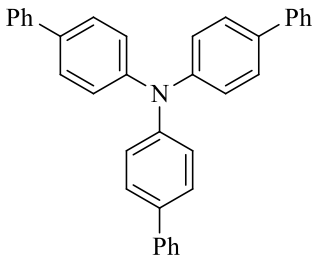

64

Tri([1,1'-biphenyl]-4-yl)amine (64) General Procedure **3** was followed using [1,1'-biphenyl]-4-amine (0.40 g, 2.3 mmol) and 4-iodo-1,1'-biphenyl (1.6 g, 5.9 mmol) $PdCl_2(PPh3)_2$ (0.0082 g, 0.011 mmol), PPh_3 (6.2 g, 0.023 mmol), NaOtBu (0.68 g, 7.1 mmol)and o-xylenes (18 mL). The product was purified by column chromatography (9:1, hexanes: ethyl acetate) (0.33 g, 30 %).

Spectroscopic data (^{1}H NMR, ^{13}C NMR and mass spectroscopy) of the purified product was identical with that previously reported.[40]

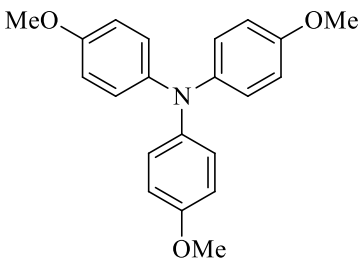

70

Tri(4-methoxyphenyl)amine (70) General Procedure **3** was followed using 4-methoxyaniline (0.20 g, 1.6 mmol) and 4-iodoanisole (0.95 g, 4.0 mmol), $PdCl_2(PPh3)_2$ (0.0057 g, 0.0082 mmol), PPh_3 (0.0042 g, 0.016 mmol) NaOtBu (0.46 g, 4.8 mmol) and o-xylenes (12 mL). Product purified by column chromatography (9:1, hexanes: ethyl acetate) (54 mg, 10 %). Spectroscopic data (^{1}H NMR, ^{13}C NMR and mass spectroscopy) of the purified product was identical with that previously reported.[40]

4.2.5 Bromination of Triphenylamine

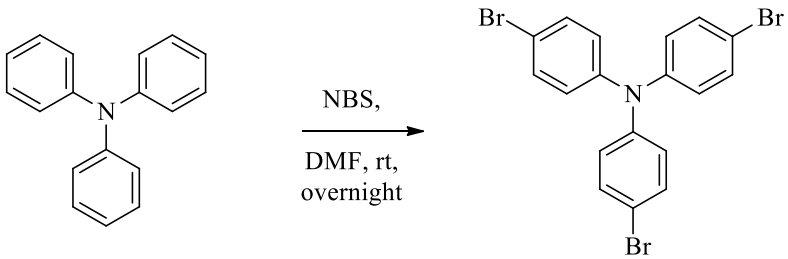

71 **72**

Tris(4-bromophenyl)amine (72) Performed similar to reported procedure.[41] A solution of triphenyl amine (2.0 g, 8.1 mmol, 1 equiv) in DMF (40 mL) was charged into a round bottom flask

with a magnetic Teflon stir bar. Fitted with an addition funnel, a solution of *N*-bromosuccinimide (4.4 g, 25 mmol, 3.1 equiv) in DMF (15 mL) was charged to the addition funnel. NBS solution was added drop wise to the triphenyl amine solution at room temperature, and the reaction mixture was stirred overnight. The reaction mixture was taken up in DCM (20 mL) and the organic layer was washed 3X with water. The organic layer was dried with sodium sulfate and concentrated under vacuum. Product was recrystalized from methanol (2.2 g, 56 %). Spectroscopic data (^{1}H NMR, ^{13}C NMR and mass spectroscopy) of the purified product was identical with that previously reported.[41]

4.2.6 General procedure 4: Oxidation of triaryl amines using antimony pentachloride[42]

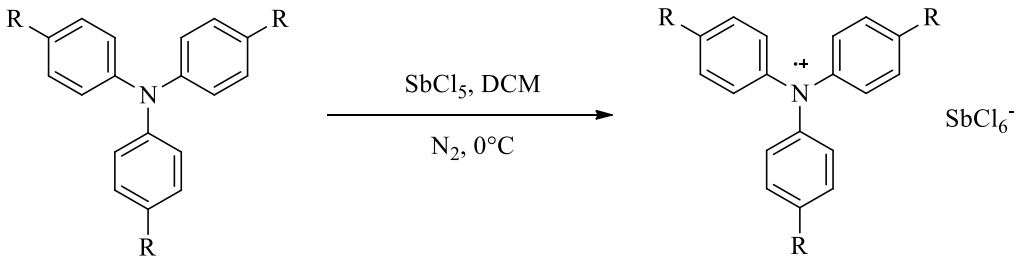

A dry three neck round bottom flask containing triaryl amine (1 equiv) sealed with rubber septum and N_2 atmosphere established on a Schlenk line. Dried, degassed dichloromethane (~5 mL) added via syringe. A solution of antimony pentachloride (1 equiv) in DCM (~5 mL) added dropwise to the triaryl amine solution at 0°C using an ice water bath. The reaction is allowed to stir for 30 minutes. Diethyl ether (~10 mL) charged to the reaction mixture and the material precipitated out. The solution decanted and product washed with cool diethyl ether to yield product without further purification.

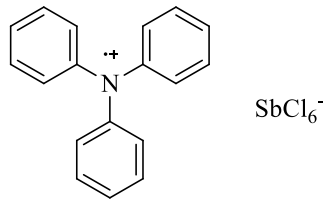

73

Trisphenylammoniumyl hexachloroantimonate (73) General Procedure **4** was followed using triphenylamine (0.4 g, 16 mmol), antimony pentachloride (0.48 g, 16 mmol), and DCM (8 mL), giving the product (0.15 g, 32%).

UV (DCM) λ_{max} nm (ε): 484 (1.90), 337 (0.34), 276 (1.18)

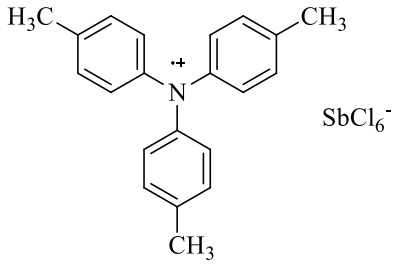

74

Tris(4-methylphenyl)ammoniumyl hexachloroantimonate (74) General Procedure **4** was followed using tri(4-methylphenyl)amine (0.008 g, 0.27 mmol), antimony pentachloride (0.0083 g, 0.27 mmol), and DCM (2 mL), giving the product (34 mg, 20%).

UV (DCM) λ_{max} nm (ε): 675 (2.34), 370 (1.84), 276 (1.54)

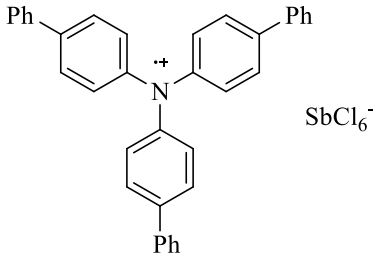

75

Tris(4-biphenyl)ammoniumyl hexachloroantimonate (75) General Procedure **4** was followed using tri(4-biphenyl)amine (0.020 g, 0.042 mmol), antimony pentachloride (0.012 g, 0.042 mmol), and DCM (1 mL) giving the product (3.4 mg, <10%). Insufficient amount isolated for spectral characterization

4.2.7: General procedure 5: Oxidation of triaryl amines using silver hexafluorophosphate[43]

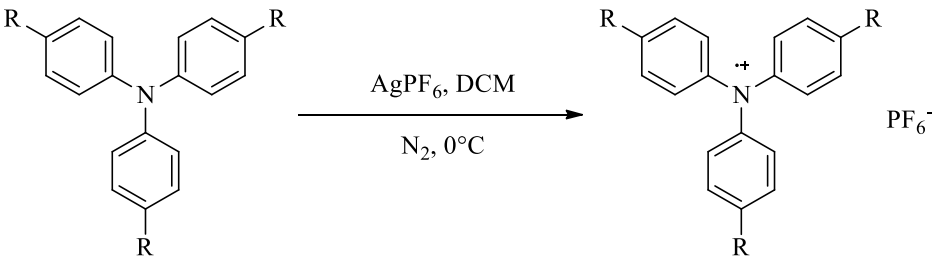

A dry three neck round bottom flask containing triaryl amine (1 equiv) is sealed with rubber septum, and a N_2 atmosphere is established on a Schlenk line. Dried, degassed dichloromethane (~3 mL) is added via syringe. A solution of silver hexafluorophosphate (1 equiv) in DCM (~3 mL) is added dropwise to the triaryl amine solution at 0°C using an ice water bath. Reaction is allowed to stir for 1 hour. Diethyl ether (~6 mL) is charged to the reaction mixture and the material

is precipitated out. Solution is decanted and product washed with cool diethyl ether to yield product without further purification.

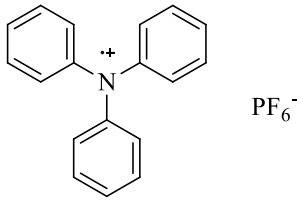

76

Trisphenylammoniumyl hexafluorophosphate (76) General Procedure **5** was followed using triphenylamine (0.20 g, 0.81 mmol) silver hexafluorophosphate (0.20 g, 0.81 mmol) and DCM (4 mL), giving the product (79 mg, 25%).

UV (DCM) λ_{max} nm (ε): 496 (0.32), 361 (1.03)

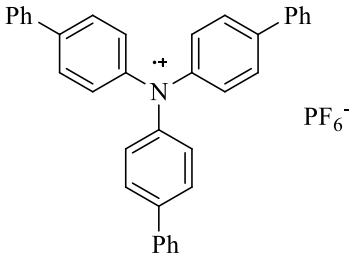

77

Tris(4-biphenyl)ammoniumyl hexafluorophosphate (77) General Procedure **5** was followed using tris(4-methylphenyl)amine (0.020 g, 0.042 mmol), silver hexafluorophosphate (0.010 g, 0.042 mmol), and DCM (1 mL), giving the product (2.6 mg, <10%).

UV (DCM) λ_{max} nm (ε): 863 (0.74), 421 (0.58), 257 (0.51)

4.2.8 General Procedure 6: Quinoline cyclocondensation initial optimization via TBPA

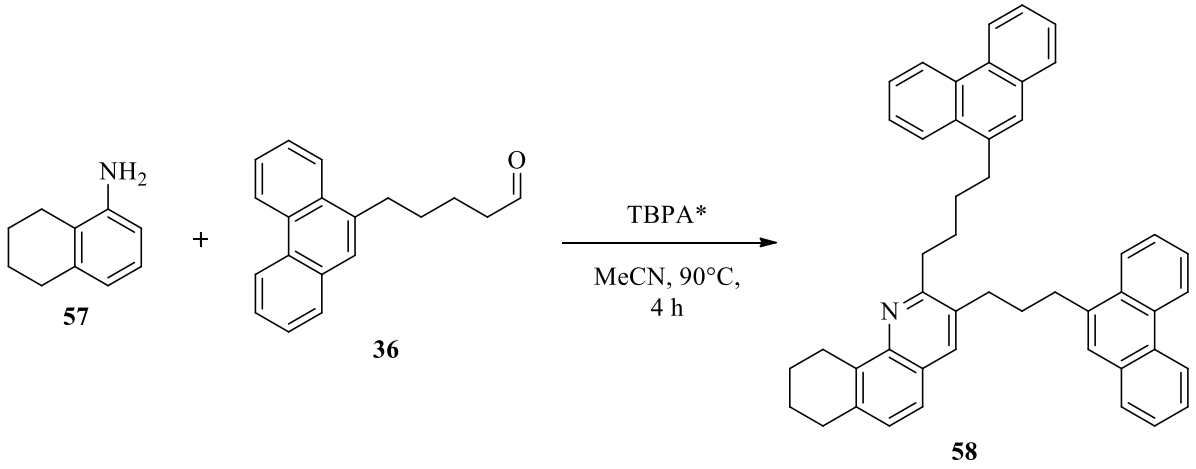

57 + **36** → **58**

5,6,7,8-Tetrahydronaphthalen-1-amine (0.023 g, 0.15 mmol, 1 equiv), 5-(phenanthren-9-yl)pentanal (0.10g, 0.39 mmol, 2.5 equiv), acetonitrile (15 mL), and a Teflon magnetic stir bar were charged to a three-neck round bottom flask. The reaction mixture allowed to stir for 10 mins. TBPA* (0.012 g, 0.015 mmol, 10 mol%) is charged to the reaction mixture and is stirred for 4 hours at 90 °C. The reaction mixture is allowed to cool to room temperature, then quenched with triethylamine (3 mL). DCM (20 mL) is charged to the reaction flask and the reaction mixture is transfered to a separatory funnel. The organic layer is washed with water, dried over sodium sulfate, and concentrated under vacuum. ^{1}H NMR analysis was performed using equimolar hexamethyldisiloxane as an internal standard.

(1A) General procedure **6** was used, TBPA* (0.012g, 0.015 mmol), MeCN (15 mL), room temperature, 4 hours (^{1}H NMR yield: 40%).

(2A) General procedure **6** was performed, TBPA* (0.012g, 0.015 mmol), MeCN (15 mL), 90°C (bath temperature), in the absence of light, 4 hours (^{1}H NMR yield: 40%).

(3A) General procedure **6** was performed, TBPA* (0.012g, 0.015 mmol), MeCN (15 mL), room temperature, 18 hours (^{1}H NMR yield: 40%).

(4A) General procedure **6** was performed, TBPA* (0.012g, 0.015 mmol), MeCN (15 mL), 90°C (bath temperature), 18 hours (^{1}H NMR yield: 66%).

(5A) General procedure **6** was performed, aldehyde (2 equiv, 0.082 g, 0.31 mmol), TBPA* (0.012g, 0.015 mmol), MeCN (15 mL), 90°C (bath temperature), 4 hours (^{1}H NMR yield: 59%).

(6A) General procedure **6** was performed, aldehyde (2.1 equivs, 0.086 g, 0.32 mmol), TBPA* (0.012g, 0.015 mmol), MeCN (15 mL), 90°C (bath temperature), 4 hours (^{1}H NMR yield: 40%).

(7A) General procedure **6** was performed, TBPA* (0.012g, 0.015 mmol), MeCN (15 mL), 90°C (bath temperature), oxygen sparged, 4 hours (^{1}H NMR yield: 74%).

(8A) General procedure **6** was performed, TBPA* (0.012g, 0.015 mmol), MeCN (15 mL), 90°C (bath temperature), sealed in a Teflon stopper, medium walled glass reactor with nitrogen atmosphere, 4 hours (^{1}H NMR yield: 70%).

(9A) General procedure **6** was performed, TBPA* (0.012g, 0.015 mmol), benzene (15 mL), 90°C (bath temperature), 4 hours (^{1}H NMR yield: 67%).

(10A) General procedure **6** was performed, TBPA* (0.012g, 0.015 mmol), anisole (15 mL), 90°C (bath temperature), 4 hours (^{1}H NMR yield: 55%).

(11A) General procedure **6** was performed, TBPA* (0.012g, 0.015 mmol), tetrahydrofuran (THF) (15 mL), 90°C (bath temperature), 4 hours (^{1}H NMR yield: 70%).

(12A) General procedure **6** was performed, TBPA* (0.012g, 0.015 mmol), dimethoxyethane (DME) (15 mL), 90°C (bath temperature), 4 hours (^{1}H NMR yield: 81%).

(13A) General procedure **6** was performed, TBPA* (0.012g, 0.015 mmol), DME (15 mL), room temperature, 4 hours (^{1}H NMR yield: 60%).

(14A) General procedure **6** was performed, TBPA* (0.012g, 0.015 mmol), MeCN (5 mL), 90°C (bath temperature), 4 hours (^{1}H NMR yield: 64%).

(15A) General procedure **6** was performed, TBPA* (0.012g, 0.015 mmol), MeCN (1.5 mL), 90°C (bath temperature), 4 hours (^{1}H NMR yield: 51%).

4.2.9: General procedure 7: radical cation salt optimization

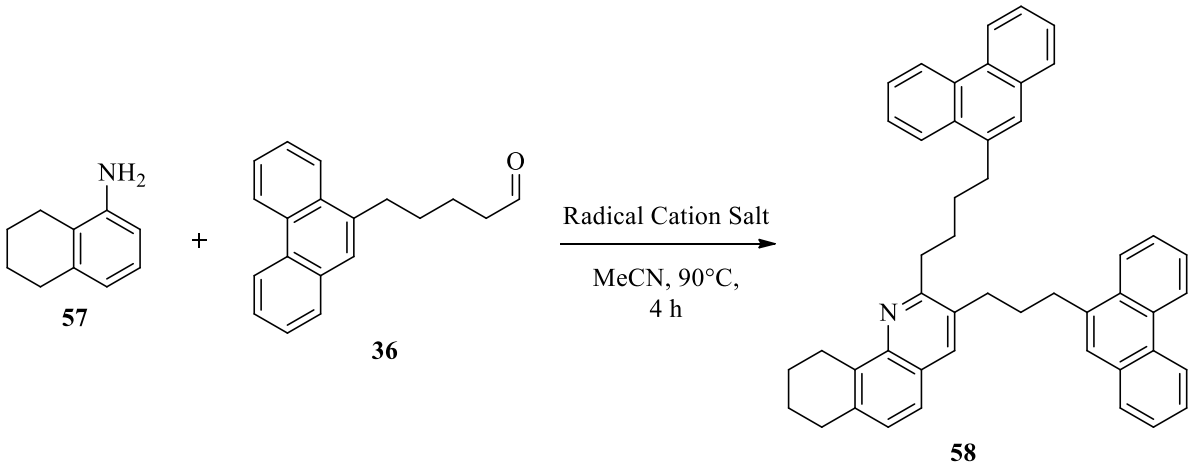

57 **36** **58**

5,6,7,8-tetrahydronaphthalen-1-amine (0.023 g, 0.15 mmol, 1 equiv), 5-(phenanthren-9-yl)pentanal (0.10 g, 0.39 mmol, 2.5 equiv), acetonitrile (15 mL) and a Teflon magnetic stir bar are charged to a three-neck round bottom flask. The reaction mixture is allowed to stir for 10 mins. The radical cation salt is charged to the reaction mixture and is stirred for 4 hours at 90 °C. The reaction mixture is allowed to cool to room temperature, then quenched with triethylamine (3 mL). DCM (20 mL) is charged to the reaction flask and the reaction mixture is transferred to a separatory funnel. The organic layer is washed with water, dried over sodium sulfate, and concentrated under vacuum. ^{1}H NMR analysis was performed using equimolar hexamethyldisiloxane (HMDSO) as an internal standard.

(1B) General procedure **7** was performed, TBPA* (0.012g , 10 mol%, 0.015 mmol), MeCN (15 mL), 90°C (bath temperature), 4 hours (^{1}H NMR yield: 80%).

(2B) General procedure **7** was performed, TBPA* (0.025g, 20 mol%, 0.031 mmol), MeCN (15 mL), 90°C (bath temperature), 4 hours (^{1}H NMR yield: 61%).

(3B) General procedure **7** was performed, TBPA* (0.0025g, 2 mol%, 0.0031 mmol), MeCN (15 mL), 90°C (bath temperature), 4 hours (^{1}H NMR yield: 80%).

(4B) General procedure **7** was performed, TBPA* (0.012g, 10 mol%, 0.015 mmol at onset of the reaction and 0.012g, 10 mol%, 0.015 mmol at two hours during the reaction), MeCN (15 mL), 90°C (bath temperature), 4 hours (^{1}H NMR yield: 95%).

(5B) General procedure **7** was performed, TBPA* (0.0012g, 1 mol%, 0.0015 mmol, addition every 15 mins), MeCN (15 mL), 90°C (bath temperature), 4 hours (^{1}H NMR yield: 64%).

(6B) General procedure **7** was performed, TTA$SbCl_6$ (0.0097g, 10 mol%, o.o15 mmol), MeCN (15 mL), 90°C (bath temperature), 4 hours (^{1}H NMR yield: 84%).

(7B) General procedure **7** was performed, TPA$SbCl_6$ (0.0093g, 10 mol%, 0.015 mmol), MeCN (15 mL), 90°C (bath temperature), 4 hours (^{1}H NMR yield: 95%).

(8B) General procedure **7** was performed, TPAPF_6 (0.0061g, 10 mol%, 0.015 mmol), MeCN (15 mL), 90°C (bath temperature), 4 hours (^{1}H NMR yield: 85%).

4.2.10: General procedure 9: quinoline cyclocondensation via radical cation scope

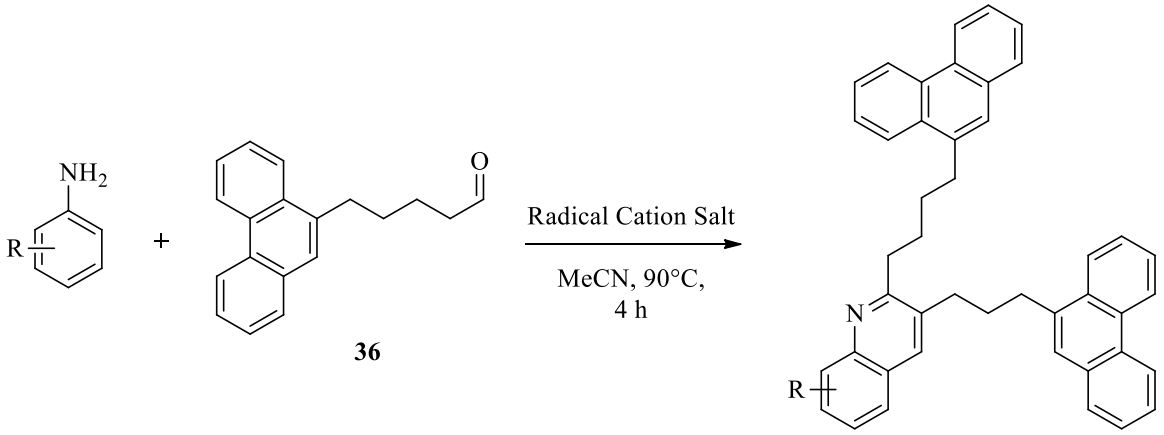

Aniline derivative (1 equiv), 5-(phenanthren-9-yl)pentanal (2.5 equiv), acetonitrile (~15 mL) and a Teflon magnetic stir bar are charged to a three-neck round bottom flask. The reaction mixture is allowed to stir for 10 mins. The radical cation salt (10 mol%) is charged to the reaction mixture and is stirred for 4 hours at 90 °C. The reaction mixture is allowed to cool to room temperature, then quenched with triethylamine (3 mL). DCM (20 mL) is charged to the reaction flask and the reaction mixture is transferred to a separatory funnel. The organic layer is washed with water, dried over sodium sulfate, and concentrated under vacuum. ^{1}H NMR analysis was performed using equimolar hexamethyldisiloxane (HMDSO) as an internal standard.

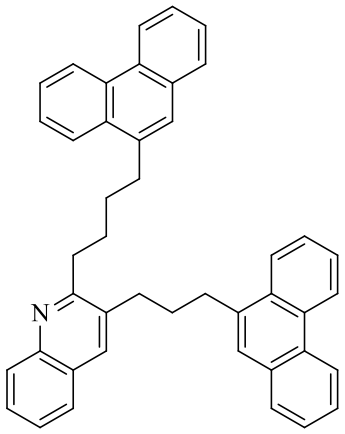

79

2-(4-(phenanthren-9-yl)butyl)-3-(3-(phenanthren-9-yl)propyl)quinoline (79) General Procedure **9** was followed using aniline (23 mg, 0.24 mmol), 5-(phenanthren-9-yl)pentanal (0.16 g, 0.61 mmol), and $TPASbCl_6$ (14 mg, 0.024 mmol) (or $TBPASbCl_6$ (20 mg, 0.024 mmol)). Hexamethyldisiloxane (52 μL, 0.24 mmol) was added as an internal standard (^{1}H NMR yield: 86%) (70% when $TBPASbCl_6$ was used). The ^{1}H NMR spectrum product was identical with that previously reported.[25]

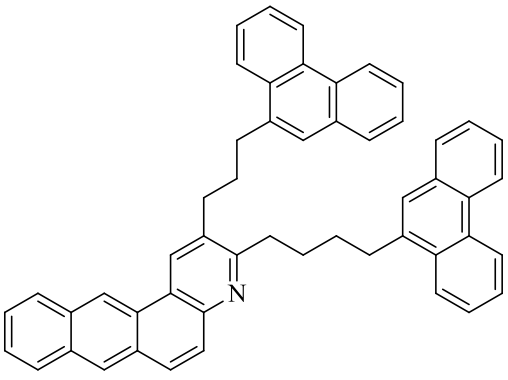

80

3-(4-(phenanthren-9-yl)butyl)-2-(3-(phenanthren-9-yl)propyl)naphtho[2,3-f]quinoline (80) General Procedure 9 was followed using 2-aminoanthracene (23 mg, 0.11 mmol), 5-(phenanthren-9-yl)pentanal (78 mg, 0.29 mmol), and $TPASbCl_6$ (6.9 mg, 0.011 mmol) (or $TBPASbCl_6$ (9.7 mg, 0.011 mmol)). Hexamethyldisiloxane (25 μL, 0.11 mmol) was added as an internal standard (^{1}H NMR yield:54%) (60% when $TBPASbCl_6$ was used). The ^{1}H NMR spectrum product was identical with that previously reported.[25]

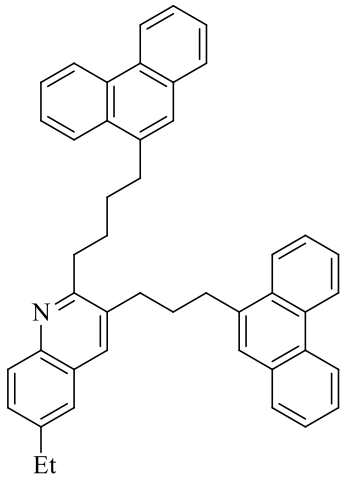

81

6-ethyl-2-(4-(phenanthren-9-yl)butyl)-3-(3-(phenanthren-9-yl)propyl)quinoline (81) General Procedure 9 was followed using 4-ethylaniline (23 mg, 0.18 mmol), 5-(phenanthren-9-yl)pentanal (0.12 g, 0.47 mmol), and $TPASbCl_6$ (11 mg, 0.018 mmol). Hexamethyldisiloxane (40 μL, 0.18 mmol) was added as an internal standard (^{1}H NMR yield: 92%). The ^{1}H NMR spectrum product was identical with that previously reported.[25]

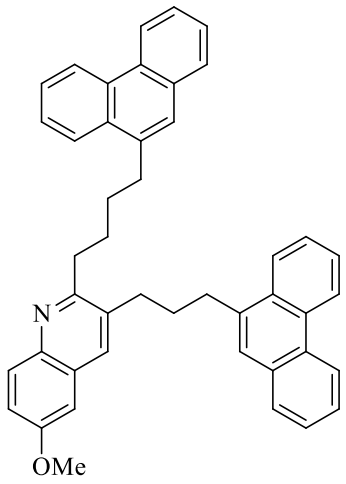

82

6-methoxy-2-(4- (phenanthren-9-yl)butyl)-3-(3-(phenanthren-9-yl)propyl)quinoline (82) General Procedure 9 was followed using 4-methoxyaniline (23 mg, 0.18 mmol), 5-(phenanthren-9-yl)pentanal (0.12 g, 0.46 mmol), and $TPASbCl_6$ (11 mg, 0.018 mmol). Hexamethyldisiloxane (39 μL, 0.18 mmol) was added as an internal standard (^{1}H NMR yield: 40%). The ^{1}H NMR spectrum product was identical with that previously reported.[25]

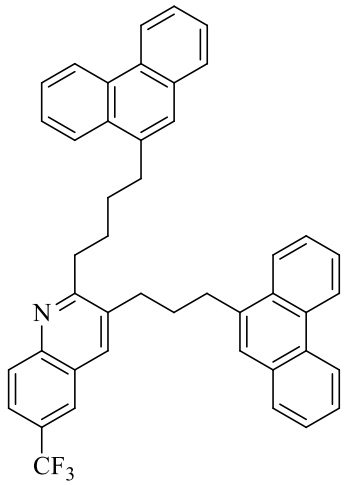

83

2-(4-(phenanthren-9-yl)butyl)-3-(3-(phenanthren-9-yl)propyl)-6-(trifluoromethyl)quinoline (83) General Procedure 9 was followed using 4-(trifluoromethyl)aniline (23 mg, 0.14 mmol), 5-(phenanthren-9-yl)pentanal (93 mg, 0.35 mmol), and $TPASbCl_6$ (8.5 mg, 0.014 mmol). Hexamethyldisiloxane (30 μL, 0.14 mmol) was added as an internal standard (^{1}H NMR yield: 41%) Further purification and continued spectroscopic analysis required.

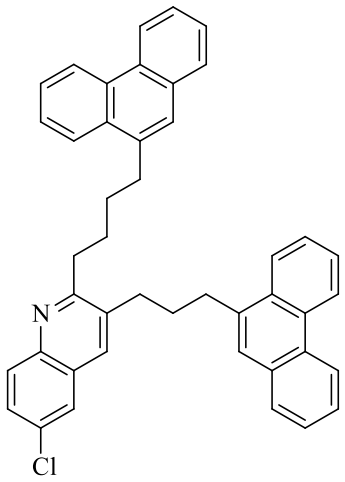

84

6-chloro-2-(4-(phenanthren-9-yl)butyl)-3-(3-(phenanthren-9-yl)propyl)quinoline (84) General Procedure 9 was followed using 4-chloroaniline (23 mg, 0.18 mmol), 5-(phenanthren-9-yl)pentanal (0.12 g, 0.45 mmol), and $TPASbCl_6$ (10 mg, 0.018 mmol). Hexamethyldisiloxane (38 μL, 0.18 mmol) was added as an internal standard (^{1}H NMR yield: 62%). Product purified by column chromatography (hexane:ethyl aceteate gradient . Further purification and continued spectroscopic analysis required.

^{1}H (500 MHz, $CDCl_3$) δ 8.73 (d, J = 6.8 Hz, 1H), 8.74 (dd, J = 7.0, 3.0 Hz, 2H), 8.55 (dd, J = 6.5, 3.5 Hz, 1H), 8.04-8.02 (m, 2H), 7.91 (d, J = 9.0 Hz, 1H), 7.80-7.78 (m, 2H), 7.76 (s, 1H), 7.66 (d,

J = 2.5 Hz, 1H), 7.65-7.62 (m, 1H), 7.60-7.56 (m, 5H), 7.55-7.54 (m, 1H), 7.52 (dd, *J* = 6.0, 3.0 Hz, 2H), 7.49 (s, 1H), 3.22 (t, *J* = 7.5 Hz, 2H), 3.03 (t, *J* = 7.0 Hz, 2H), 2.91 (quart, *J* = 8.5 Hz, 4H), 2.20 (quint, *J* = 7.5 Hz, 2H), 1.91-1.87 (m, 2H), 1.85-1.79 (m, 2H)

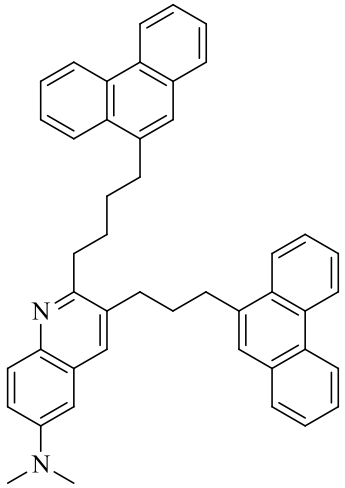

85

N,N-dimethyl-2-(4-(phenanthren-9-yl)butyl)-3-(3-(phenanthren-9-yl)propyl)quinolin-6-amine (85) General Procedure 9 was followed using *N,N*-dimethyl-4-phenylenediamine (23.0 mg, 0.16 mmol), 5-(phenanthren-9-yl)pentanal (0.11 g, 0.42 mmol), and $TBPASbCl_6$ (13 mg, 0.016 mmol). Hexamethyldisiloxane (35 μL, 0.16 mmol) was added as an internal standard (^{1}H NMR yield: 85%). The ^{1}H NMR spectrum product was identical with that previously reported.[25]

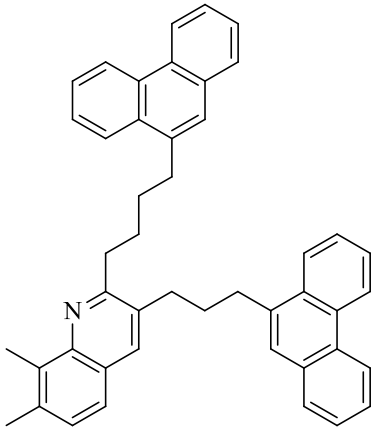

86

7,8-dimethyl-2-(4-(phenanthren-9-yl)butyl)-3-(3-(phenanthren-9-yl)propyl)quinoline (86)

General Procedure 9 was followed using 2,3-dimethylaniline (23 mg, 0.18 mmol), 5-(phenanthren-9-yl)pentanal (0.124 g, 0.47 mmol), and $TBPASbCl_6$ (15 mg, 0.018 mmol). Hexamethyldisiloxane (40 μL, 0.18 mmol) was added as an internal standard (^{1}H NMR yield: 48%). The ^{1}H NMR spectrum product was identical with that previously reported.[25]

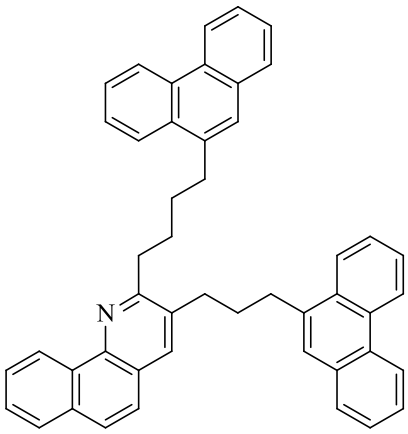

87

2-(4-(phenanthren-9-yl)butyl)-3-(3-(phenanthren-9-yl)propyl)benzo[h]quinoline (87)

General Procedure 9 was followed using 1-napthylamine (23 mg, 0.16 mmol), 5-(phenanthren-9-yl)pentanal (0.10 g, 0.40 mmol), and $TBPASbCl_6$ (13 mg, 0.016 mmol). Hexamethyldisiloxane (34 μL, 0.16 mmol) was added as an internal standard (^{1}H NMR yield: 62%). The ^{1}H NMR spectrum product was identical with that previously reported.[25]

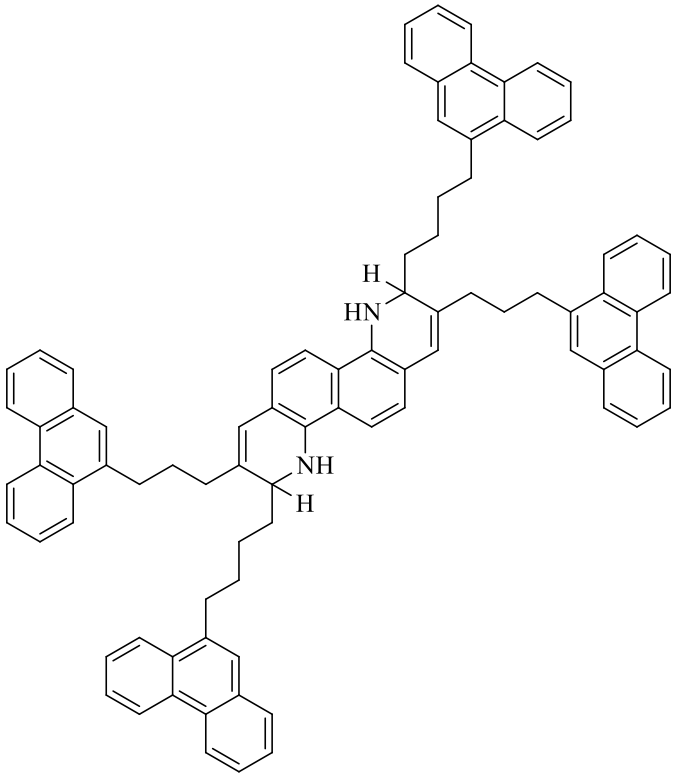

88

3,9-bis(4-(phenanthren-9-yl)butyl)-2,8-bis(3-(phenanthren-9-yl)propyl)-3,4,9,10-tetrahydroquinolino[8,7-h]quinoline (88) General Procedure 9 was followed using 1,5-diaminonapthylene (23 mg, 0.14 mmol), 5-(phenanthren-9-yl)pentanal (0.19 g, 0.70 mmol), and $TPASbCl_6$ (17 mg, 0.016 mmol). Hexamethyldisiloxane (34 μL, 0.16 mmol) Product attempted to

be purified by column chromatography (hexane:ethyl acetate gradient). ^{1}H NMR analysis was inconclusive. Further purification and continued spectroscopic analysis required.

HRMS-ESI (m/z): [M]+ calcd for $C_{96}H_{84}N_4$ 1134.5; found, 1135.5.

4.3 Experimental Procedures for Chapter 3

All techniques performed using the electrochemical equipment from IKA. The Electrosyn 2.0 and the electrodes were all purchased through IKA and used according to the manufacturer's guidelines. For reactions performed in tandem, a six-position carousel was used in place of a single use slot.

4.3.1: Cyclic Voltammetry of the Triaryl Amines

Cyclic voltammetric measurements were performed using a glassy carbon as the working electrode, platinum as the counter electrode, and silver wire in a glass frit for the reference electrode. The experiments were stirred in a solution of 0.1 M tetrabutylammonium hexafluorophosphate in acetonitrile. Triaryl amine substrates (0.02 mmol) were measured and with ferrocene (0.02 mmol) used as an internal reference for voltage.

Tri(4-bromophenyl)amine (72)

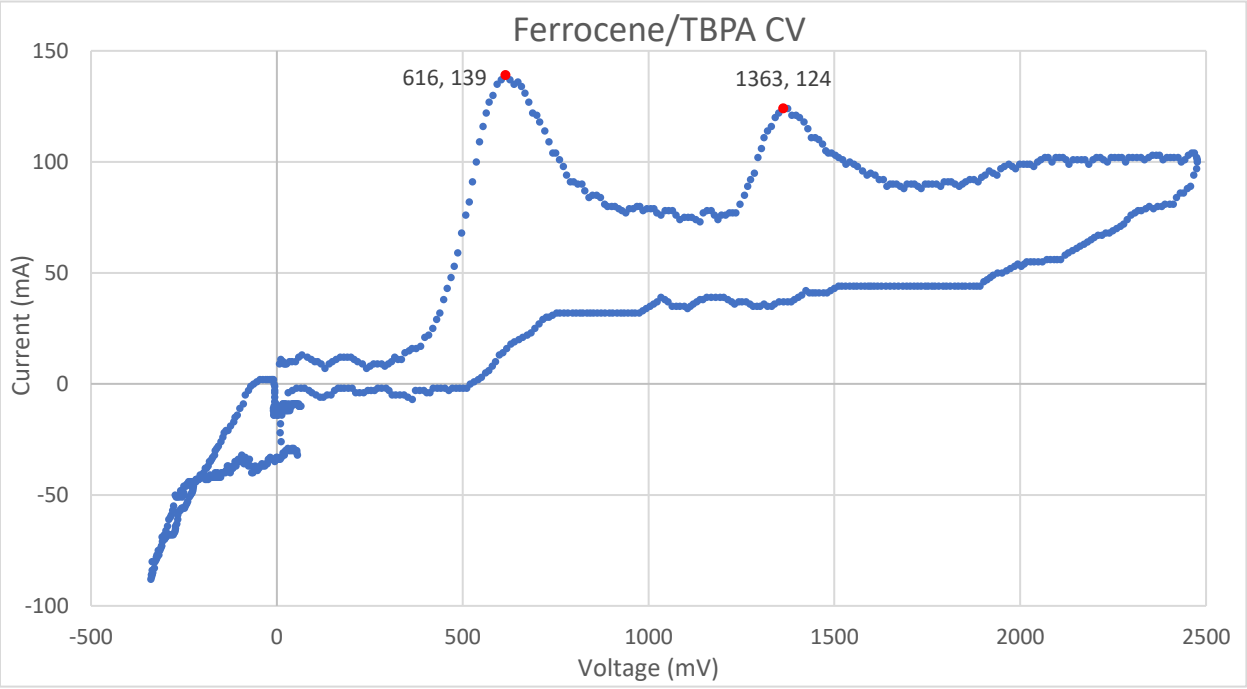

Triphenylamine (71)

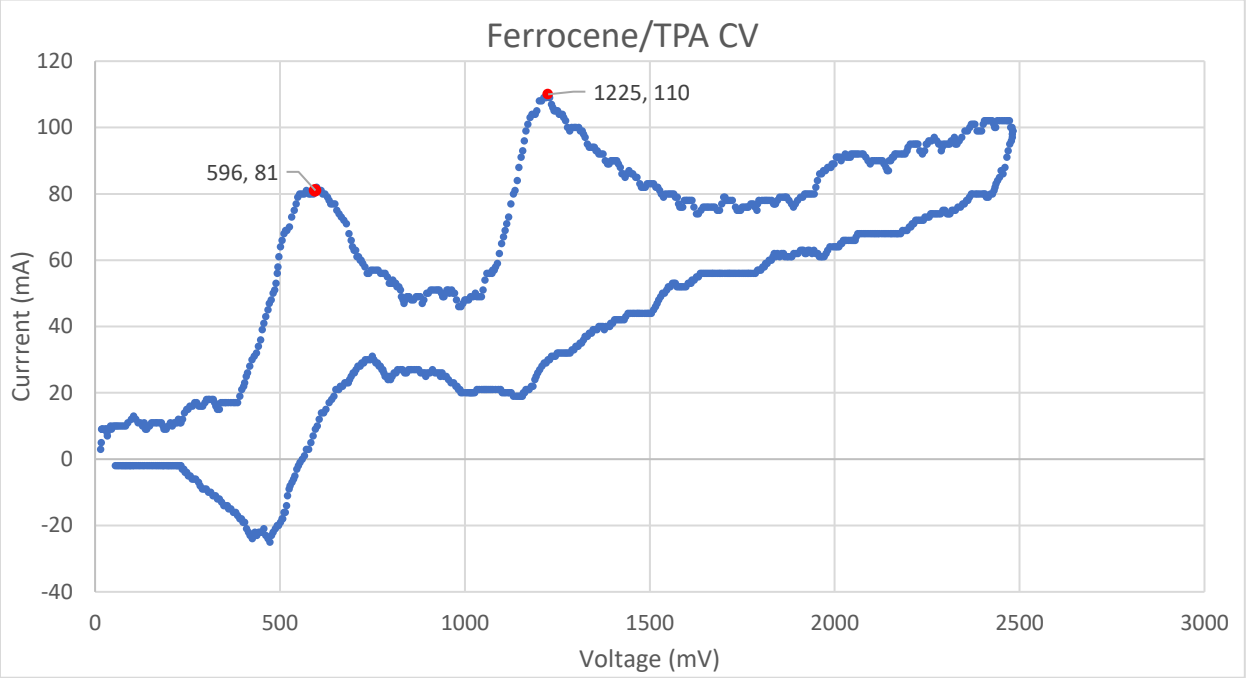

Tri(tolyl)amine (63)

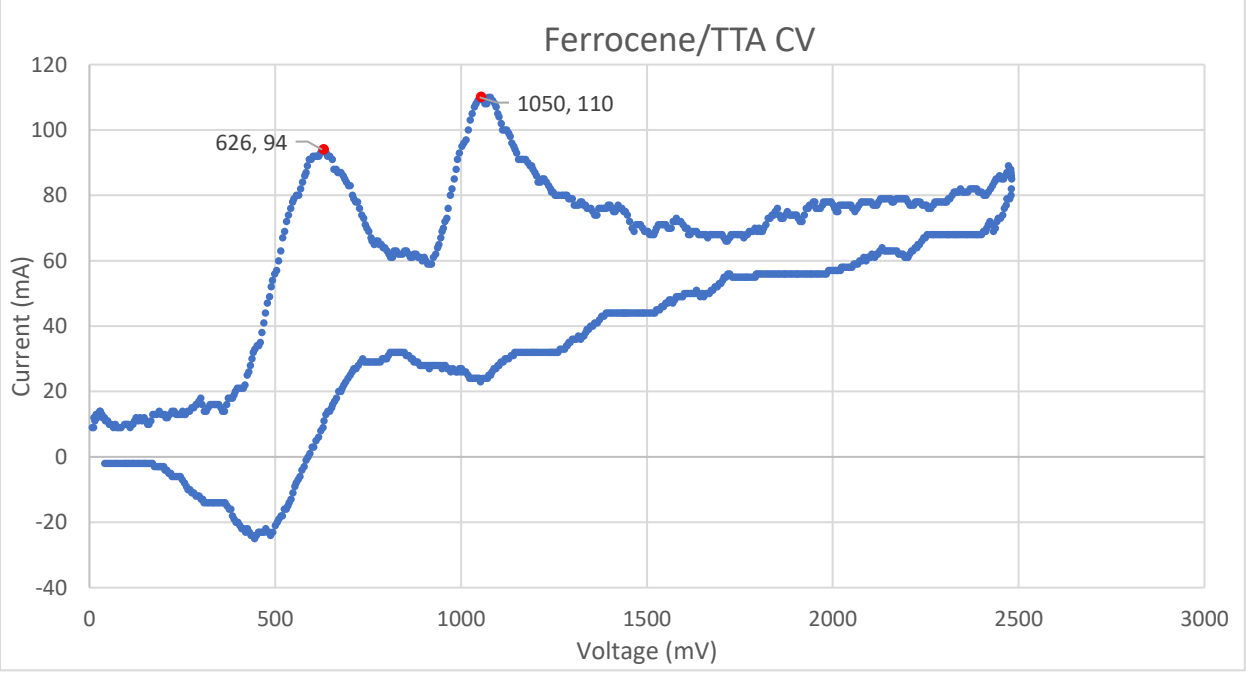

Tri([1,1'-biphenyl]-4-yl)amine (64)

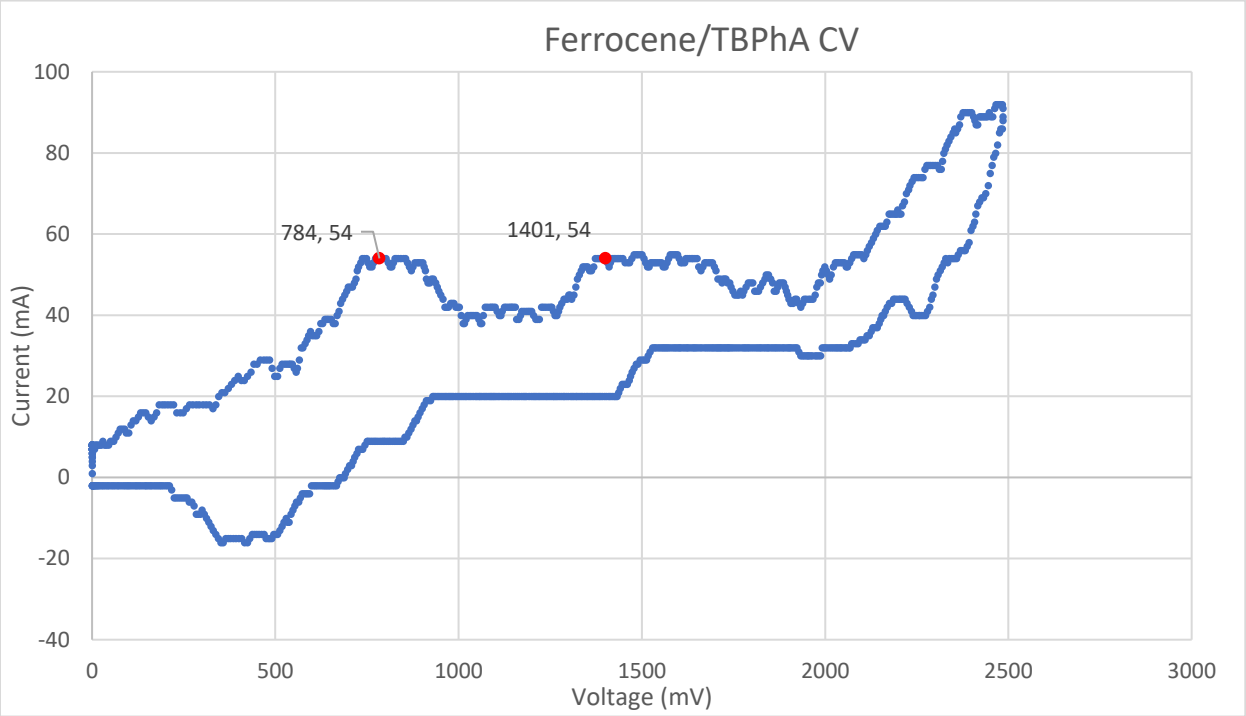

4.3.2: General procedure 10: Electrochemical quinoline synthesis

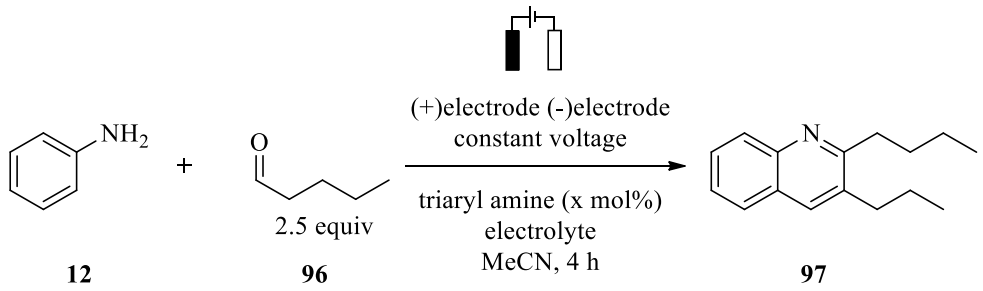

12 **96** **97**

Aniline (0.020 g, 0.21 mmol, 1 equiv), pentanal (0.046 g, 0.53 mmol, 2.5 equiv), tri(4-bromophenyl)amine (TBPA) (0.010 g, 0.021 mmol, 10 mol%), the electrolyte (3.6 equiv), and acetonitrile (8 mL) were all charged into a 10 mL IKA undivided electrochemical cell. The desired electrodes were positioned onto the cap of the cell and the cap screwed onto the cell. The assembled electrochemical cell was positioned onto an Electrosyn 2.0 instrument. The information for an experiment was then programed into the device: concentration of the cell, desired voltage, 4 hours for the reaction time, and no alternating polarity. Upon completion, reaction mixture was filtered through a pad of silica and concentrated by vacuum. . ^{1}H NMR analysis was performed using equimolar hexamethyldisiloxane (45 μL, 0.21 mmol , 1 equiv) as an internal standard. The ^{1}H NMR spectrum was identical with that previously reported.[72]

4.3.3 Electrolyte Screening

Trials for the electrolyte was carried out following the general procedure **10**. The varying electrolyte (3.6 equiv) is summarized in the table below.

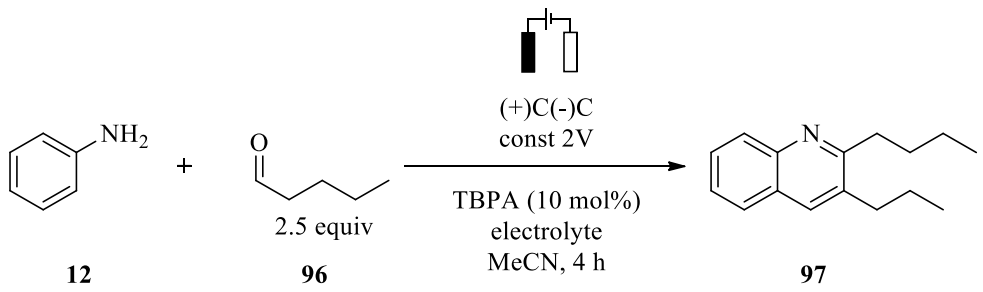

12 **96** **97**

Entry	Electrolyte	Yield*
1	$TBAPF_6$	8
2	LiBr	30
3	LiCl	8
4	LiI	9
5	TBACl	2
6	TBABr	3
7	TBAI	2

*By ^{1}H NMR analysis

4.3.4 Electrode Screening

Trials for the variation of the different electrodes were carried out following the general procedure **10**. The varied anodes and cathodes used are summarized in the following table.

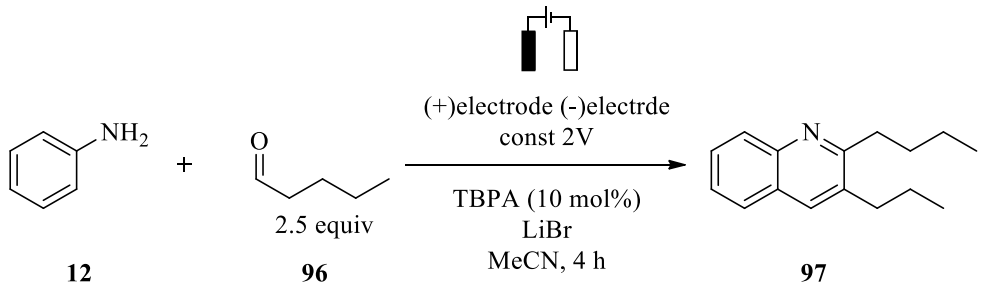

12 **96** **97**

Entry	Anode (+)	Cathode (-)	Yield (%)*
1	C (graphite)	C (graphite)	30
2	Mg	Stainless Steel	13
3	Zn	Stainless Steel	20
4	Ni	Stainless Steel	19
5	RVC	Platinum	5

*By 1H NMR analysis

4.3.5 Voltage Survey

Trials for the range of voltages were carried out following the general procedure **10**. The cell voltages were summarized in the following table.

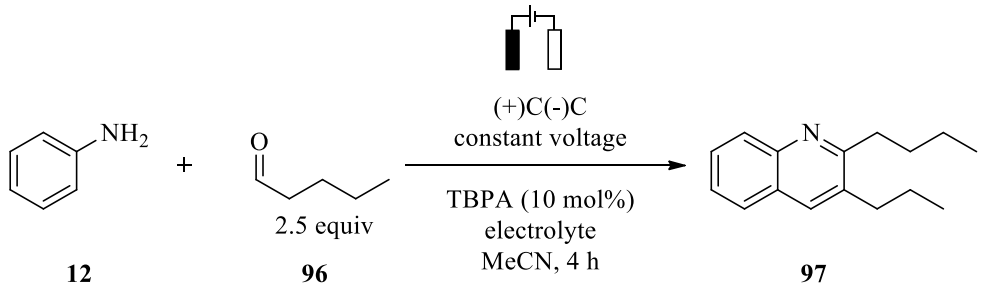

12 **96** **97**

Entry	Voltage (V)	Yield*
1	1.5	23
2	1.8	32
3	1.9	38
4	2.0	30
5	2.2	26
6	2.5	22
7	3.0	25

*By ^{1}H NMR analysis

4.3.6 Triaryl amine mediator screening

Trials for different triaryl amine mediator and the loadings of the mediaotrs were carried out following the general procedure **10**. The observed yields are summarized in the following table

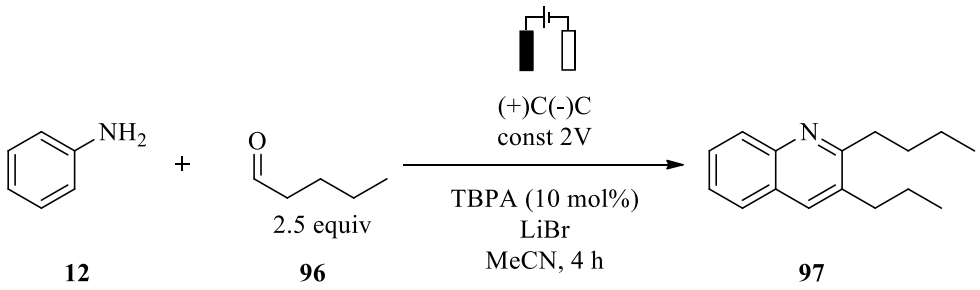

12 **96** **97**

Entry	Additive (mol%)	Yield[a]
1	TBPA (10%)	30
2	TBPA (20%)	37
3	TBPA (1 equiv)	40
4	TPA (10%)	32
5	TPA (20%)	32
6	TPA (1 eq)	30
7	TBPhA (10%)	29
8	TTA (10%)	30

[a] ^{1}H NMR conversion using HMDSO as an internal standard.

4.3.7 Other electrochemical controls

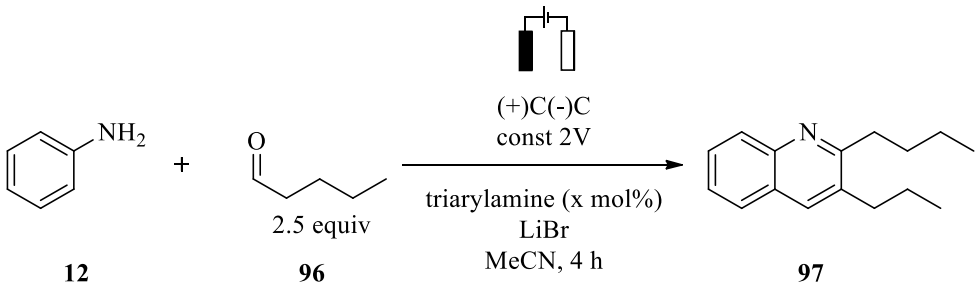

Equation 3.2: General procedure **10** was performed. Direction of the current was alternated between the anode and the cathode in intervals of 30 mins., for 4 hr (^{1}H NMR yield: 11%).

Equation 3.3(1): General procedure **10** was performed. TBPA was charged to the cell containing LiBr and MeCN and a constant 2.0 V was applied for 10 mins. Aniline and pentanal were then charged to the cell (^{1}H NMR yield: 41%).

Equation 3.3(2): General procedure **10** was performed. TBPA was charged to the cell containing LiBr and MeCN and a constant 2.0 V was applied for 10 mins. Aniline and pentanal were then added and the voltage was turned off. Reaction stirred at room temp for 4 hr (^{1}H NMR yield: 22%).

Equation 3.4: General procedure **10** was performed. TMEDA (89 mg, 0.77 mmol, 3.6 equiv) was added at the onset of the reaction (^{1}H NMR yield: 2%).

Equation 3.5: General procedure **10** was performed. No TBPA was added to the reaction (^{1}H NMR yield: 35%).

Bibliography

(1) World Energy Resources: 2010 Survey https://www.worldenergy.org/publications/entry/world-energy-resources-2010-survey (accessed 2021 -08 -18).

(2) Gray, M. R. Introduction. In *Upgrading Oilsands Bitumen and Heavy Oil*; University of Alberta Press, 2015; pp 1–12.

(3) Gray, M. R. Density and Phase Behaviour. In *Upgrading Oilsands Bitumen and Heavy Oil*; University of Alberta Press, 2015; pp 15–67.

(4) Crude oil blends by API gravity and by sulfur content https://corporate.exxonmobil.com:443/Crude-oils/Crude-trading/Crude-oil-blends-by-API-gravity-and-by-sulfur-content (accessed 2021 -08 -17).

(5) Gray, M. R.; Jokuty, P.; Yeniova, H.; Nazarewycz, L.; Wanke, S. E.; Achia, U.; Krzywicki, A.; Sanford, E. C.; Sy, O. K. Y. The Relationship between Chemical Structure and Reactivity of Alberta Bitumens and Heavy Oils. *The Canadian Journal of Chemical Engineering* **1991**, *69* (4), 833–843. https://doi.org/10.1002/cjce.5450690404.

(6) Holý, M.; Remišová, E. Analysis of Influence of Bitumen Composition on the Properties Represented by Empirical and Viscosity Test. *Transportation Research Procedia* **2019**, *40*, 34–41. https://doi.org/10.1016/j.trpro.2019.07.007.

(7) Gray, M. R. Chemical Composition. In *Upgrading Oilsands Bitumen and Heavy Oil*; Univeristy of Alberta Press, 2015; pp 91–147.

(8) Strausz, O. P.; Lown, E. M. *The Chemistry of Alberta Oil Sands, Bitumen and Heavy Oils*; Alberta Energy Research Institute, 2003.

(9) Strong, D.; Filby, R. H. Vanadyl Porphyrin Distribution in the Alberta Oil-Sand Bitumens. In *Metal Complexes in Fossil Fuels*; ACS Symposium Series; American Chemical Society, 1987; Vol. 344, pp 154–172. https://doi.org/10.1021/bk-1987-0344.ch010.

(10) Gray, M. R. Separation Processes. In *Upgrading Oilsands Bitumen and Heavy Oil*; University of Alberta Press, 2015; pp 276–294.

(11) Schuler, B.; Meyer, G.; Peña, D.; Mullins, O. C.; Gross, L. Unraveling the Molecular Structures of Asphaltenes by Atomic Force Microscopy. *J. Am. Chem. Soc.* **2015**, *137* (31), 9870–9876. https://doi.org/10.1021/jacs.5b04056.

(12) Schuler, B.; Zhang, Y.; Collazos, S.; Fatayer, S.; Meyer, G.; Pérez, D.; Guitián, E.; Harper, M. R.; Kushnerick, J. D.; Peña, D.; Gross, L. Characterizing Aliphatic Moieties in Hydrocarbons with Atomic Force Microscopy. *Chem. Sci.* **2017**, *8* (3), 2315–2320. https://doi.org/10.1039/C6SC04698C.

(13) Mullins, O. C.; Sabbah, H.; Eyssautier, J.; Pomerantz, A. E.; Barré, L.; Andrews, A. B.; Ruiz-Morales, Y.; Mostowfi, F.; McFarlane, R.; Goual, L.; Lepkowicz, R.; Cooper, T.; Orbulescu, J.; Leblanc, R. M.; Edwards, J.; Zare, R. N. Advances in Asphaltene Science and the Yen−Mullins Model. *Energy Fuels* **2012**, *26* (7), 3986–4003. https://doi.org/10.1021/ef300185p.

(14) Sheremata, J. M.; Gray, M. R.; Dettman, H. D.; McCaffrey, W. C. Quantitative Molecular Representation and Sequential Optimization of Athabasca Asphaltenes. *Energy Fuels* **2004**, *18*, 1377. https://doi.org/10.1021/ef049936+

(15) Gray, M. R.; Tykwinski, R. R.; Stryker, J. M.; Tan, X. Supramolecular Assembly Model for Aggregation of Petroleum Asphaltenes. *Energy Fuels* **2011**, *25* (7), 3125–3134. https://doi.org/10.1021/ef200654p.
(16) Scott, D. E.; Schulze, M.; Stryker, J. M.; Tykwinski, R. R. Deciphering Structure and Aggregation in Asphaltenes: Hypothesis-Driven Design and Development of Synthetic Model Compounds. *Chem. Soc. Rev.* **2021**, 10.1039.D1CS00048A. https://doi.org/10.1039/D1CS00048A.
(17) Rakotondradany, F.; Fenniri, H.; Rahimi, P.; Gawrys, K. L.; Kilpatrick, P. K.; Gray, M. R. Hexabenzocoronene Model Compounds for Asphaltene Fractions: Synthesis & Characterization. *Energy Fuels* **2006**, *20* (6), 2439–2447. https://doi.org/10.1021/ef060130e.
(18) Schulze, M.; Lechner, M. P.; Stryker, J. M.; Tykwinski, R. R. Aggregation of Asphaltene Model Compounds Using a Porphyrin Tethered to a Carboxylic Acid. *Org. Biomol. Chem.* **2015**, *13* (25), 6984–6991. https://doi.org/10.1039/C5OB00836K.
(19) Diner, C.; Scott, D. E.; Tykwinski, R. R.; Gray, M. R.; Stryker, J. M. Scalable, Chromatography-Free Synthesis of Alkyl-Tethered Pyrene-Based Materials. Application to First-Generation "Archipelago Model" Asphaltene Compounds. *J. Org. Chem.* **2015**, *80* (3), 1719–1726. https://doi.org/10.1021/jo502650m.
(20) Ugi, I.; Dömling, A.; Hörl, W. Multicomponent Reactions in Organic Chemistry. *Endeavour* **1994**, *18* (3), 115–122. https://doi.org/10.1016/S0160-9327(05)80086-9.
(21) Ramann, G. A.; Cowen, B. J. Recent Advances in Metal-Free Quinoline Synthesis. *Molecules* **2016**, *21* (8), 986. https://doi.org/10.3390/molecules21080986.
(22) Kozlov, N. G.; Basalaeva, L. I.; Firgang, S. I.; Shashkov, A. S. Reaction of Methylcyclohexanones with Substituted Benzaldehydes and 2-Naphthylamine. *Russ. J. Org. Chem.* **2004**, *40* (4), 7. https://doi.org/10.1023/B:RUJO.0000036073.49961.28.
(23) Wang, X.-S.; Li, Q.; Yao, C.-S.; Tu, S.-J. An Efficient Method for the Synthesis of Benzo[*f*]Quinoline and Benzo[*a*]Phenanthridine Derivatives Catalyzed by Iodine by a Three-Component Reaction of Arenecarbaldehyde, Naphthalen-2-Amine, and Cyclic Ketone. *Eur. J. Org. Chem.* **2008**, *2008* (20), 3513–3518. https://doi.org/10.1002/ejoc.200800287.
(24) Schulze, M.; Scott, D. E.; Scherer, A.; Hampel, F.; Hamilton, R. J.; Gray, M. R.; Tykwinski, R. R.; Stryker, J. M. Steroid-Derived Naphthoquinoline Asphaltene Model Compounds: Hydriodic Acid Is the Active Catalyst in I_2 -Promoted Multicomponent Cyclocondensation Reactions. *Org. Lett.* **2015**, *17* (23), 5930–5933. https://doi.org/10.1021/acs.orglett.5b03193.
(25) Scott, D. E.; Aloisio, M. D.; Rodriguez, J. F.; Morimoto, M.; Hamilton, R. J.; Brown, O.; Tykwinski, R. R.; Stryker, J. M. Optimizing the Iodide/Iodonium/O2 Oxidation Cycle Enhances the Scope, Selectivity, and Yields of Hydroiodic Acid-Catalyzed Multicomponent Cyclocondensation Reactions. *Advanced Synthesis & Catalysis* **2021**, *n/a* (n/a). https://doi.org/10.1002/adsc.202100657.
(26) Teja, C.; Khan, F. R. N. Radical Transformations towards the Synthesis of Quinoline: A Review. *Chemistry – An Asian Journal* **2020**, *15* (24), 4153–4167. https://doi.org/10.1002/asia.202001156.
(27) Jia, X.; Peng, F.; Qing, C.; Huo, C.; Wang, X. Catalytic Radical Cation Salt Induced C_{sp^3} –H Functionalization of Glycine Derivatives: Synthesis of Substituted Quinolines. *Org. Lett.* **2012**, *14* (15), 4030–4033. https://doi.org/10.1021/ol301909g.

(28) Yuan, Y.; Zhang, S.; Sun, Z.; Su, Y.; Ma, Q.; Yuan, Y.; Jia, X. Tris(4-Bromophenyl)Aminium Hexachloroantimonate-Initiated Oxidative Povarov-Type Reaction between Glycine Esters and (Cyclopropylidenemethyl)Benzenes Using the Counterion as a Chlorine Donor. *Org. Lett.* **2020**, *22* (16), 6294–6298. https://doi.org/10.1021/acs.orglett.0c02054.
(29) Jia, X.; Peng, F.; Qing, C.; Huo, C.; Wang, Y.; Wang, X. Synthesis of 2,3-Disubstituted Quinolines from in Situ Generated Imines and Its Enamine Tautomer under Radical Cation Induced Conditions. *Tetrahedron Letters* **2013**, *54* (36), 4950–4952. https://doi.org/10.1016/j.tetlet.2013.07.014.
(30) Klapars, A.; Buchwald, S. L. Copper-Catalyzed Halogen Exchange in Aryl Halides: An Aromatic Finkelstein Reaction. *J. Am. Chem. Soc.* **2002**, *124* (50), 14844–14845. https://doi.org/10.1021/ja028865v.
(31) Amara, R.; Bentabed-Ababsa, G.; Hedidi, M.; Khoury, J.; Awad, H.; Nassar, E.; Roisnel, T.; Dorcet, V.; Chevallier, F.; Fajloun, Z.; Mongin, F. Synthesis of N-Aryl and N-Heteroaryl γ-, δ-, and ε-Lactams Using Deprotometalation–Iodination and N-Arylation, and Properties Thereof. *Synthesis* **2017**, *28* (19), 4500–4516. https://doi.org/10.1055/s-0036-1590798.
(32) Rennels, R. A.; Maliakal, A. J.; Collum, D. B. Ortholithiation of Anisole by *n* -BuLi−TMEDA: Reaction via Disolvated Dimers. *J. Am. Chem. Soc.* **1998**, *120* (2), 421–422. https://doi.org/10.1021/ja972610d.
(33) Larock, R. C.; Leung, W.-Y.; Stolz-Dunn, S. Synthesis of Aryl-Substituted Aldehydes and Ketones via Palladium-Catalyzed Coupling of Aryl Halides and Non-Allylic Unsaturated Alcohols. *Tetrahedron Letters* **1989**, *30* (48), 6629–6632. https://doi.org/10.1016/S0040-4039(00)70636-8.
(34) Barton, D. H. R.; Crich, D.; Motherwell, W. B. N e w and Improved Methods for the Radical Decarboxylation of Acids. *J. Chem. Soc., Chem. Commun.* **1983**, 3. https://doi.org/10.1039/C39830000939.
(35) Sreenath, K.; Suneesh, C. V.; Ratheesh Kumar, V. K.; Gopidas, K. R. Cu(II)-Mediated Generation of Triarylamine Radical Cations and Their Dimerization. An Easy Route to Tetraarylbenzidines. *J. Org. Chem.* **2008**, *73* (8), 3245–3251. https://doi.org/10.1021/jo800349n.
(36) Talipov, M. R.; Hossain, M. M.; Boddeda, A.; Thakur, K.; Rathore, R. A Search for Blues Brothers: X-Ray Crystallographic/Spectroscopic Characterization of the Tetraarylbenzidine Cation Radical as a Product of Aging of Solid Magic Blue. *Org. Biomol. Chem.* **2016**, *14* (10), 2961–2968. https://doi.org/10.1039/C6OB00140H.
(37) Dorel, R.; Grugel, C. P.; Haydl, A. M. The Buchwald–Hartwig Amination After 25 Years. *Angewandte Chemie International Edition* **2019**, *58* (48), 17118–17129. https://doi.org/10.1002/anie.201904795.
(38) Tlili, A.; Monnier, F.; Taillefer, M. Selective One-Pot Synthesis of Symmetrical and Unsymmetrical Di- and Triarylamines with a Ligandless Copper Catalytic System. *Chem. Commun.* **2012**, *48* (51), 6408. https://doi.org/10.1039/c2cc32252h.
(39) Liu, Y.-H.; Chen, C.; Yang, L.-M. Diazabutadiene: A Simple and Efficient Ligand for Copper-Catalyzed N-Arylation of Aromatic Amines. *Tetrahedron Letters* **2006**, *47* (52), 9275–9278. https://doi.org/10.1016/j.tetlet.2006.10.103.

(40) Barham, J. P.; John, M. P.; Murphy, J. A. Contra-Thermodynamic Hydrogen Atom Abstraction in the Selective C–H Functionalization of Trialkylamine *N* -CH $_3$ Groups. *J. Am. Chem. Soc.* **2016**, *138* (47), 15482–15487. https://doi.org/10.1021/jacs.6b09690.
(41) Li, Z.; Ishizuka, H.; Sei, Y.; Akita, M.; Yoshizawa, M. Extended Fluorochromism of Anthracene Trimers with a Meta-Substituted Triphenylamine or Triphenylphosphine Core. *Chemistry – An Asian Journal* **2012**, *7* (8), 1789–1794. https://doi.org/10.1002/asia.201200310.
(42) Huo, C.; Wang, C.; Wu, M.; Jia, X.; Wang, X.; Yuan, Y.; Xie, H. Catalytic Amounts of Triarylaminium Salt Initiated Aerobic Oxidative Coupling of N-Aryl Tetrahydroisoquinolines. *Org. Biomol. Chem.* **2014**, *12* (19), 3123–3128. https://doi.org/10.1039/C3OB42454E.
(43) Reichl, K. D.; Ess, D. H.; Radosevich, A. T. Catalyzing Pyramidal Inversion: Configurational Lability of P-Stereogenic Phosphines via Single Electron Oxidation. *J. Am. Chem. Soc.* **2013**, *135* (25), 9354–9357. https://doi.org/10.1021/ja404943x.
(44) Murata, H.; Lahti, P. M. Synthesis and Oxidation of Triarylamine Derivatives Bearing Hydrogen-Bonding Groups. *J. Org. Chem.* **2007**, *72* (13), 4974–4977. https://doi.org/10.1021/jo070318a.
(45) Bender, T. P.; Graham, J. F.; Duff, J. M. Effect of Substitution on the Electrochemical and Xerographic Properties of Triarylamines: Correlation to the Hammett Parameter of the Substituent and Calculated HOMO Energy Level. *Chem. Mater.* **2001**, *13* (11), 4105–4111. https://doi.org/10.1021/cm010281p.
(46) Scopus - Analyze search results https://www.scopus.com/term/analyzer.uri?sid=9bb534882fc73a0d65d883aecbabbb2d&origin=resultslist&src=s&s=TITLE-ABS-KEY%28Electrochemical+synthesis%29&sort=plf-f&sdt=b&sot=b&sl=40&count=82980&analyzeResults=Analyze+results&txGid=06cf16d8c70e89c57e64ae8cf6cc877e (accessed 2021 -08 -19).
(47) Yan, M.; Kawamata, Y.; Baran, P. S. Synthetic Organic Electrochemical Methods Since 2000: On the Verge of a Renaissance. *Chem. Rev.* **2017**, *117* (21), 13230–13319. https://doi.org/10.1021/acs.chemrev.7b00397.
(48) Horn, E. J.; Rosen, B. R.; Baran, P. S. Synthetic Organic Electrochemistry: An Enabling and Innately Sustainable Method. *ACS Cent. Sci.* **2016**, *2* (5), 302–308. https://doi.org/10.1021/acscentsci.6b00091.
(49) Kingston, C.; Palkowitz, M. D.; Takahira, Y.; Vantourout, J. C.; Peters, B. K.; Kawamata, Y.; Baran, P. S. A Survival Guide for the "Electro-Curious." *Acc. Chem. Res.* **2020**, *53* (1), 72–83. https://doi.org/10.1021/acs.accounts.9b00539.
(50) Steckhan, E. Indirect Electroorganic Syntheses—A Modern Chapter of Organic Electrochemistry [New Synthetic Methods (59)]. *Angewandte Chemie International Edition in English* **1986**, *25* (8), 683–701. https://doi.org/10.1002/anie.198606831.
(51) Shono, T.; Hamaguchi, H.; Matsumura, Y. Electroorganic Chemistry. XX. Anodic Oxidation of Carbamates. *J. Am. Chem. Soc.* **1975**, *97* (15), 4264–4268. https://doi.org/10.1021/ja00848a020.
(52) Shono, T.; Matsumura, Y.; Tsubata, K. Electroorganic Chemistry. 46. A New Carbon-Carbon Bond Forming Reaction at the .Alpha.-Position of Amines Utilizing Anodic Oxidation as a Key Step. *J. Am. Chem. Soc.* **1981**, *103* (5), 1172–1176. https://doi.org/10.1021/ja00395a029.

(53) Hou, Z.-W.; Mao, Z.-Y.; Zhao, H.-B.; Melcamu, Y. Y.; Lu, X.; Song, J.; Xu, H.-C. Electrochemical C−H/N−H Functionalization for the Synthesis of Highly Functionalized (Aza)Indoles. *Angewandte Chemie International Edition* **2016**, *55* (32), 9168–9172. https://doi.org/10.1002/anie.201602616.
(54) Park, Y. S.; Wang, S. C.; Tantillo, D. J.; Little, R. D. A Highly Selective Rearrangement of a Housane-Derived Cation Radical: An Electrochemically Mediated Transformation. *J. Org. Chem.* **2007**, *72* (12), 4351–4357. https://doi.org/10.1021/jo070190x.
(55) Wu, X.; Davis, A. P.; Fry, A. J. Electrocatalytic Oxidative Cleavage of Electron-Deficient Substituted Stilbenes in Acetonitrile−Water Employing a New High Oxidation Potential Electrocatalyst. An Electrochemical Equivalent of Ozonolysis. *Org. Lett.* **2007**, *9* (26), 5633–5636. https://doi.org/10.1021/ol7026416.
(56) Platen, M.; Steckhan, E. Oxidative Deblocking of the 4-Methoxybenzyl Thioether Protecting Group: Application to the Directed Synthesis of Poly-Cystinyl Peptides. *Liebigs Annalen der Chemie* **1984**, *1984* (9), 1563–1576. https://doi.org/10.1002/jlac.198419840905.
(57) Li, L.-J.; Jiang, Y.-Y.; Lam, C. M.; Zeng, C.-C.; Hu, L.-M.; Little, R. D. Aromatic C–H Bond Functionalization Induced by Electrochemically in Situ Generated Tris(*p* -Bromophenyl)Aminium Radical Cation: Cationic Chain Reactions of Electron-Rich Aromatics with Enamides. *J. Org. Chem.* **2015**, *80* (21), 11021–11030. https://doi.org/10.1021/acs.joc.5b02222.
(58) Heard, D. M.; Lennox, A. J. J. Electrode Materials in Modern Organic Electrochemistry. *Angewandte Chemie International Edition* **2020**, *59* (43), 18866–18884. https://doi.org/10.1002/anie.202005745.
(59) Bahlake, A.; Ansari, M. R.; Talkhoncheh, S. K. Experimental Investigation of an Electrochemical Cell from the Power Generation View Point. *Advances in Applied Science Research* **2012**, *3*, 1738–1743.
(60) Lv, J.; Tan, Y.-X.; Xie, J.; Yang, R.; Yu, M.; Sun, S.; Li, M.-D.; Yuan, D.; Wang, Y. Direct Solar-to-Electrochemical Energy Storage in a Functionalized Covalent Organic Framework. *Angewandte Chemie International Edition* **2018**, *57* (39), 12716–12720. https://doi.org/10.1002/anie.201806596.
(61) Ingelsson, M.; Yasri, N.; Roberts, E. P. L. Electrode Passivation, Faradaic Efficiency, and Performance Enhancement Strategies in Electrocoagulation—a Review. *Water Research* **2020**, *187*, 116433. https://doi.org/10.1016/j.watres.2020.116433.
(62) Hilt, G. Basic Strategies and Types of Applications in Organic Electrochemistry. *ChemElectroChem* **2020**, *7* (2), 395–405. https://doi.org/10.1002/celc.201901799.
(63) Vinogradov, M. G.; Turova, O. V.; Zlotin, S. G. Catalytic Asymmetric Aza-Diels-Alder Reaction: Pivotal Milestones and Recent Applications to Synthesis of Nitrogen-Containing Heterocycles. *Advanced Synthesis & Catalysis* **2021**, *363* (6), 1466–1526. https://doi.org/10.1002/adsc.202001307.
(64) Shi, M.; Shao, L.-X.; Xu, B. The Lewis Acids Catalyzed Aza-Diels−Alder Reaction of Methylenecyclopropanes with Imines. *Org. Lett.* **2003**, *5* (4), 579–582. https://doi.org/10.1021/ol0275365.
(65) Armstrong, D. A.; Huie, R. E.; Lymar, S.; Koppenol, W. H.; Merényi, G.; Neta, P.; Stanbury, D. M.; Steenken, S.; Wardman, P. Standard Electrode Potentials Involving Radicals in Aqueous Solution: Inorganic Radicals. *BioInorganic Reaction Mechanisms* **2013**, *9* (1–4). https://doi.org/10.1515/irm-2013-0005.

(66) Nicolaescu, A. R.; Wiest, O.; Kamat, P. V. Radical-Induced Oxidative Transformation of Quinoline. *J. Phys. Chem. A* **2003**, *107* (3), 427–433. https://doi.org/10.1021/jp027112s.
(67) Galus, Z.; Adams, R. N. Anodic Oxidation of N-Methylaniline and N,N-Dimethyl-p-Toluidine. *J. Phys. Chem.* **1963**, *67* (4), 862–866. https://doi.org/10.1021/j100798a035.
(68) De, A. K.; Ganguly, T. Investigations on nonradiative transitions in different environments using excited (or ground state) 1,2,3,4-tetrahydroquinoline (THQ) as donor and ground state (or excited) 9-fluorenone (9FL) or 2-nitro-9-fluorenone (2N9FL) as acceptors *Canadian Journal of Chemistry* **2000**, *78* (1), 139–150. https://doi.org/10.1139/v99-224
(69) Kauffman, G. B.; Fang, L. Y.; Viswanathan, N.; Townsend, G. Purification of Copper (i) Iodide. In *Inorganic Syntheses*; John Wiley & Sons, Ltd, 1984; pp 101–103. https://doi.org/10.1002/9780470132531.ch20.
(70) Stark, T.; Suhartono, M.; Göbel, M. W.; Lautens, M. A Palladium-Catalyzed Domino Reaction as Key Step for the Synthesis of Functionalized Aromatic Amino Acids. *Synlett* **2013**, *24* (20), 2730–2734.
(71) Lo, C.-Y.; Kumar, M. P.; Chang, H.-K.; Lush, S.-F.; Liu, R.-S. Regioselective Haloaromatization of 1,2-Bis(Ethynyl)Benzene via Halogen Acids and PtCl2. Platinum-Catalyzed 6-π Electrocyclization of 1,2-Bis(1‘-Haloethenyl)Benzene Intermediates. *J. Org. Chem.* **2005**, *70* (25), 10482–10487. https://doi.org/10.1021/jo0518295.
(72) Cho, C. S.; Lee, N. Y.; Kim, T.-J.; Shim, S. C. Ruthenium-Catalyzed Formal Alkyl Group Transfer: Synthesis of Quinolines from Nitroarenes and Alkylammonium Halides. *Journal of Heterocyclic Chemistry* **2004**, *41* (3), 423–429. https://doi.org/10.1002/jhet.5570410320.